CHARACTERIZATION OF COUPLED BODY RESPONSE IN RANDOM SEA

A Thesis

by

CHEN XIE

Submitted to the Office of Graduate Studies of
Texas A&M University
in partial fulfillment of the requirements for the degree of

MASTER OF SCIENCE

December 2005

Major Subject: Ocean Engineering

CHARACTERIZATION OF COUPLED BODY RESPONSE IN RANDOM SEA

A Thesis

by

CHEN XIE

Submitted to the Office of Graduate Studies of
Texas A&M University
in partial fulfillment of the requirements for the degree of

MASTER OF SCIENCE

Approved by:

Chair of Committee,	John M. Niedzwecki
Committee Members,	H. Joseph Newton
	Jun Zhang
Head of Department,	David V. Rosowsky

December 2005

Major Subject: Ocean Engineering

ABSTRACT

Characterization of Coupled Body Response in Random Sea. (December 2005)
Chen Xie,
Diplôme d'Ingénieur, Ecole Spéciale des Travaux Publics, Paris, France
Chair of Advisory Committee: Dr. John M. Niedzwecki

The frequent use of two or more closely positioned vessels during offshore operations makes the study of multi-body hydrodynamics an important topic, especially for the design of deepwater offshore systems. This research investigation studies the response behavior of a coupled mini-TLP / barge system in both head and beam sea conditions. The design sea conditions were selected to represent the combined wind, wave and current conditions for a target location off the coast of West Africa. Both the mini-TLP and the barge were designed to have independent mooring systems. Coupling between the two vessels is introduced through a connection consisting of two breast lines and a fender system. This connection is designed to restrain the horizontal movements of the two vessels while keeping a constant distance between them and avoiding collisions.

The main focus of this study is to analyze the experimental data obtained during the model testing, especially the motions of the two bodies and the values related to the fender system, in order to characterize the behavior of the uncoupled and coupled system configurations. A statistical approach is used for the data analysis and interpretation. Statistical parameters are used to provide an overall characterization of system behavior, and Gaussian and Weibull distribution functions are utilized to detect the importance of non-linearity in the data with particular attention to extreme values. Correlations between the two vessels in time domain and frequency domain are investigated. In addition, auto and cross spectrum analyses of the data are used to contrast the motion behavior of the uncoupled and coupled configurations. It is shown that the connection

system reduces the horizontal vessel motions; however the forces exerted on the fender system show significant variation depending on sea heading conditions.

DEDICATION

To my family

ACKNOWLEDGEMENTS

This research study was supported in part by the Texas Advanced Technology Program (C04-00174), the Texas Engineering Experiment Station and the R.P. Gregory ’32 Chair endowment. Each of these funding sources is gratefully acknowledged. The data for this study was made available as a result of a collaborative research program between the Offshore Technology Research Center and Statoil, Norway. The permission to utilize the data is gratefully acknowledged, as is the contributions of the OTRC technicians and students in successfully executing the model test program.

I would like to express my gratitude and thanks to my advisor, Dr. John M. Niedzwecki, for his guidance and advice during my studies. I would also like to thank my advisory committee members: Dr. H. Joseph Newton and Dr. Jun Zhang, for their guidance throughout this research project.

I wish also to thank my parents, all the members of my family, as well as my friends for their support and help.

TABLE OF CONTENTS

Page

LIST OF FIGURES

Page

Page

LIST OF TABLES

Page

1. INTRODUCTION

In many offshore operations, two or more closely positioned structures are used, with or without connections between them. Some of the practical examples of two-body hydrodynamic systems are: a ship floating adjacent to an offshore structure; a tanker moored to a floating buoy for offloading oil; and more recently, the side-by-side mooring configurations proposed for the loading and offloading of LNG vessels. A good understanding of the basic two-body hydrodynamic behavior is needed for the design of real offshore systems. For instance, the ability to better predict heave motion of an LNG tanker moored to a deep water terminal could better facilitate the necessary product transfer between the platforms. Similarly, improving the prediction of the LNG tanker surge, sway and roll motions could help designer to avoid collisions between the two vessels.

The hydrodynamic behavior of a two-body system is different from that of a single-body system since the motions of each body will be influenced by the presence of its neighboring structure. Besides tie-offs and soft or hard connections for product transfer, the hydrodynamic interaction effects such as diffraction / radiation and amplitude of the wave field between the platforms present significant design problems. The response behavior is much influenced by the configuration of the two-body system, in particular the size and the shape of the structures, the separation distance between them and by the stiffness of the various mooring and docking connections.

1.1. Literature review

Over the years, multi-body hydrodynamic problems, particularly two-body systems, have been investigated by researchers attempting to estimate the vessel response motions. Linear potential theory has been widely used for this purpose and this requires that the following conditions are satisfied: the fluid is incompressible, inviscid, irrotational, and the motion of the structures are small compared to their size. Three

---

This thesis follows the style of Ocean Engineering.

main numerical simulation methods based on the linear potential theory have been developed for this use. These include the strip theory method, the boundary integral method, and the finite element method. Brief summaries of the technical articles used in this literature review for numerical methods are presented in Tables 1, 2 and 3, classified by the type of method and by the chronicle order.

Strip theory was developed for slender bodies which have one length-dimension substantially greater than the others. In this case, it is assumed that the local force at one section of the body is not affected by the shape of the other parts of the body. In a two-body system, this means that there is interaction only between the corresponding sections of the two structures. Using this method, the studied structures are divided longitudinally into a number of transverse sections for which the hydrodynamic coefficients are estimated. These sectional characteristics are then integrated along the length to obtain global coefficients. The work by Korvin-Kroukovsky (1955) provided the foundation for the application of the strip method to ship motion problem, its use on multi-body systems appeared about one decade later. The strip theory method was used to evaluate the hydrodynamic forces and moments on a twin hull ocean platform by Kim (1972). Later, Ohkusu (1976) proposed a method to calculate the interaction forces for a multi-body system. Further study by Ikegami and Matsuura (1981) incorporated the behavior of ship systems that had mooring lines and connections. Two-body ship systems subject to oblique waves were studied by Kodan (1984).

Unlike the strip theory approach, the boundary integral method (BIM), also known as panel method, can be used for ship hulls and ocean structures that have more arbitrary geometries. Its formulation uses the Green's theorem to express the velocity potential in term of the surface distribution of singularities over the boundary surfaces which are discretized into small panels. The wave exciting forces, the added mass and the damping coefficients can be thus found, as well as the equations of motion. The three dimensional source distribution method is one of the most common forms of the BIM method, its use was extended for the two-body system by Van Oortmerssen (1979). Inoue *et al.* (1996) developed a general method for evaluating dynamic responses of multiple-body systems

having arbitrary connections. Buchner *et al*. (2001) conducted studies for a time-domain analysis of a side-by-side mooring FPSO system. More recently, Hong *et al.* (2005) used a higher-order boundary element method for a more accurate analysis of a two-body system. A thorough review of the state-of-the-art using first and second order panel method can be found in the technical article by Lee and Newman (2004).

The advantage of the finite element method (FEM) when compared to the boundary integral method is that it is not subject to the phenomenon of irregular frequencies. At these frequencies, the solution of the surface integral equation is not unique, which causes poor numerical conditioning. Taylor and Zietsman (1982) employed a combined method which uses the FEM to describe the close field of the fluid region and the BIM for the far field. Huang *et al.* (1985) developed a finite element method to solve 3D wave diffraction/radiation problems by using a radiation boundary damper approach where the boundary condition is local in both space and time. Chen *et al.* (1991) analyzed the coupled motion of waves and floating twin bodies by applying the finite element method derived from the Galerkin approximation. Two-dimensional finite element method was used by Sannasiraj *et al.* (2001) to study the dynamics of multiple floating structures in directional waves.

Parallel to these numerical simulation methods, studies based on experimental results from model tests present another view of the study of the two or multi-body system hydrodynamics, especially for real industrial projects. Teigen and Niedzwecki (1999) presented a fully coupled mini-TLP / barge system with a connection consisted of breast lines and a fender system. Different combinations of external excitations such as wave, current, and wind were experimentally tested and the measurements were analyzed in the study of the system behavior. The LNG FPSO / shuttle tanker system has been investigated by Hong *et el.* (2002) by comparing the side-by-side and tandem mooring system. Both motion responses and drift forces were studied. Similarly, these two mooring features have been tested and compared by Van der Valk and Watson (2005) in a recent study of the mooring of LNG carriers to a weathervaning floater, based on the environmental conditions and operational feasibility for the transfer system.

Table 1. A brief summary of selected technical articles using strip theory to solve ship hydrodynamic problems

Year	Author(s)	Journal / Report Title	Summary
1972	Kim	The hydrodynamic interaction between two cylindrical bodies floating in beam seas	The hydrodynamic interactions between two different rigidly connected or freely floating cylindrical bodies in beam seas have been analyzed by using the strip method. The application on a twin hull ocean platform in beam seas has been described. Hydrodynamic forces and moments are evaluated, and the wave exciting forces are found by using force coefficients for rigidly coupled bodies. The strip method is recommended for the systematic calculations of a Catamaran hull in oblique seas. It can be also extended to further studies of freely floating bodies in oblique seas.
1976	Ohkusu	Ship motions in vicinity of a structure	A method has been purposed, by which the sectional interaction effects on the added mass, on the damping coefficients and on the wave exciting forces are evaluated by analyzing incoming waves generated by the oscillatory motion of corresponding sections of the two floating bodies. A system consisted of a moored structure and a ship in regular wave has been considered. Both the motions and drift forces have been studied. The comparison between the computed and experimental results shows good agreement.
1981	Ikegami & Matsuura	Study on motions of floating bodies under composite external loads	The equations of motions in regular wave have been derived by using the strip method. An added coefficients matrix due to mooring and connecting members has been used. Model tests of different mooring and connection configuration have been conducted: floating body moored by linear spring; floating body moored by a spud; two floating bodies brought alongside freely; two floating bodies connected alongside with semi-rigid link; floating bodies connected rigidly; several floating bodies connected with pin-joints, several floating bodies connected rigidly.
1984	Kodan	The motions of adjacent floating structures in oblique waves	Effects of hydrodynamic interaction between two parallel slender structures in oblique waves have been described, based on Ohkusu's theory. A combination of a ship and a rectangular barge has been studied. It is found that the influence of the existence of the other structure on the wave exciting force in oblique waves is substantial, that the different wave frequency, separation distance, and wave encounter angle will cause different interaction effects. In random wave, the prediction of the significant wave motion responses shows that the best separation distance between two structures can be chosen if the mean wave period of the field is known in advance.

Table 2. A brief summary of selected technical articles using the Boundary Integral Approach to solve ship hydrodynamic problems

Year	Author	Journal / Report Title	Summary
1979	Van Oortmerssen	Hydrodynamic interaction between two structures, floating in waves	Theoretical formulations have been derived for hydrodynamic interactions between two floating structures in vicinity of each other, by using the 3D source distribution method. An extended NSMB (Netherlands Ship Model Basin)'s 3D diffraction program is used to obtain numerical results for a model consisting of separately moored box and cylinder in regular long crested wave, this with different frequencies and separation distances. Besides an overestimation of pitch and roll at resonance due to the fact that the viscous effect is neglected, the comparison with experimental results is quite satisfactory.
1996	Inoue *et al.*	Motion analysis of parallely connected FPSO unit and LNG carrier	Linear stiffness matrices are introduced into the equation of motions to represent the effect of the mooring lines and the connections. These matrices are determined by the locations of the attachment points and the constant stiffness of the connection. The case of a parallely connected FPSO unit and LNG carrier is studied. The general analysis of the system only requires the frequency domain simulation. But for detail analysis such as design of the connection, a time domain analysis should be considered in order to take account of the nonlinear effects.
2001	Buchner & Van Dijk & De Wilde	Numerical multiple-body simulations of side-by-side mooring to an FPSO	A combination of the BIM and the impulse response theory (which states that the response to an arbitrary force is the superposition of the responses to unit impulses) is used in a time domain simulation to overcome the problems related to the non-linearity of a multi-body system. A diffraction analysis in frequency domain is performed in order to obtain added mass and damping coefficients which are used to calculate the retardation functions in time domain. The time traces of the wave forces and drift forces can then be obtained which will allow the analysis of the simulation in time domain.
2003	Lee & Newman	Computation of wave effects using the panel method	This text is a thorough review of the panel method (e.g. BIM). The general formulation of the method including the calculation of the equations of motion and the drift forces is presented. Two different numerical methods are described along with computation examples: low-order and high-order methods. The latter provides more accuracy and efficiency. The PFFT (Precorrected Fast Fourier Transform) method is discussed as well. Finally, the calculation of the second-order drift forces and the time domain impulse-response functions are presented, they are computationally more complicated but important when dealing with the second-order problems and the nonlinearity of the system.
2005	Hong *et al.*	Numerical and experimental study on hydrodynamic interaction of side-by-side moored multiple vessels	A higher-order boundary element method combined with generalized mode approach is used for the analysis of a moored multiple-vessel system. Both the numerical results of motions and drift forces show good agreement with experimental results in regular and irregular seas. An accuracy of total wave drift force can be assured even if strong interactions may occur due to Helmholtz resonance. The strength of the Helmholtz resonance caused interaction is less significant in head sea than in beam sea.

Table 3. A brief summary of selected technical articles using the Finite Element Method to solve ship hydrodynamic problems

Year	Author	Journal / Report Title	Summary
1982	Taylor & Zietsman	Hydrodynamic loading on multi-component bodies	A combined method is used for the analysis of multi-component systems: FEM for fluid region near the body and BIM for the far field region. It is an economical numerical technique which provides an accurate prediction of the hydrodynamic interaction between structures. The formulation of the method is reviewed including the choice of element mesh, symmetry, and equation solution. This method was applied to different multi-body configurations including two horizontal cylinders, floating box & cylinder, and semi-submersible catamaran. The comparison between the results obtained by the present method and those obtained by using other methods gives a good agreement.
1985	Huang & Hudspeth & Leonard	FEM solution of 3D wave interference problems	FEM is used to investigate the wave diffraction/radiation and body responses of multiple 3D bodies. A radiation boundary damper (both cylindrical and plane) approach is used where the boundary condition is local in both space and time. This text extended some of the same authors' previous works for the 2D wave diffraction/radiation problem (1983) by considering the 3D end effects. Both permeable and impermeable boundaries are treated and a fictitious bottom boundary is considered. The numerical results are compared to experimental results for the following cases: 3D catamaran, and multi-body loading/unloading facilities. It is found that the numerical solutions are more accurate by using the cylindrical dampers.
1991	Chen & Mahrenholtz & Zhu	Gravity waves and their interaction with floating twin bodies	A finite element method derived from the Galerkin approximation is used for the analysis of the dynamic responses of a twin body system. This approximation helps to solve the velocity potential thus find the hydrodynamic coefficients. The accuracy and applicability of the method has been checked on a single half circular cylinder before applied to a twin body system. The calculations are performed for 20 different frequencies. It is observed that the added mass coefficients and the wave damping coefficients behave differently with respect to frequencies. The effects of the water depth, the distance between two bodies and the body shapes are discussed.
2001	Sannasiraj & Sundaravad-ivelu & Sundar	Diffraction-radiation of multiple floating structures in directional waves	A numerical method based on the 2D finite element technique is used to study the dynamics of multiple floating structures under a directional wave. For this, the 2D FEM is first applied to evaluate hydrodynamic coefficients and forces in an oblique waves. The motions responses are then extrapolated under directional waves by using linear filter. The responses in sway, heave and roll modes are studied for different directional homogeneous waves. The force ratio and the response ratio are evaluated numerically for frequency-independent and frequency-dependent spreading cases in a directional sea state.

1.2. Statistical interpretation and the thesis objective

Many of the studies reported in the open literature address theoretical formulations and numerical simulations. Further, their focus is generally limited to the prediction of the hydrodynamic forces and the motions of two-body systems subject to regular sea conditions. The results for irregular seas or random seas, when considered, are typically obtained by linearly superposing regular wave components according to the linear theory. In the majority of cases, no ship nor offshore structures is identical to another, model testing plays an important role in understanding and refining numerical simulation tools used for design.

This thesis research focuses upon the interpretation of a data from an experimental study of a fully coupled mini-TLP and tender barge system. This side-by-side moored system was conceived for deployment in West Africa and was first studied by Teigen and Niedzwecki (1999). As shown in Fig. 1, the two platforms are connected by breast lines and separated by a fender system. The model tests included a variety of wind, random wave and current conditions, for both head and beam sea configurations. A 1:62 scaled model mini-TLP and barge were utilized in the test program.

A statistical approach is adopted in this research study to characterize and interpret the data obtained during the model testing. This choice is based on the fact that the external excitation forces are random and are so expected the corresponding structure responses. By using statistical tools, both linear and nonlinear systems can be analyzed directly and the behavior of the system can be interpreted in term of different statistical parameters such as extreme values and correlation coefficients which are important for design process. The primary objective of this study is to investigate the relative motions of the mini-TLP/barge system as it responds to the combined external forces; and to assess the influence consequently the efficiency of the connection system.

This study consists of three main parts. The first part presents the theoretical background and including definitions and formulae used in this study. These tools include the basic characterization parameters such as variance and extreme values, statistical distributions (Normal and Weibull distributions), time domain parameters such

as correlation coefficients, as well as frequency domain spectral analysis parameters. The methods used for single and two-body systems are reviewed separately. The second part provides a detailed description of the mini-TLP/barge system and the corresponding model tests. Characteristics of the prototype and the model are given in this section, together with the description of the design environment. Finally, in the third part, the data obtained during the model tests are analyzed and discussed. In particular, time series concerning the motion of each platform which includes the surge, sway and heave of the mini-TLP and the barge, the wave elevation between the platforms and the fender force are discussed. Both the uncoupled and coupled data are analyzed in order to better understand the influence of the connection system.

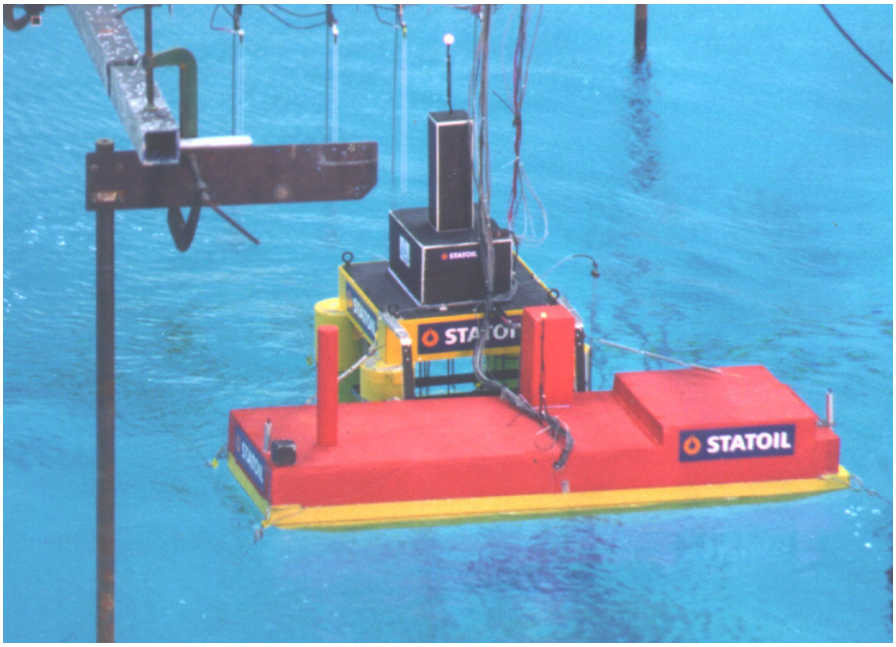

Fig. 1. Photograph of the mini-TLP and tender barge from the model test study, showing the coupled configuration

2. STATISTICAL METHODS

Offshore structures are subject to the combined environmental forces resulting from wind, waves and currents, which are often characterized as random processes. Consequently the resulting marine structure motions are also at times complex and hard to understand and interpret for design. Statistical analysis methods can be at great help in trying to characterize those random time series, especially in determining some parameters important for the design of the offshore systems.

The statistical methods used in the current study are described in this section. The formulae and the notations of the presented statistical notions follow that used in "Timeslab: A time series analysis laboratory" (Newton, 1996). In addition, formulae from MATLAB are included since some analysis utilized some of the built-in MATLAB functions. Another source which influenced the used notations is the online version of the "Handbook of Statistical Methods" provided by the National Institute of Standards and Technology (NIST).

2.1. Basic characterization parameters

A data set can be characterized by using some basic statistical parameters such as its mean, variance, minimum, maximum, skewness and kurtosis. These parameters provide a quick and general idea of how the measured time series behave and will be utilized in this study.

Before giving any definitions, a clear distinction should be made between a population and a data set. A population is the ensemble of realizations for a random variable; whereas a data set is one possible realization of an infinite number of possibilities. In pure statistics, the equations for a same parameter are slightly different depending on whether it is for a population or for a data set. This study is based on measured data, thus only the sampling properties will be considered.

For a random variable $x(t)$ sampled at n constant intervals. The sample mean $\overline{x}$, also called the first moment, is defined as:

$$\bar{x} = \frac{1}{n}\sum_{t=1}^{n} x(t) \tag{1}$$

It is important to know the value of the mean because zero-mean data are frequently used in statistical analysis. This simplifies the calculations of the parameters such as variance, skewness and kurtosis by subtracting by advance the mean value.

Extreme values such as data minima and data maxima are also important parameters for they set the limit values for the design process. These values are simply obtained by observing the data.

The variance (or the second moment) of a data is a non-negative number which is used to measure how spread out the distribution of a data is about its average value, and it is defined as followed:

$$Var(x) = \frac{1}{n}\sum_{t=1}^{n} (x(t) - \bar{x})^2 \tag{2}$$

Note that as stated earlier, if zero-mean data are used then it is no use to subtract the mean value in the above formula.

The larger the variance, the further the corresponding observation is from the data mean. The square root of the variance $\sigma = \sqrt{Var(x)}$ is called the standard deviation which indicates how tightly the values in a normally distributed data are gathered around the sample mean. It is estimated that 68% of the data values are within the range $[\bar{x} - \sigma, \bar{x} + \sigma]$ and 95% within the range $[\bar{x} - 2\sigma, \bar{x} + 2\sigma]$.

The distributions functions are studied in detail in the next section, but two related parameters are presented here as basic statistical parameters. One of them is the skewness s which is defined in MATLAB as:

$$s = \frac{E(x - \bar{x})^3}{\sigma^3} \tag{3}$$

with $E(.)$ the expected value of the quantity in parenthesis. This parameter measures the asymmetry of a distribution relative to its sample mean. If it is negative, the data are spread out more to the left of the mean than to the right (i.e. longer tail at the left). If it

is positive, the data are spread out more to the right (i.e. longer tail at the right). It is equal to 0 for a Normal distribution since it is a perfectly centered distribution.

The second parameter used to characterize a distribution is the kurtosis k :

$$k = \frac{E(x-\overline{x})^4}{\sigma^4} \tag{4}$$

It measures the size of the tail of a distribution. A big value of kurtosis corresponds to a distribution with large tails, as a consequence the distribution curve is relatively flattened; a small value of kurtosis corresponds to a distribution with small tails which has a narrow and steep figure. The kurtosis is equal to 3 for a Normal distribution.

2.2. Distribution functions

Probability distributions are a fundamental statistical concept. Typically, a probability distribution is defined in terms of the probability density function (PDF) and the cumulative density function (CDF). Since the experimental measurements are usually considered as continuous random variables, the formulae used in this section are those for continuous distributions.

Mathematically, the continuous probability density function $p(x)$ is a non-negative function which expresses the probability that a variable X of a random process take a value between two points a and b, usually the interval [a, b] tend to be very small:

$$\int_a^b p(x)dx = \Pr\left[a \le X \le b\right] \tag{5}$$

Note that in the case of a continuous variable, the height of the probability function can be greater than 1 if the interval [a, b] is small enough, because the probability (which must be less than or equal to 1) is defined by the area under the curve for each interval. However, the sum of all the $p(x)$ for a data set should be equal to 1.

The cumulative distribution function $P(x)$ is the probability that X is less than or equal to a specific value x, it is actually the integral of the probability density function over the whole interval at the left hand side of x :

$$P(x) = \int_{-\infty}^{x} p(x')dx' = \Pr\left[X \le x\right] \tag{6}$$

As it is a cumulative value, the CDF increases from 0 at the left extreme of the horizontal axis to 1 at the right extreme. This is consistent with the property of the PDF which states that the total probability is 1.

Every time series has its own distribution pattern. However, some standard distribution functions are well studied, thus it is often useful to determine a reasonable distributional model for the data in order to simplify the analysis of the time series. These standard distributions include Normal distribution, Weibull distribution, Rayleigh distribution, and so on.

The most common distribution function is the Normal or Gaussian distribution. For a data set $x(t)$, the density functions of the normal distribution are:

$$\text{PDF:} \quad p(x) = \frac{1}{\sigma\sqrt{2\pi}} e^{-(x-\bar{x})^2/(2\sigma^2)} \tag{7}$$

$$\text{CDF:} \quad P(x) = \frac{1}{\sigma\sqrt{2\pi}} \int_{-\infty}^{x} e^{-(x'-\bar{x}')^2/(2\sigma^2)} dx' \tag{8}$$

Sometimes the sample mean $\bar{x}$ is called the location parameter and the standard deviation σ the scale parameter. The standard Normal distribution refers to the case where $\bar{x} = 0$ and $\sigma = 1$.

As shown in Fig. 2, the Normal distribution has a symmetrical bell shaped probability distribution curve about its mean. Note that the area under the probability distribution function should be equal to 1 which is the sum of all the probabilities. Since the cumulative distribution function is the integral of the probability distribution function, it should increase from 0 to 1 as stated earlier. In the practice, for a data which is expected to be normally distributed, some deviations can be observed. They are measured by the skewness and the kurtosis which have been presented in the previous section. A perfect Normal distribution has a skewness equal to 0 and 3 for kurtosis.

The Normal distribution is a very good model for many continuous distributions that occur in real situations. Actually, the statistical theories of sea waves are based on the assumption that the instantaneous wave elevations can be expressed by a normal distribution. Other environmental forces such as wave or current are also supposed to be

random processes with normal distributions. In a linear system, the structure motions are expected to be Gaussian when a Gaussian excitation is applied. By studying the Normal distribution of a data one can detect if the system has any nonlinear behaviors.

The most fitted model of distribution for the extreme values such as local maxima and local minima is the Weibull distribution. As mentioned before, the study of the extreme values is important for the design process. A Weibull distribution can be characterized by three parameters: shape parameter α which measures the sharpness of the peak, scale parameter β which indicates the expansion of the tail, and location parameter γ which locates the distribution along the abscissa. In this study, only the two-parameter Weibull distribution will be used, meaning that the location parameter is considered to be 0.

The two-parameter equations of the Weibull distribution are:

$$\text{PDF:} \quad p(x) = \alpha\beta^{-\alpha} x^{\alpha-1} e^{-(x/\beta)^{\alpha}} \tag{9}$$

$$\text{CDF:} \quad P(x) = 1 - e^{-(x/\beta)^{\alpha}} \tag{10}$$

Fig. 3 presents the PDF and the CDF of a Weibull distribution with shape parameter equal to 1 and scale parameter equal to 2. Similar to the normal distribution, the area under the probability distribution curve should be equal to 1 as well as the converged value of the cumulative probability. Note that the Rayleigh distribution is a special case of the Weibull distribution with the shape parameter α equal to 2; it is a very useful distribution especially for the study of narrow-band data.

(a)

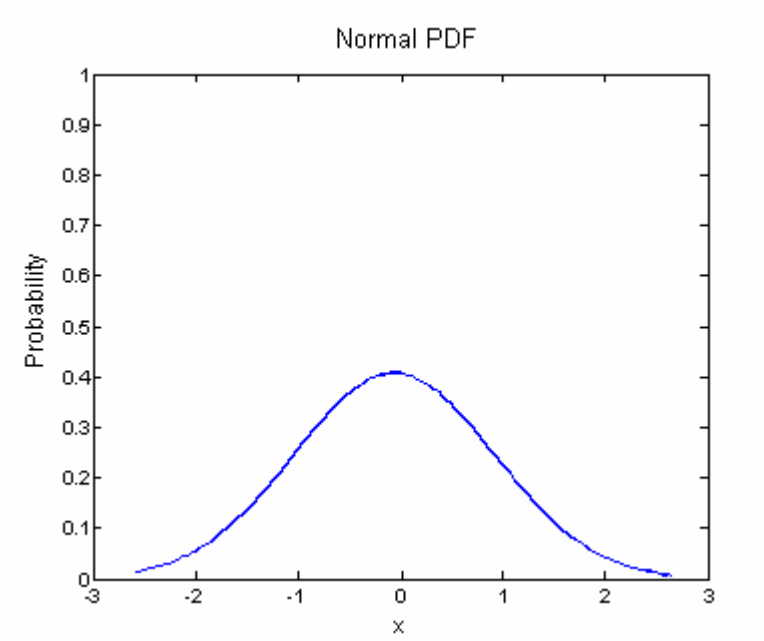

(b)

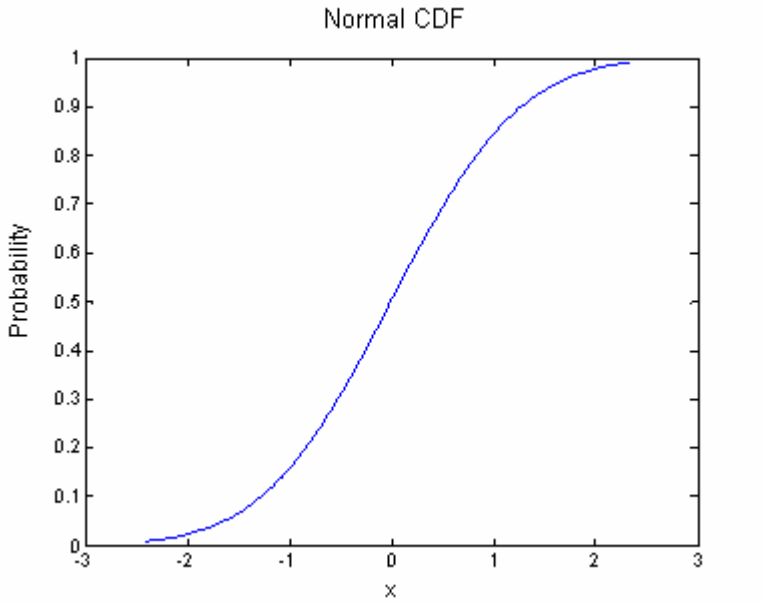

Fig. 2. a) PDF and b) CDF for a MATLAB randomly generated normal distribution data

(a)

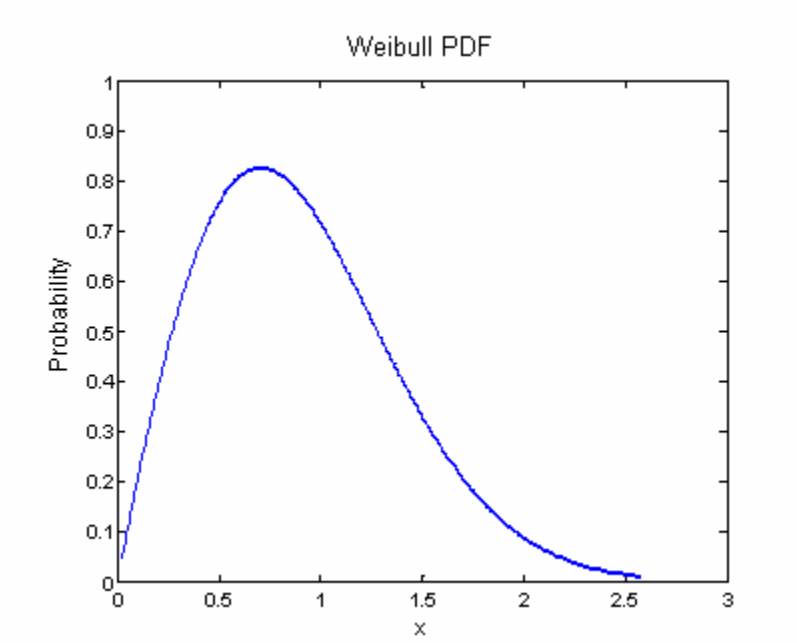

(b)

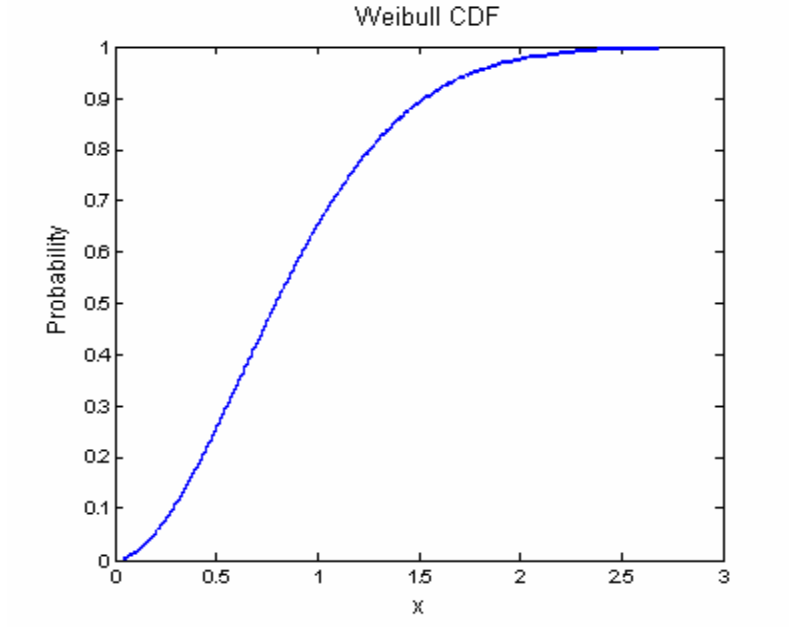

Fig. 3. a) PDF and b) CDF for a MATLAB randomly generated Weibull distribution data with $\alpha=1$ and $\beta=2$

2.3. Correlation

2.3.1. Auto-covariance and auto-correlation

A time series typically exhibits a correlation that varies over time. This means that the value of one point of the data can influence the behavior of another point of the same data separated by a time lag τ. In order to measure the relationship between $x(t)$ and $x(t-\tau)$, the auto-covariance is considered. It is formulated as followed for a data of size n:

$$\hat{R}_{xx}(\tau) = \frac{\sum_{t=1}^{n-|\tau|}(x(t)-\overline{x})(x(t+|\tau|)-\overline{x})}{n}, \qquad \tau < n \tag{11}$$

Another parameter, the sample auto-correlation coefficient $\hat{\rho}$, gives a more visual indication of the correlation between $x(t)$ and $x(t-\tau)$. It is defined as:

$$\begin{aligned}\hat{\rho}_{xx}(\tau) &= Corr(x(t), x(t+\tau)) = \frac{Cov(x(t), x(t+\tau))}{\sqrt{Var(x)Var(x)}} \\ &= \frac{\hat{R}_{xx}(\tau)}{\hat{R}_{xx}(0)} = \frac{\sum_{t=1}^{n-|\tau|}(x(t)-\overline{x})(x(t+|\tau|)-\overline{x})}{\sum_{t=1}^{n}(x(t)-\overline{x})^2}\end{aligned} \qquad , \ \tau < n \tag{12}$$

$\hat{\rho}(\tau)$ is a variable between -1 and 1. The plot of $\hat{\rho}(\tau)$ versus τ for $\tau = 1, 2, ..., M$, with $M < n$ an arbitrarily chosen maximum time lag, is called the correlogram of the data. It shows the correlation of a data set for different time lags. A large absolute value of $\hat{\rho}(\tau)$, e.g. $\hat{\rho}(\tau)$ close to 1 or -1, indicates a high correlation thus a strong linear predictability in the data. The correlogram may also indicate the possible periodicity in the data and the memory type of the time series. A large value of $\hat{\rho}(\tau)$ indicates a possible periodicity of τ time units in the data. As for the memory type, a correlogram that decays rapidly to zero as τ increases means that the series is short memory, in other words there are no apparent deterministic patterns in the data except some similitude for small time lags. Otherwise the data is long memory type which is almost a deterministic function of time; it is closely related to the past and can be perfectly extrapolated far into the future. White noise type data gives a correlogram around 0 over the whole time lag range.

2.3.2. Cross-correlation

For a two-body system, the cross-correlation coefficient is used to measure the linear correlation between the different time series records. For two random data $x(t)$ and $y(t)$ of size n, the cross-correlation coefficient $\hat{\rho}_{xy}(\tau)$ which is a normalized measure is defined as followed:

$$\hat{\rho}_{xy}(\tau) = Corr(x(t), y(t+\tau))$$
$$= \frac{\hat{R}_{xy}(\tau)}{\sqrt{\hat{R}_{xx}(0)\hat{R}_{yy}(0)}} = \frac{\sum_{t=1}^{n-|\tau|}(x(t)-\overline{x})(y(t+|\tau|)-\overline{y})}{\sqrt{\sum_{t=1}^{n}(x(t)-\overline{x})^2 \sum_{t=1}^{n}(y(t)-\overline{y})^2}} \quad , \tau < n \tag{13}$$

With $\hat{R}_{xx}$ and $\hat{R}_{yy}$ the usual auto-covariance functions defined earlier for respectively $x(t)$ and $y(t)$. And

$$\hat{R}_{xy} = \frac{\sum_{t=1}^{n-|\tau|}(x(t)-\overline{x})(y(t+|\tau|)-\overline{y})}{n} \tag{14}$$

is the covariance between the data $x(t)$ and $y(t)$.

A correlogram similar to the one of the auto-correlation coefficient can be drawn. If $\hat{\rho}_{xy}(\tau)$ is near to 0 for all values of τ, then the data $x(t)$ and $y(t)$ are not correlated. A large cross-correlation of time lag τ indicates that the two studied data may have similar behavior with a phase shift of time τ. It helps to show the effect of one structure in relation to the other one in a two-body system, and suggests that it is possible to predict the behavior of data record from the other with a time lag τ.

2.4. Spectrum analysis

2.4.1. Auto-spectral density function

The auto-covariance and auto-correlation functions are used as statistical analysis tools in time domain. Alternatively, the auto-spectral density function can be employed in frequency domain to study the time series.

This quantity is related to the auto-covariance function defined earlier. They form a Fourier transform pair.

Auto-spectral density function: $\hat{S}_{xx}(\omega) = \sum_{\tau=-n}^{n} \hat{R}_{xx}(\tau) e^{-i\omega\tau}$ (15)

Auto-covariance function: $\hat{R}_{xx}(\tau) = \int_{-\pi}^{\pi} \frac{\hat{S}_{xx}(\omega) e^{i\omega\tau}}{2\pi} d\omega$ (16)

The auto-spectral density function is 2π -periodic, real and even which means that $\hat{S}_{xx}(\omega) = \hat{S}_{xx}(-\omega)$.

The auto-covariance and the auto-spectral density function contain the same information about the process, but with two different representations. The spectral density helps to determine the percentage of energy that falls within a given frequency band. If time series has a strong sinusoidal signal for some frequency, then there will be a peak in the spectrum plot at that frequency. It can be used to find the natural period of a time series. In linear theory, a multi-peak spectrum generally indicates coupling effect.

2.4.2. Cross-spectral density

Similar to the auto-covariance and spectral density function, the cross-variance and cross-spectral density also form a Fourier pair.

Cross-spectral density: $\hat{S}_{xy}(\omega) = \sum_{\tau=-n}^{n} \hat{R}_{xy}(\tau) e^{-i\omega\tau}$ (17)

Cross-covariance: $\hat{R}_{xy}(\tau) = \int_{-\pi}^{\pi} \frac{\hat{S}_{xy}(\omega) e^{i\omega\tau}}{2\pi} d\omega$ (18)

Contrary to the auto-spectral density, the cross-spectral density is not symmetric and it is a complex value, with its real part called the cospectral density which is the in-phase signal and the imaginary part the quadrature spectral density which is the out-of-phase signal:

$$\hat{S}_{xy}(\omega) = c_{xy}(\omega) - iq_{xy}(\omega) \quad (19)$$

Where $c_{xy}(\omega) = \mathrm{Re}(\hat{S}_{xy}(\omega))$ and $q_{xy}(\omega) = -\mathrm{Im}(\hat{S}_{xy}(\omega))$

The cross-spectral density can be also written in terms of its amplitude and phase:

$$\hat{S}_{xy}(\omega) = A_{xy}(\omega) e^{i\phi_{xy}(\omega)} \quad (20)$$

Where $A_{xy}(\omega) = \left|\hat{S}_{xy}(\omega)\right|$ and $\phi_{xy}(\omega) = \arctan\dfrac{-q_{xy}(\omega)}{c_{xy}(\omega)}$

$A_{xy}(\omega)$ contains the information about the amplitude of the spectrum and is called the amplitude spectrum. $\phi_{xy}(\omega)$ is called the phase spectrum, it is a number between $-\pi$ and π, containing the information about the phase between the two data. $\phi_{xy}(\omega) = 0$ means that the two data are in phase for the frequency ω whereas they are completely out of phase if this value is equal to π or $-\pi$.

2.4.3. Coherence function

The cross-spectral density has various standardized forms, among which the complex coherency function:

$$w_{xy}(\omega) = \frac{\hat{S}_{xy}(\omega)}{\sqrt{\hat{S}_{xx}(\omega)\hat{S}_{yy}(\omega)}} \tag{21}$$

We define the coherency function as:

$$W_{xy}(\omega) = \left|w_{xy}(\omega)\right| = \frac{A_{xy}(\omega)}{\sqrt{\hat{S}_{xx}(\omega)\hat{S}_{yy}(\omega)}} \tag{22}$$

This value is between 0 and 1 if the auto-spectral densities of both data are positive. The squared value of the coherency function $W_{xy}^{\,2}(\omega)$ is a correlation coefficient; it has the function as the correlation coefficient $\hat{\rho}_{xy}(\tau)$ except that instead of measuring the correlation between the two data in time domain it is used for frequency domain to measure the correlation between the cyclical components of two time series. Actually, the peak of the normalized cross-correlation after being filtered to contain a single frequency is identical to the magnitude of the coherence function at the frequency of the filter.

The time series are uncorrelated at the frequency ω if $W_{xy}^{\,2}$ converges to 0 at that frequency and correlated if this value converges to 1. When two time series of data are highly correlated it suggests that the behavior of one time series can be predicted from

the value of the other once an appropriate transfer function is determined. Note that it is useless to examine the coherency function for all the frequencies, because only those where high density is involved are interesting for the investigation.

Precaution should be made while the analysis of the coherency functions: they should not be interpreted by themselves. This because when two time series with small spectrum amplitudes can still have a high coherency value for the divisor will be very small, even when they do not have strong cyclical components.

3. MINI-TLP/BARGE EXPERIMENT

3.1. Presentation of the system

In 1999, Teigen and Niedzwecki first reported on a series of model tests involving a side-by-side two-body system typical for deepwater operations for the offshore industry. Their experiments involved two platforms, a mini-TLP and a tender barge, in uncoupled and coupled configurations. A mini-TLP is a relatively small unmanned deepwater platform which has limited deck space and storage capacity. Thus the use of a tending vessel, a barge in this case, is required for drilling and maintenance operations. This new unmanned platform concept was based upon proven technology and was viewed as a cost effective solution for offshore operations in benign environments like those found off the coast of West Africa. The target location for this system was the Gulf of Guinea, off the coast of Nigeria, where the water depth is typically 1000 meters. Besides wave, wind and current is also a problem at that area. The basic information on the environment at that location is listed in the Table 4.

Both offshore platforms have their own mooring system. The mini-TLP was designed to have eight tethers, two in each corner; and the tender barge had its spread catenary mooring system including eight mooring lines assisted by submerged buoys. In addition to that, the two platforms were connected together by a ‘soft’ connection consisting of a fender system and a pair of breast lines. The fender system was designed to avoid direct contact of the two hulls, and the breast lines to restrain the separation distance which is to be maintained at 10 meters. Note that the mini-TLP has 12 risers which furnished an important horizontal restoring force. The main characteristics of the prototype mini-TLP and of the prototype tender barge are given in Tables 5 and 6.

Table 4. Environmental parameters specified for the West Africa site

Parameter	Value
Significant wave height - H_s	4.0 m
Peak period - T_p	16.0 s
Peakedness factor – γ	2.0
Current velocity - V_c	0.95 m/s
Wind velocity at z_0 = 10 m	25.65 m/s
Wind velocity at platform reference height z_r = 17.2 m	27.41 m/s

Table 5. Some characteristics of the prototype mini-TLP design

Parameter	Prototype
Draught	28.50 m
Column diameter	8.75 m
Column separation distance	28.50 m
Pontoon height	6.25 m
Pontoon width	6.25 m
Deck clearance	10.00 m
Center of gravity (X)	0 m
Center of gravity (Y)	0 m
Center of gravity (Z)	27.04 m
Total weight of TLP	6620 t
Displacement	10320 t
Number of tethers	8
Number of risers (excluding catenaries)	12
Total tendon and riser pretension	3700 t
Natural period surge / sway	133 s
Natural period yaw	121 s

Table 6. Some characteristics of the prototype tender barge design

Parameter	Prototype
Draught	3.70 m
Length at water line	89.40 m
Overall length	91.50 m
Width	27.5 m
Length of flat part of barge bottom	72.9 m
Center of gravity (X)	0 m
Center of gravity (Y)	0 m
Center of gravity (Z)	6.8 m
Weight of barge	8533 t
Number of mooring lines	8
Total vertical pretension from mooring lines	101 t
Natural period surge	107 s
Natural period sway	125 s
Natural period yaw	48 s

3.2. Experimental set-up

The models were constructed at a scale of 1:62 and the tests were conducted at the Offshore Technology Research Center (OTRC). The data used in this study are from these model basin tests. The characteristics of the models as built are presented in Tables 7 and 8. A series of data sets were selected from this comprehensive model test program and these selected measurements are analyzed in this research investigation.

In order to simplify the model test set up, the number of tether is reduced from 8 to 4 to have one tether in each corner. However, all the 12 risers (including gas, water injection, and production risers) were represented in the model to replicate the prototype so that the responses could be as realistic as possible. The target water depth was 1000 meters, which at model scale is about 16.1 meters. The pit in the model basin at OTRC has a depth of 16.8 meters, which allowed the mini-TLP tether and risers to be modeled at full length. In the case of the barge, the spread mooring was reduced to one mooring line at each corner with departing angles of 45 degrees from the longitudinal axis instead of 2 (30 and 60 degrees angles) mooring lines in each corner as specified in the prototype case. These mooring lines were modeled by using two in-line linear springs which allow matching the global offset curve. Note that the deck of the mini-TLP has been raised compared to the original design for testing in a wider range of sea states, namely mild Gulf of Mexico design sea conditions.

Table 7. Characteristics of the 1:62 model scale mini-TLP as built

Parameter	1:62 scale
Draught	0.460 m
Column diameter	0.141 m
Column separation distance	0.460 m
Pontoon height	0.101 m
Pontoon width	0.101 m
Deck clearance	0.161 m
Center of gravity (X)	0 m
Center of gravity (Y)	0 m
Center of gravity (Z)	0.436 m
Total weight of TLP	27.09 kg
Displacement	43.22 kg
Number of tethers	4
Number of risers (excluding catenaries)	12
Total tendon and riser pretension	15.14 kg

Table 8. Characteristics of the 1:62 model scale tender barge as built

Parameter	1:62 scale
Draught	0.060 m
Length at water line	1.442 m
Overall length	1.476 m
Width	0.444 m
Length of flat part of barge bottom	1.176 m
Center of gravity (X)	0 m
Center of gravity (Y)	0 m
Center of gravity (Z)	0.110 m
Weight of barge	34.90 kg
Number of mooring lines	4
Total vertical pretension from mooring lines	0.415 kg

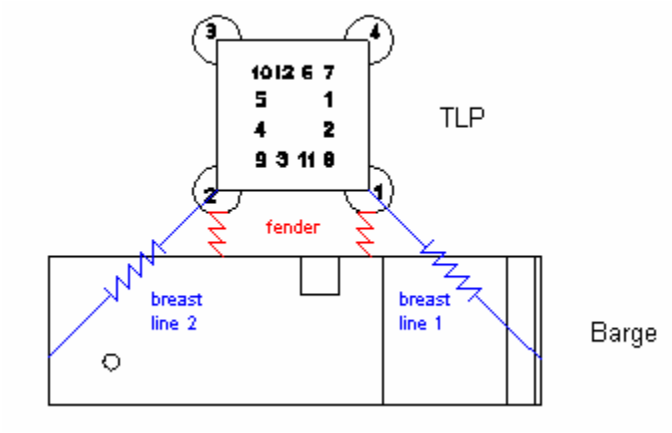

Fig. 4. The mini-TLP and the barge with their fender/breast lines connection system

The connection system was designed to restrain the relative surge, sway and yaw motions. The stiffness between the two bodies in these three directions was carefully matched in the modeling of the system; this resulted in the fender/breast line model combination illustrated in Fig. 4. The breast lines and the fender were modeled utilizing a spring system that matches the design specifications. For example, the breast line spring had a constant of 33.97 N/m compared to 33.80 N/m for target system and the compression spring for the fender system had a constant of 25.92 N/m as compared to 25.92 N/m for target system. The compressive loads were measured using a shear cell that was attached to a bar where the compression springs were mounted. To reduce the friction between the barge and the fender system during the testing, Teflon pads were used at the contact points.

3.3. Test configurations and instrumentation

Because of the mild wave conditions at the target location, the contribution of the wind and the current has as much influence on the motion of the offshore platforms as the waves. Different combinations of environmental conditions were simulated including wind, wave, current alone and the case which combined all these three environmental forces. At this particular offshore site, most of the bad weather comes from one particular direction which simplified the test matrix. Each model test for a specified environment and platform configuration lasted 3 hours at prototype scale. Often a sequence of 3 realizations was produced providing the equivalent of 9-hour storm.

Two environmental force heading conditions have been tested: 0 degree heading (head sea condition) and -90 degree heading (beam sea condition). The corresponding schematics of the mini-TLP/barge configurations are shown in Fig. 5 with the risers and columns numbered. Note that during the model tests, the center of the mini-TLP is aligned with the center of the OTRC model basin's deep pit. When the system is rotated, the barge is rotated around the mini-TLP.

For each of these configurations, both uncoupled and coupled cases are considered. The uncoupled system refers to the case where there is no tie-off between the two bodies and the coupled case when the barge is restrained (by breast lines and fender system) to the mini-TLP. Fig. 6 and Fig. 7 show respectively the uncoupled system in calm water and the coupled system in head sea condition during the tests under the various environmental forces.

The combination of different simulated environmental conditions with the two configurations, uncoupled or coupled, gave different sets of time series data. Parameters that are essential for the understanding of the system were measured. The measurements relevant to this investigation were measured during the model tests and are as follows:

- The motion in 3 DOF (translations) for the mini-TLP, and in 6 DOF for the barge, measured by camera tracking system;
- The compression force between the two bodies, measured by the shear cell fixed on the bar where the compression springs are mounted. This is also called the fender force.

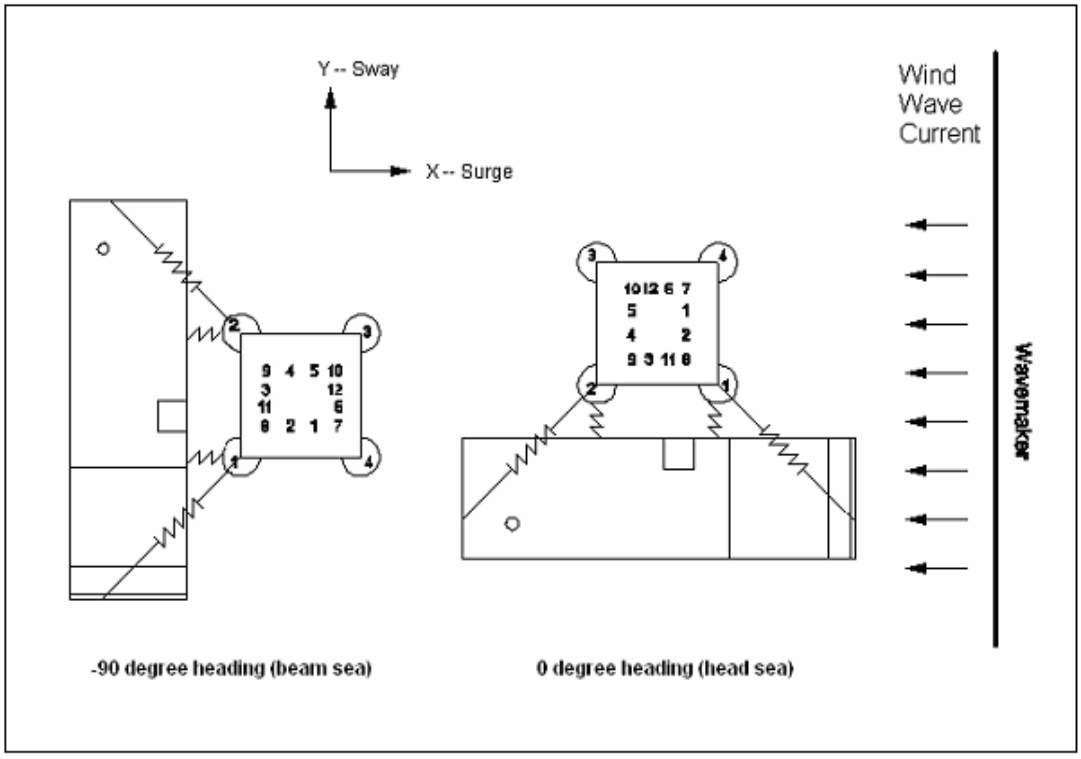

Fig. 5. Mini-TLP/barge system in 0° and -90° heading conditions

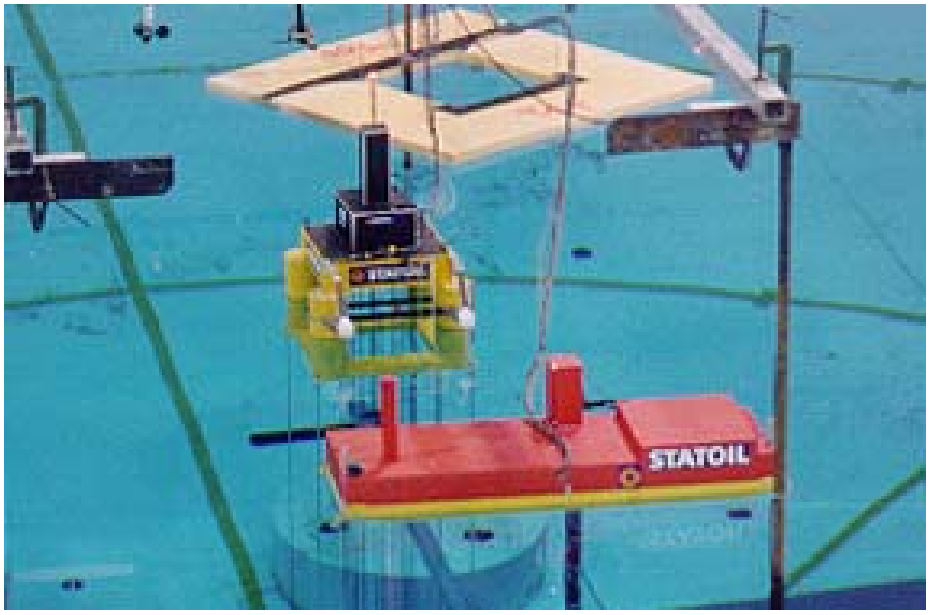

Fig. 6. Uncoupled system in calm water

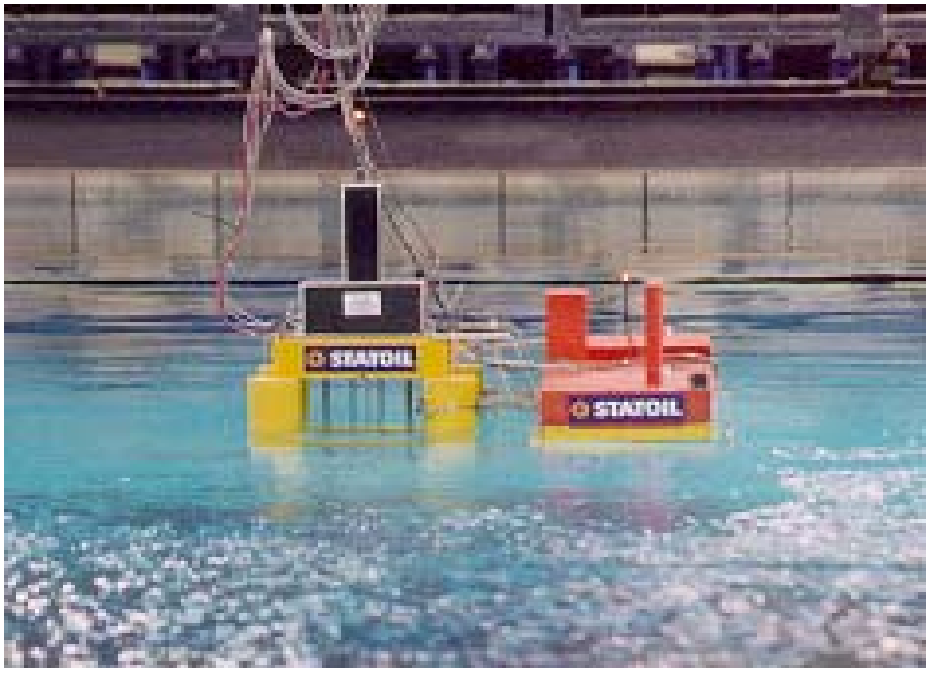

Fig. 7. The coupled system in head sea condition during the experimental tests

4. ANALYSIS OF THE MINI-TLP / BARGE SYSTEM

This section aims at visualizing and interpreting the experimental data from the mini-TLP / barge model testing, this in order to characterize the two-body system and its connection system. These data were analyzed by using the statistical tools presented earlier in this study, under the MATLAB programming environment.

Both 0° and -90° heading configurations are studied in detail in order to compare the behavior of the system in head and beam seas. The unidirectional environmental excitations include wind, wave and current. Among all the combinations of environmental forces, only the wind-wave-current combined case will be studied, for it is the most interesting feature for the design purpose and also because the data for other cases are not complete for both 0° and -90° heading configurations. Thus 4 series of tests are studied here: uncoupled and coupled cases in both 0° and -90° configurations for combined environment condition. The corresponding time series have each 42105 sample points which correspond to 3 hours of simulation.

Main emphasis is put on the analysis of the motion of the two vessels: how their behavior changes in the uncoupled and coupled cases. The motions studied in the present research are the following:

- TLP surge, sway, heave
- Barge surge, sway, heave, roll, pitch, yaw

The wave elevation between the mini-TLP and the barge as well as the fender force is also studied as a consequence of the coupled motion of the two-body system. Thereby, a total of 11 output data are analyzed in this study. Note that all the original data are obtained from the model test, but they have already been scaled so that they can be analyzed directly for a prototype size system.

It is impossible to show all the results in the main text since a relatively considerable amount of plots and tables have been generated during the study of this project. The complete results can be found in the appendices at the end of the dissertation.

4.1. Characterization of the environmental forces

Before analyzing the time series of the structure motions, it is necessary to first examine the input data which are in this case the external environmental forces such as wind, wave and current. Although it is impossible to recreate exactly the same environmental condition at the point of measurement on the mini-TLP/barge system for different tests, similar environments are simulated for the 0° and -90° configurations so that the comparison becomes possible. Fig. 8 shows the truncated time series of these external forces with their means in the coupled 0° case.

It is to be reminded that all the three excitations are in the same direction X (direction of the surge). There exists a secondary current in the Y direction (direction of the sway); it is not a deliberately generated excitation but merely a result of the circular effect due to the reflection of the main current at the limitation of the basin.

The basic statistical characterization parameters and the natural periods of the environmental forces in the uncoupled and coupled cases for both 0° and -90° configurations measured on a particular point of the mini-TLP/barge system are listed in Tables 9 and 10.

The similarity between the basic statistical values of the environmental excitations of each coupling/heading condition confirms the fact that the environments simulated for the tests are comparable. They also have same visible periodicity for every combination of environmental forces and the auto-spectrum amplitudes are similar as well (Appendix C). These time series are all normally distributed as shown by the kurtosis and the skewness parameters in Table 11. However it can be seen that these simulated external conditions have different profiles. The current and especially the wave have quite big standard variations which indicate big fluctuations: respectively 39% and 1000% of the mean. At the other hand, the wind seems to have a relatively small standard variation which is less than 10% of the mean. In practice it is reasonable to consider it as a steady force although we can observe a certain periodicity.

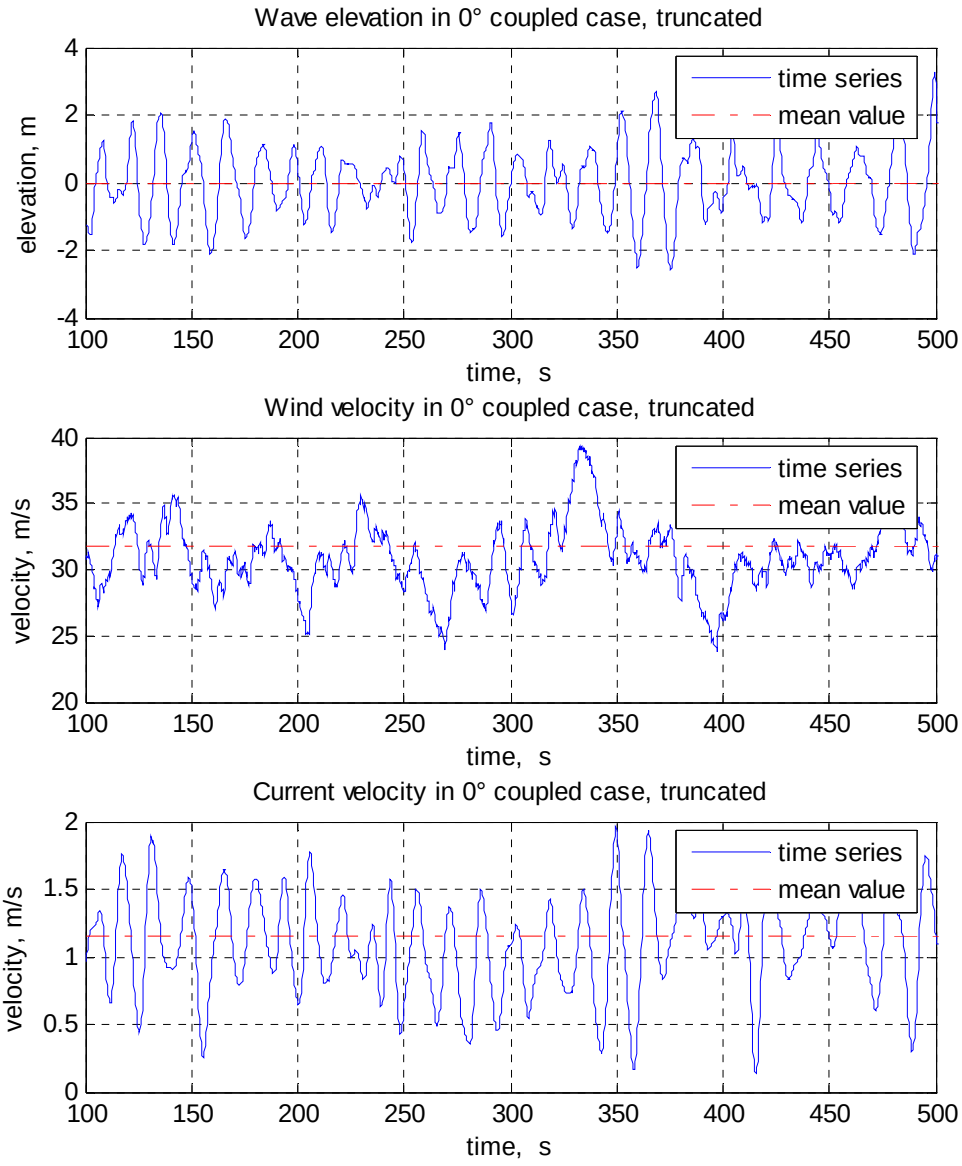

Fig. 8. Time series of the environmental excitations in the 0° coupled case

Table 9. Basic statistical characteristics of the environmental excitations

(a) 0º - head sea

	Uncoupled				Coupled			
	max	Min	μ	σ	max	min	μ	σ
Current (m/s)	2.46	-0.54	0.98	0.38	2.42	-0.23	1.15	0.35
Wind (m/s)	40.67	22.37	31.63	2.71	42.40	21.42	31.73	2.92
Wave (m)	4.11	-3.70	0.09	0.93	4.19	-3.84	-0.03	0.92

(b) -90º - beam sea

	Uncoupled				Coupled			
	max	Min	μ	σ	max	min	μ	σ
Current (m/s)	2.21	-0.11	1.06	0.35	2.39	-0.14	1.15	0.35
Wind (m/s)	42.21	22.99	31.53	2.61	41.62	22.12	31.77	2.27
Wave (m)	4.31	-3.84	0.04	0.95	4.17	-3.47	0.02	0.92

Table 10. Natural periods of the environmental excitations

	0º Uncoupled	0º Coupled	-90º Uncoupled	-90º Coupled
Current (s)	16	16	16	16
Wind (s)	65	65	65	65
Wave (s)	16	16	16	16

Table 11. Kurtosis and skewness of the environmental excitations

	0º Uncoupled		0º Coupled		-90º Uncoupled		-90º Coupled	
	k	s	k	s	k	s	k	s
Current	2.93	-0.05	2.86	-0.09	2.81	-0.15	3.02	-0.16
Wind	2.92	-0.06	2.83	-0.12	2.84	-0.04	2.87	-0.007
Wave	3.21	0.06	3.28	0.12	3.22	0.09	3.46	-0.13

4.2. Basic characterization of the time series

The output data are studied in the present and the following sections by using different statistical tools. Those data include the motions of each of the platforms in both uncoupled and coupled cases as well as the fender force and the fender wave (the wave elevation between the two platforms when connected) in the coupled case.

In this section, the basic statistic characteristics such as the sample mean and the standard deviation of the time series are computed. Fig. 9 gives an example of these time series, the truncated mini-TLP surge, barge heave and fender force data are plotted. The calculated parameters for all the test configurations are listed in Table 12. Note that the data for both the mini-TLP and barge sway motions are of poor quality probably due to some measuring problems during the testing, thus the results should be interpreted with precaution when these data are involved.

The knowledge of the mean value of each time series can reveal to be very useful. For example, in the considered 0° head sea configuration, the surges of both mini-TLP and barge, which should be 0 in the calm water condition in the chosen reference, are negative. It means that the system is displaced mostly toward the direction following the external forces. It can have important implications, for instance the barge catenary mooring lines at the weather side would have more load than those located at the lee side of the system, and thus precaution should be taken in the design of the mooring lines considering this phenomenon. The maximum and minimum values are to be used for the design process as limit values. Note that the presented measured extreme values are obtained from a single realization, thereby they are only indicative.

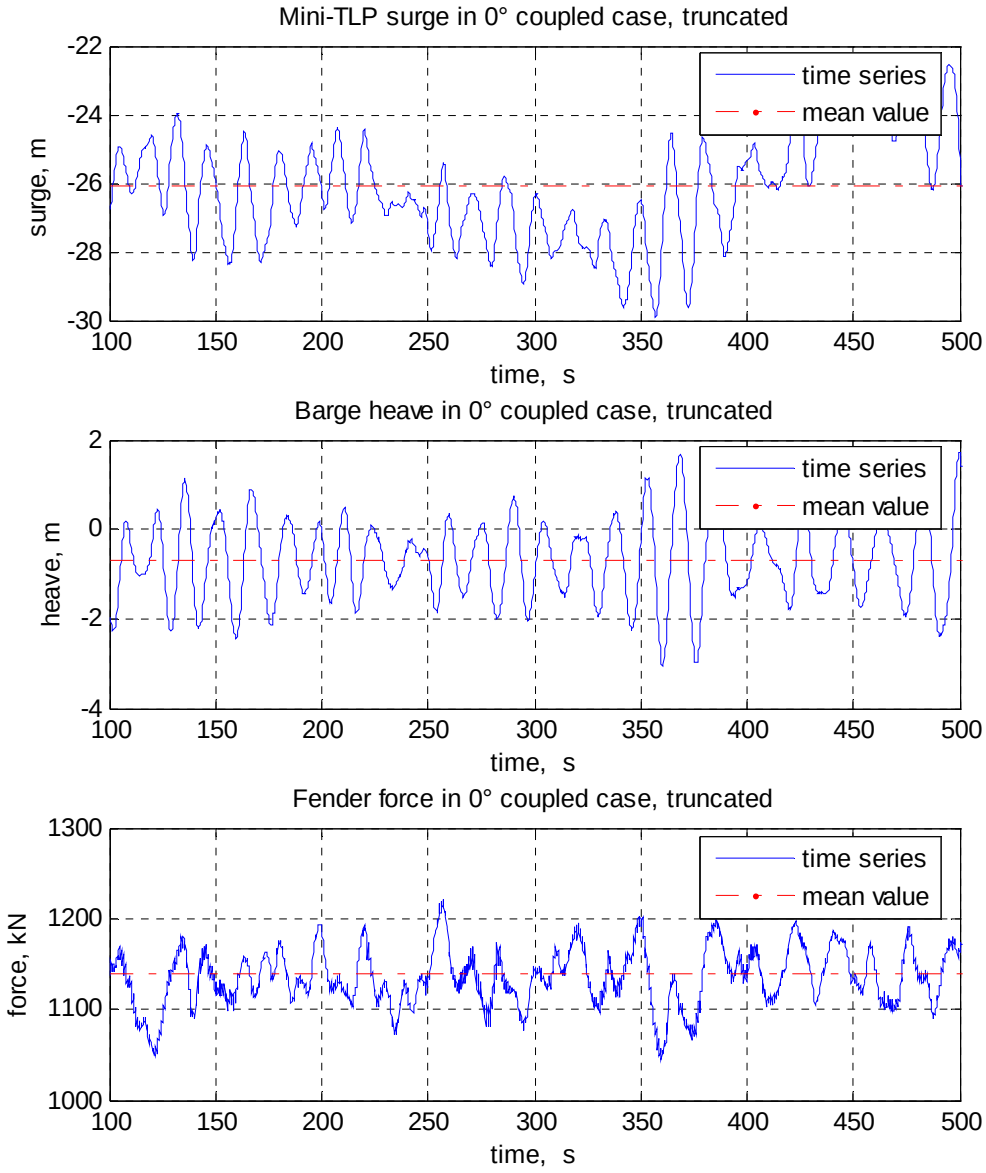

Fig. 9. Time series of mini-TLP surge, barge heave and fender force in the 0° coupled case

Table 12. Basic statistical characteristics of the vessel motions and fender force

(a) 0º - heading sea

	Uncoupled				Coupled			
	max	min	μ	σ	max	min	μ	σ
TLP surge (m)	-25.36	-43.60	-34.01	2.67	-17.72	-33.84	-26.06	2.18
TLP sway (m)	3.03	-3.19	0.07	1.15	4.31	-1.95	1.43	0.92
TLP heave (m)	-0.17	-0.87	-0.51	0.09	-0.01	-0.48	-0.24	0.07
Barge surge (m)	-4.11	-18.86	-10.89	2.19	-13.86	-28.00	-21.46	1.87
Barge sway (m)	-37.65	-45.58	-41.85	1.40	-37.44	-44.26	-40.62	0.94
Barge heave (m)	3.05	-3.91	-0.39	0.82	2.50	-4.11	-0.70	0.80
Barge roll (deg)	2.02	-0.82	0.62	0.40	1.46	-1.44	-0.002	0.33
Barge pitch (deg)	4.53	-4.04	0.06	1.12	4.20	-4.25	0.09	1.07
Barge yaw (deg)	1.51	-1.81	-0.21	0.48	5.89	0.51	3.35	0.74
Fender wave (m)	NA	NA	NA	NA	3.82	-3.81	-0.002	0.89
Fender force (kN)	NA	NA	NA	NA	1275.6	986.4	1139.9	37.9

(b) -90º - beam sea

	Uncoupled				Coupled			
	max	min	μ	σ	max	min	μ	σ
TLP surge (m)	-20.70	-36.79	-29.07	2.25	-21.55	-35.73	-28.62	2.03
TLP sway (m)	7.90	-1.24	2.98	1.59	5.62	-1.87	1.93	1.15
TLP heave (m)	-0.14	-0.72	-0.41	0.07	-0.18	-0.66	-0.42	0.06
Barge surge (m)	-61.23	-81.14	-68.67	2.66	-62.70	-77.34	-69.84	2.10
Barge sway (m)	3.06	-2.22	0.57	0.85	5.94	-0.99	2.25	0.93
Barge heave (m)	1.76	-6.16	-2.20	0.97	2.00	-6.34	-2.24	0.96
Barge roll (deg)	6.53	-6.02	0.30	1.57	5.54	-6.20	-0.29	1.34
Barge pitch (deg)	0.86	-0.78	-0.05	0.19	0.76	-0.96	-0.05	0.22
Barge yaw (deg)	-86.69	-94.83	-90.61	1.03	-88.00	-92.32	-90.11	0.64
Fender wave (m)	NA	NA	NA	NA	4.68	-2.28	1.47	0.77
Fender force (kN)	NA	NA	NA	NA	2719.7	486.9	1292.9	195.5

It is not surprising to notice from the standard deviation that the barge has a more important heave motion than the mini-TLP; because the barge has a much larger water plane surface thus is more sensible to the vertical motion of the wave; whereas the mini-TLP is more sensible to the current with its deep draft. This difference in heave was not reduced in the coupled case. It seems that the connection system does not have a significant impact on the heave motion, as well as on the roll and pitch motion. However the surge, sway and yaw seem to be noticeably affected by the existence of the tie-off: the surge and sway motions are reduced for both structures in the two heading conditions and the yaw is increased by the connection in the head sea and reduced under the beam sea condition. Note that the barge sway has unexpectedly a bigger fluctuation in the -90° coupled case compared to the uncoupled case, since the mini-TLP sway is smaller in the coupled case the most probable explanation is the existence of some measuring errors in the data. In general, the differences observed between the uncoupled and coupled cases suggest that the connection system does have the characteristics anticipated by the design, which means the restriction on the surge, sway and yaw motions without significant effect on heave, roll and pitch. In the coupled case the offset of the COG shows that the separation distance between the two platforms is kept around 10 meters as designed, which shows once again that the breast lines and the fender system work correctly.

In general, the different sea heading conditions do not seem to have a big impact on the behavior of the two structures. A certain shielding effect can be observed in the beam sea condition but it is not significant since the mini-TLP is relatively small: it can not provide a substantial shield to the barge against the environmental forces. The major impact due to this shielding effect is that the fender wave, which is the wave elevation between the two structures when they are connected, is higher in the beam sea condition. This because the wave is ‘trapped’ between the two structures since the barge is on the lee side and has a big water plane area whereas the mini-TLP is at the weather side and has a much smaller water plane area. Another consequence of the -90° heading is that

the fender force is much more important than in the 0° heading condition for the external forces are in the same direction as the compression force of the fender system.

The previous analysis based on the basic parameters only gives a general idea of the system behavior. More detailed results will be found in the following sections of the study by using other statistical methods.

4.3. Distribution functions

The response time series were investigated to see if they follow any well known distribution functions. As stated earlier, the environmental forces are normally distributed. If the responses follow also Normal distribution, then one can assume that the system is linear. A MATLAB built-in function 'normplot' was used to verify whether the data is normally distributed: when the output of this function is a linear plot then the data are Gaussian. Next, both the probability density function (pdf) and the cumulative density function (cdf) of each time series were compared to the ones of the ideal normal distribution for the same mean and standard deviation.

The probability plot, the pdf and the cdf of the TLP surge in 0° coupled case were plotted in the Fig. 10 as an example. It can be observed that the data fit quite well Normal distribution, with slight deviations that were measured by the kurtosis and skewness parameters listed in Table 13. Like the mini-TLP surge data, most of the response time series from the model tests follow the Normal distribution. However, in all the cases the probability plot lost more or less its linearity at the both extremities of the data; it means that those values follow some other distribution function. Especially for the fender force in the -90° coupled configuration where the large value of kurtosis indicates a big tail toward the right of the distribution plot, which explains why a large non-linearity is observed for big values (Fig. 11).

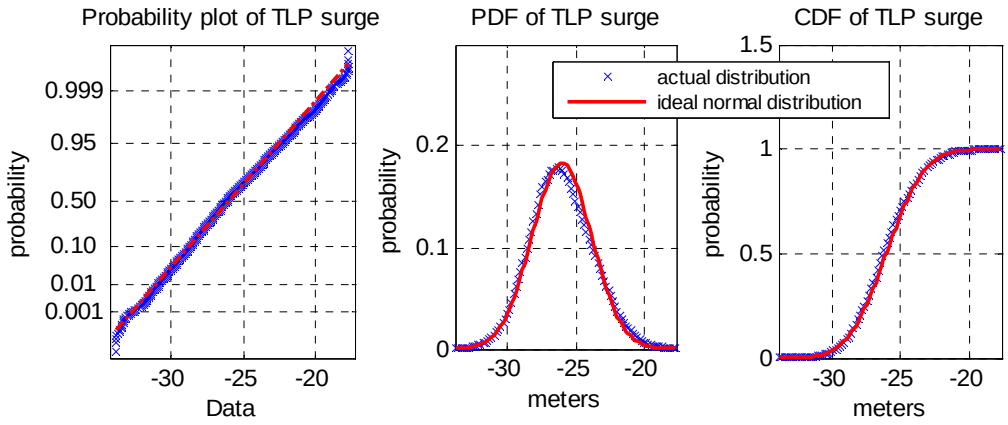

Fig. 10. Distribution plots of the mini-TLP surge in coupled 0° case

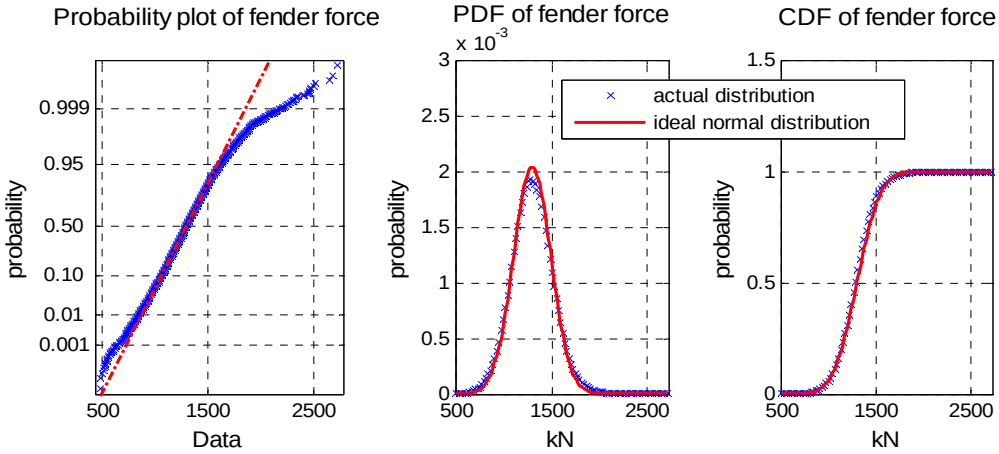

Fig. 11. Distribution plots of the fender force in coupled -90° case

Table 13. Kurtosis and skewness of the time series

	0º Uncoupled		0º Coupled		-90º Uncoupled		-90º Coupled	
	k	s	k	s	k	s	k	s
TLP surge	2.78	-0.08	3.07	0.21	2.86	0.13	2.77	0.04
TLP sway	2.61	0.05	3.23	-0.16	2.89	0.20	2.85	0.04
TLP heave	2.86	-0.24	2.71	-0.12	2.84	-0.11	2.96	-0.06
Barge surge	2.81	-0.04	3.42	0.10	3.49	-0.38	2.81	-0.01
Barge sway	2.60	0.09	3.21	-0.14	2.97	-0.21	3.24	0.02
Barge heave	3.23	0.02	3.21	-0.01	3.23	0.01	3.26	0.02
Barge roll	2.93	-0.02	3.20	-0.04	3.11	-0.09	3.31	-0.07
Barge pitch	3.03	0.02	3.03	0.02	3.17	-0.01	3.28	-0.10
Barge yaw	2.96	0.12	3.19	-0.04	3.39	0.13	2.95	0.15
Fender wave	NA	NA	3.58	-0.10	NA	NA	3.20	-0.32
Fender force	NA	NA	3.12	-0.005	NA	NA	4.40	0.31

A model other than Normal distribution needs to be found for the data of extreme values. Extreme values considered in this study are local and the definition of the local maxima and minima was given by Ochi (1998). Fig .12 is an illustration of the definition. A program written under MATLAB by Liagre and Niedzwecki (2000) was used to find the local extreme values as defined by Ochi. For a Gaussian random process, the positive maxima and the negative minima follow the same probability law, whereas the positive minima and the negative maxima have the same kind of distribution. Only the positive maxima and the negative minima were investigated in this study because they are interesting for the design process and risk analysis.

Weibull distribution, as a commonly used distribution for extreme values, was chosen to compare with the actual distributions of the local extremes. Again, both pdf and cdf of the data were plotted, and the MATLAB function 'wblplot' was used to assess graphically if the data follow a Weibull distribution. It reveals that most of them fit quite well to the Weibull distribution as shown by the example of the mini-TLP surge in Fig. 13. The positive maxima and the negative minima (the absolute value is used here) have similar distribution. In both cases, the logarithmic probability plots show a visible linearity for the values higher than 1 (approximately) in absolute value and an increasing nonlinearity below this value.

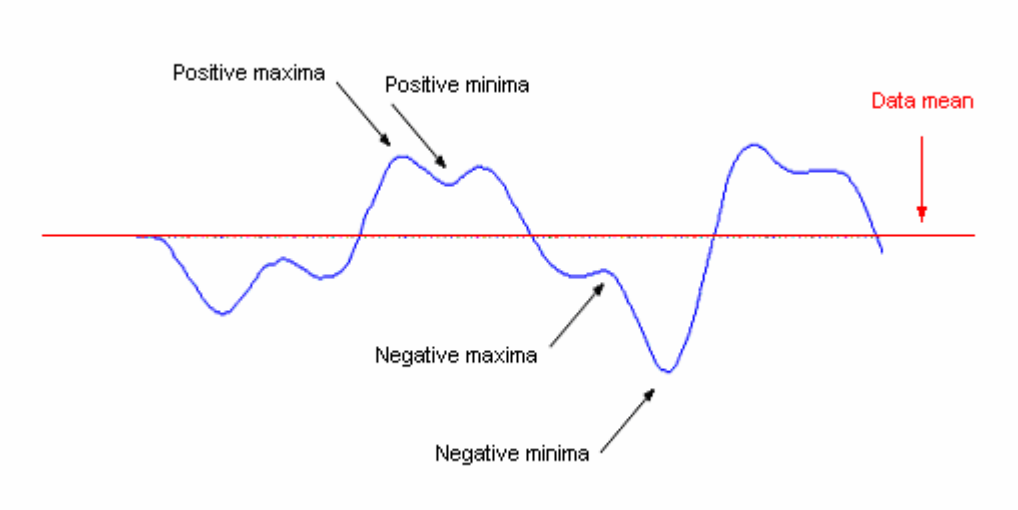

Fig. 12. Definition of local extreme values

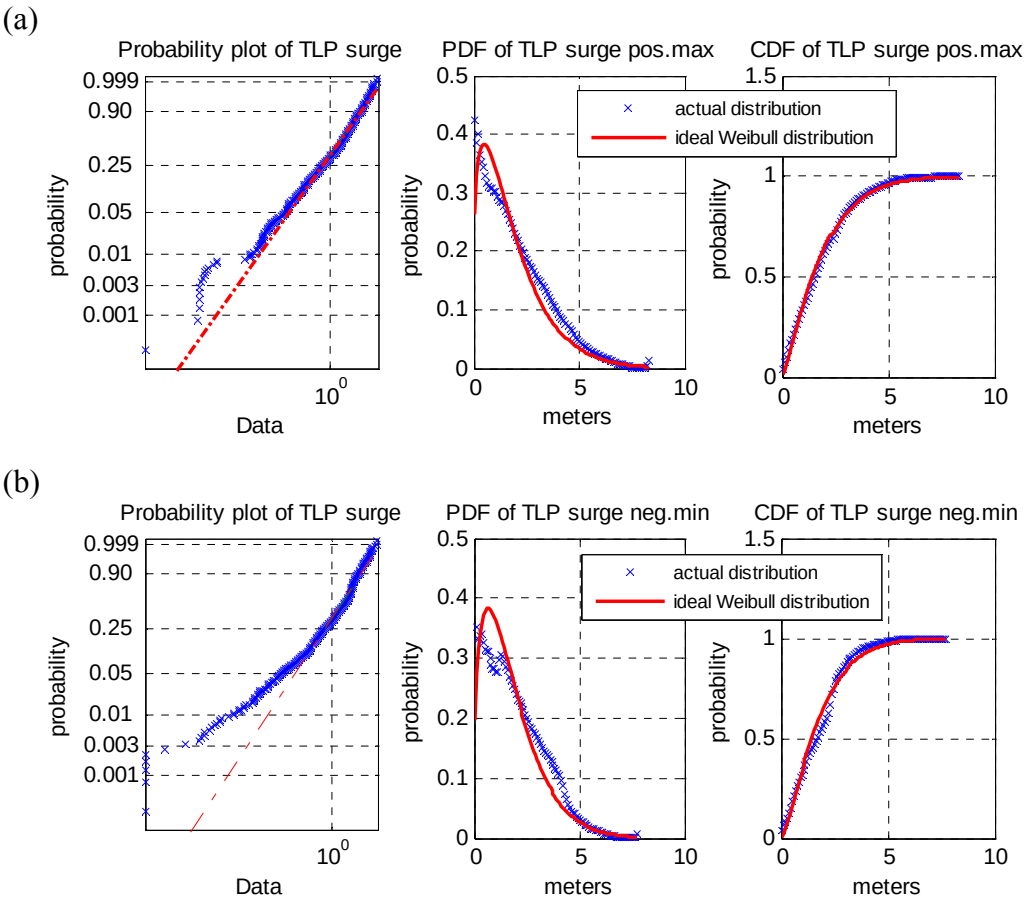

Fig. 13. Distribution plots of the TLP surge (a) local maxima, (b) local minima, in the 0° couple case

Table 14. Shape and scale parameters for Weibull distribution in the 0° coupled case

	Shape parameters		Scale parameters	
	p_max	n_min	p_max	n_min
TLP surge	1.22	1.32	1.96	1.92
TLP sway	1.65	1.15	0.90	0.73
TLP heave	1.73	1.39	0.07	0.06
Barge surge	1.30	1.27	1.78	1.56
Barge sway	1.27	1.21	0.82	0.81
Barge heave	1.37	1.25	0.76	0.74
Barge roll	1.72	1.72	0.44	0.44
Barge pitch	1.77	1.81	1.43	1.43
Barge yaw	1.24	1.27	0.63	0.65
Fender wave	1.24	0.86	0.89	0.47
Fender force	1.29	1.27	34.51	34.34

However, this nonlinearity does not discredit the fit of the data into Weibull distribution: considering that most of the absolute extreme values are bigger than 1, and the biggest value of the positive maxima relative to the data mean is around 8 and the negative minima around -8 (shown by the cdf and pdf), a good linearity for local extremes bigger than 1 is sufficient for the design purpose. Thereby, the extremes values of each time series can be reasonably considered as a Weibull distribution, with the shape and scale parameters listed in Table 14. Appendix A contains a complete list of those characterization parameters for different studied cases.

Nevertheless, one can not consequently assume that Weibull distribution is the optimal distribution model for the studied data. Fig. 14 gives an enlarged view of the pdf tail of each extreme value data. The ideal Weibull distribution tends to overestimate the large values. But the discrepancy is not substantial and as long as one can not find a better model, it is better to be conservative rather than underestimate the extreme values. The unexpected high probability of the biggest extreme values compared to the estimated one is probably due to some measure errors.

4.4. Cross-correlation

With the tie-off, the 2-body system is completely coupled. The ultimate goal of the connection is to restrain some relative movements between the mini-TLP and the barge by matching the corresponding stiffness. In order to measure the effect of the connection system over the relative movement between two motions, one may compare the cross-correlation between these motions in uncoupled and coupled cases. The larger the correlation, the more linearly coupled the motions. The complete set of correlograms can be found in Appendix B.

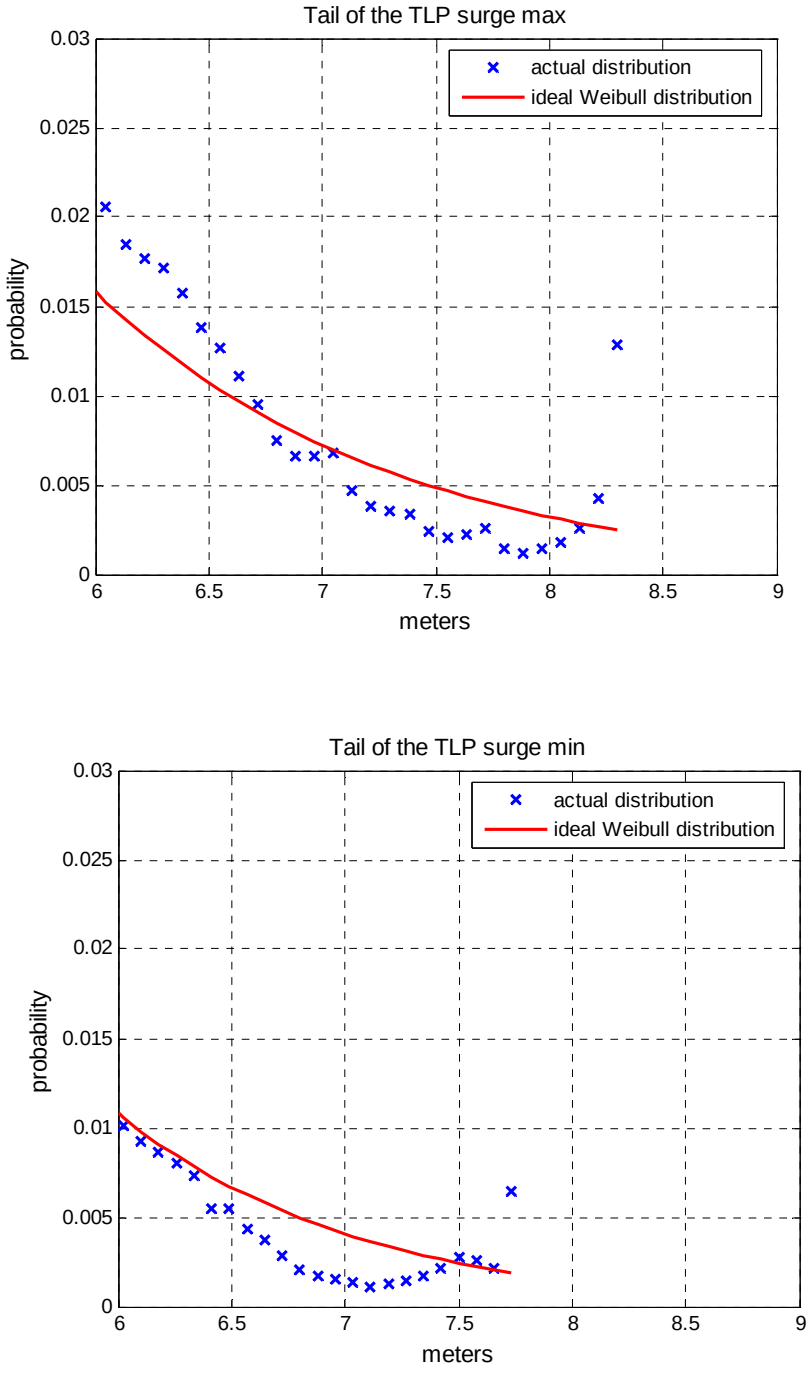

Fig. 14. Tails of the extreme value pdfs in the 0° coupled case for the TLP surge

Different features are observed. First, for some pairs the adding of the connection system causes the cross-correlation to increase significantly compared to the one obtained in the initial uncoupled case. For instance, the correlation between the mini-TLP and the barge surge is very small in the uncoupled case, but it becomes considerable for small time lags when the mooring system is put into application (Fig. 15). Under the similar environmental condition, this increase of correlation suggests that the fender system highly affected the two-body system in the surge/surge relative motion. This phenomenon can be also observed in the following pairs of motions in the 0 degree heading configuration: mini-TLP sway / barge sway, mini-TLP heave / barge surge.

A second feature is when the connection system does not change visibly the correlation, which implies that it has little influence over the considered relative motion. The TLP-heave / barge heave is in this category (Fig. 16): the initial correlation is not high and the adding of the connection system only increased slightly this value. Knowing that the connection system is not designed to restrain the heave/heave relative motion, it is not surprising to see that the coupling effect is small. However, it shows that the using of the connection system can still have a slight effect of restriction on the heave motion thought this was not the primary purpose of the system. Other pairs of motions which have the similar feature are: TLP surge / barge heave, TLP surge / barge pitch, TLP heave / barge pitch, TLP surge / barge yaw and TLP heave / barge yaw.

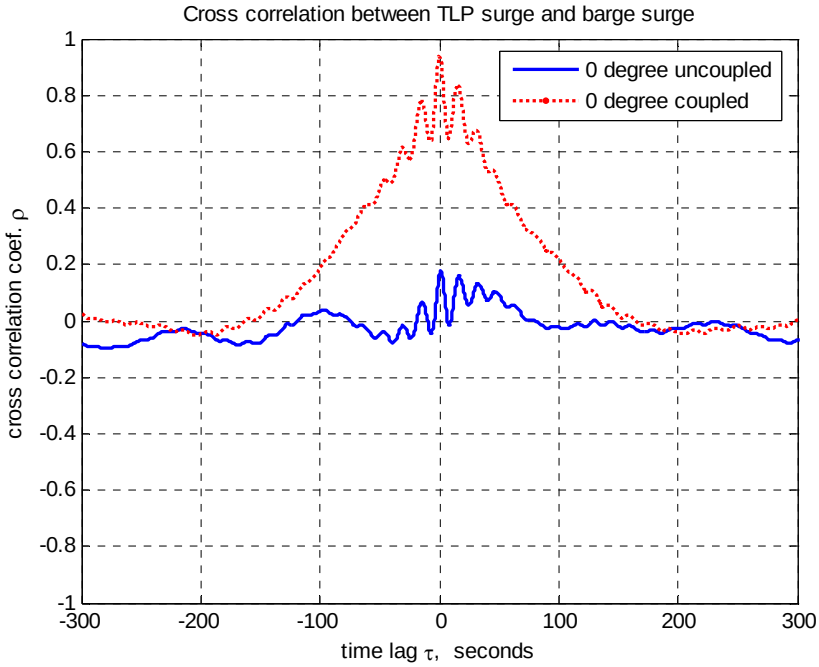

Fig. 15. Cross correlation between the mini-TLP surge and the barge surge in the 0° uncoupled and coupled cases

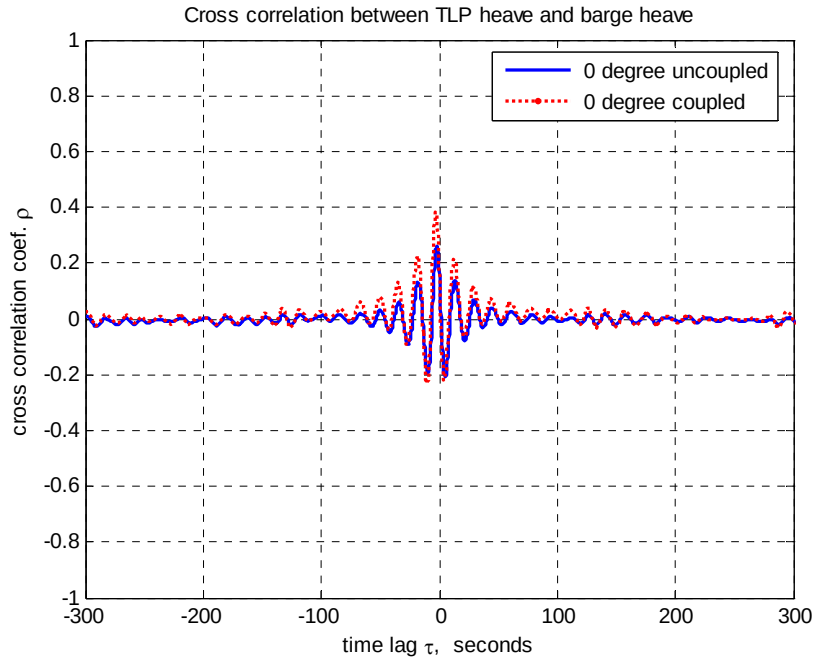

Fig. 16. Cross correlation between the mini-TLP heave and barge heave in the 0° uncoupled and coupled cases

The remaining pairs can all be considered as not correlated in either uncoupled nor coupled cases for the correlation coefficients are insignificant. This indicates that the connection system has no apparent effect on these relative motions.

In general, the cross-correlation between a pair of motion in the 0° heading case is similar to the one for the -90° heading case with some exceptions. One interesting observation is that the correlation between the fender force and the fender wave (elevation of the wave between the two vessels) in the coupled case is very different depending on the heading configuration. As shown by Fig. 17, the correlation is much higher in the -90° heading which indicate a high linear coupling effect. This is likely due to the fact that in the -90 degree case, the water is trapped between the two platforms and it applies a linear force on the system in the direction of the compression spring of the fender system.

In the -90 degree heading configuration, a high correlation can be observed in the coupled case for the following pairs: mini-TLP surge / barge surge, mini-TLP sway / barge sway, and mini-TLP heave / barge surge, the same as in the 0 degree heading sea. However, the relative motions mini-TLP surge / barge surge and mini-TLP heave / barge surge have already very high correlation when uncoupled. The example of the surge / surge case is presented in Fig. 18. This difference between the 0 degree and -90 degree headings may be explained by the fact that for the -90 degree configuration, the system is more sensible to the external influences since a larger area (barge) is exposed to the unidirectional environmental forces which are common for both vessels, thus there may be a higher linearity related to these forces even without the connection system.

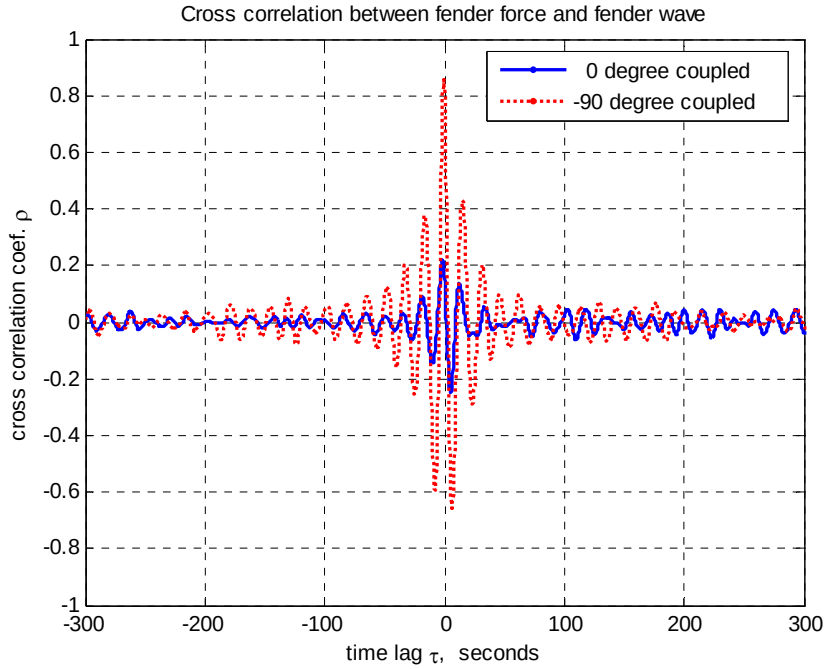

Fig. 17. Cross correlation between the fender force and fender wave in 0° and -90° heading cases

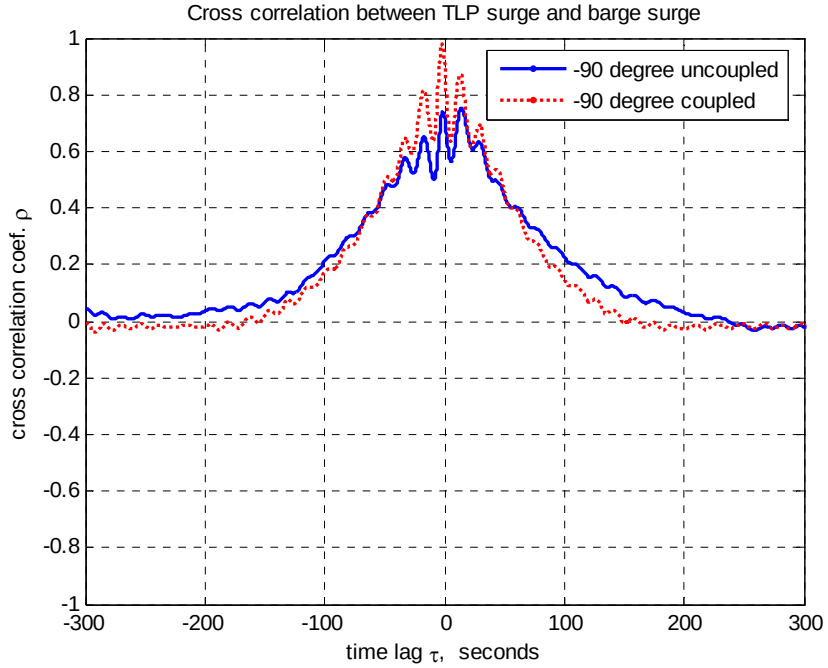

Fig. 18. Cross correlation between the mini-TLP surge and the barge surge in -90° uncoupled and coupled cases

4.5. Spectral analysis

The correlation method used earlier is a time domain based statistical tool. The study of the spectrums allows a similar analysis of the data in frequency domain. In order to study a time series in frequency domain, a Fourier transform is needed. In general, the higher the number of the Fourier transform is, the more accurate but also the more complex is the representation. The MATLAB functions used for this analysis are based on Fast Fourier transform, the number of NFFT is chosen to be 512 for it is considered that the information it provides is sufficient for this study.

4.5.1. Auto-spectral analysis

The auto-spectrums give an estimation of the natural period of each motion which is the period corresponding to the frequency where the highest peak of the spectral occurs.

The time series used here for the natural period estimation come from the decay tests. In these tests, the mini-TLP or the barge is alone in the test basin and totally free of the interaction caused by the other body. Moreover, the environmental conditions are set such that they do not present any significant periodic behavior thus will not influence the value of the natural periods of the studied motions. Fig. 19 gives the example of the mini-TLP heave; it shows how different the spectrums could be between a decay test and a test under periodic environmental forces. In the first one, the peak indicates clearly the natural period of the motion; whereas in the second case the dominating periods are those of the wave (16 seconds) and other long period horizontal motions (128 seconds) due probably to the heave set down.

Table 15. Natural periods of the mini-TLP and barge motions (NFFT = 512 unless otherwise stated)

	Prototype	1:62 scale model	
TLP surge (s)	133	128	
TLP sway (s)	133	128	
TLP heave (s)	2.6	3.0	
Barge surge (s)	107	103	NFFT = 2048
Barge sway (s)	125	128	
Barge heave (s)	NA	6.5	
Barge roll (s)	NA	7.2	
Barge pitch (s)	NA	7.6	
Barge yaw (s)	48	47	NFFT = 2048

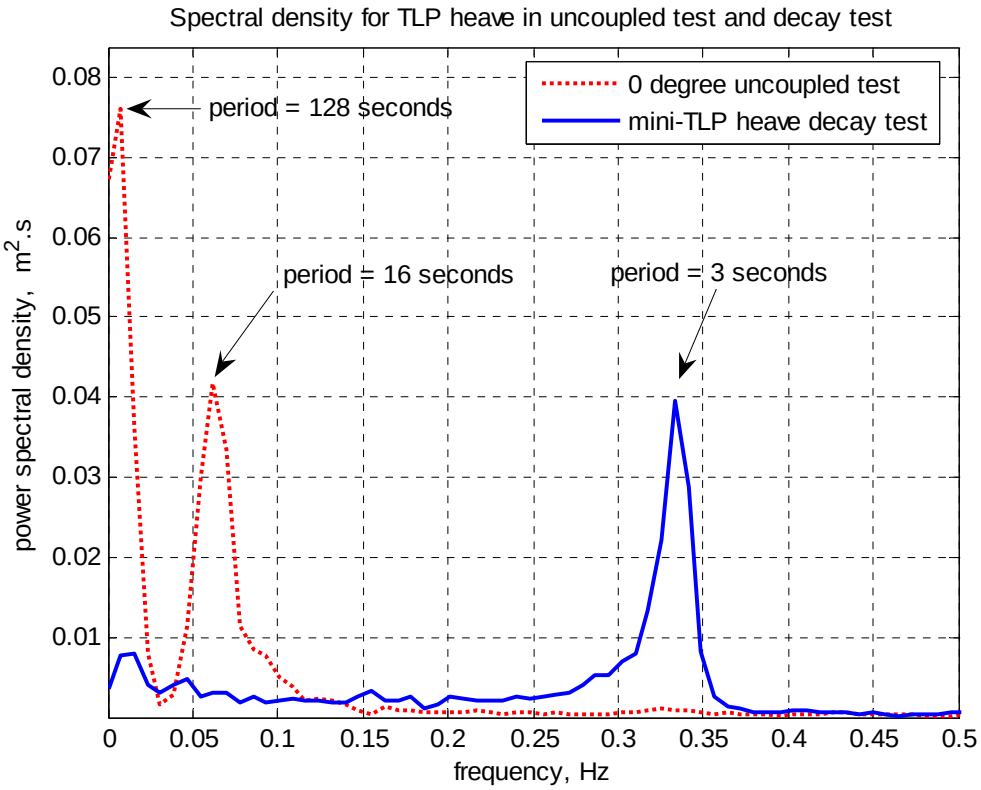

Fig. 19. The auto-spectrums of the mini-TLP heave motion in the decay test and the uncoupled 0° test

The natural periods measured in the 1:62 scaled model are listed in Table 15, along with the corresponding values of the prototype. Note that for the barge surge and yaw, the values are more accurate if a higher NFFT (2048) was used. However, NFFT = 512 is kept for the following spectral analysis for two reasons: first, the sensitivity analysis shows that NFFT = 512 and NFFT = 2048 give very close results for all the other time series and that the plots using lower NFFT show much clearer peaks for the study; the second reason is that although slight inaccuracy exists for the barge surge and yaw motions, the results obtained by using NFFT = 512 is sufficient for the qualitative study of the system aimed by the current research.

Besides the calculation of the natural period, the auto-spectrums also allow studying the behavior of the time series. Note that the following spectrums are those of the data measured under the combined environmental condition, thereby unlike in the decay test the spectrums show the influence of these external forces. The spectrums of the uncoupled and coupled cases are compared to assess the effect of the connection system. It is to be reminded that while the data of all the six DOF are available for the barge, only those of the three translation motions are available for the study of the mini-TLP.

The spectrums of the mini-TLP motions in the uncoupled and coupled cases are similar, in both 0° and 90° heading configurations. By similar, it means that these spectrums have the same shape with the same main peaks, and little difference is observed in the amplitudes of the curves. Fig. 20 gives the example of the mini-TLP surge in the 0° head sea. It is a low frequency motion with a period of 128 seconds but somehow strongly influenced by the wave frequency motions at the wave period which is 16 seconds. It is obvious that the spectrums in the uncoupled and coupled cases are similar. It implies that the connection system does not have a visible influence on the surge motion of the mini-TLP. This can be explained by the fact that the mini-TLP is relatively stiff due to the mooring effect of its tendons and risers, thus the connection system does not affect significantly its motions, not only the surge motion but also the sway and heave motions.

In the case of the barge however, the spectrums of some of its motions are visibly affected after the adding of the connection system, for instance the barge surge motion in the 0° degree heading as shown in Fig. 21. Although the frequencies of the main peaks remain the same, the amplitude of the low frequency peak is reduced significantly. Actually, the barge is moored with a spread mooring system which gives not much stiffness to the structure compared to the mooring system of the mini-TLP. When coupled to this latter one, a large portion of the load on the barge is taken by the mini-TLP via the connection system. As the result of the coupling, the surge and sway motions of the barge are reduced significantly and tend to become similar to the corresponding TLP motions (Fig. 22).

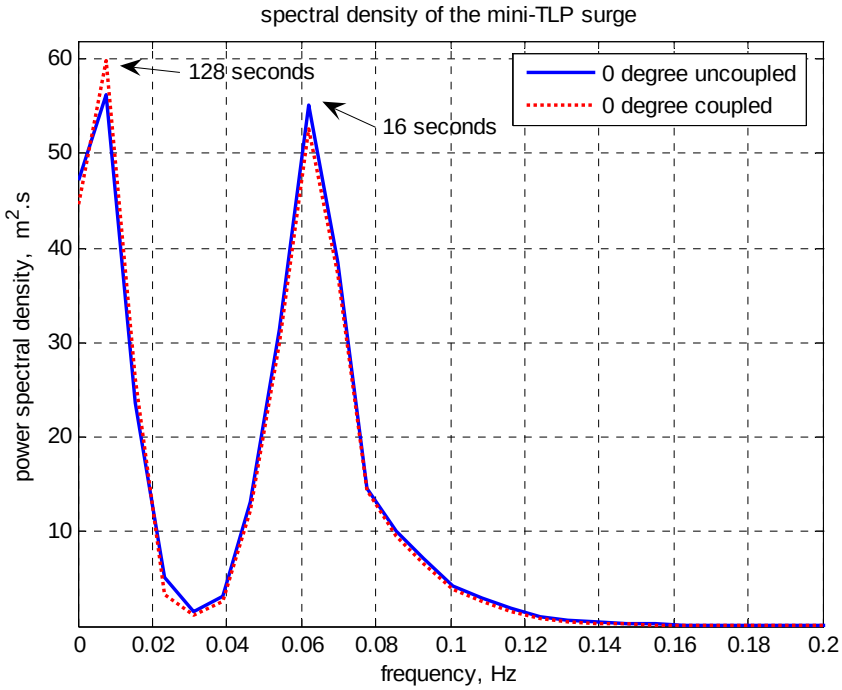

Fig. 20. Spectral density of the mini-TLP surge in the 0° uncoupled and coupled cases

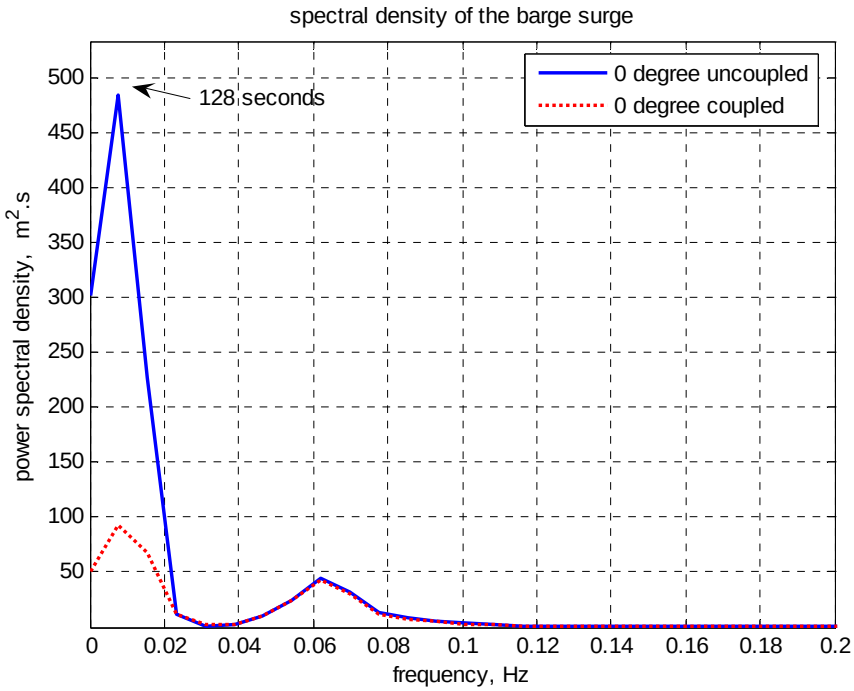

Fig. 21. Spectral density of the barge surge in the 0° uncoupled and coupled cases

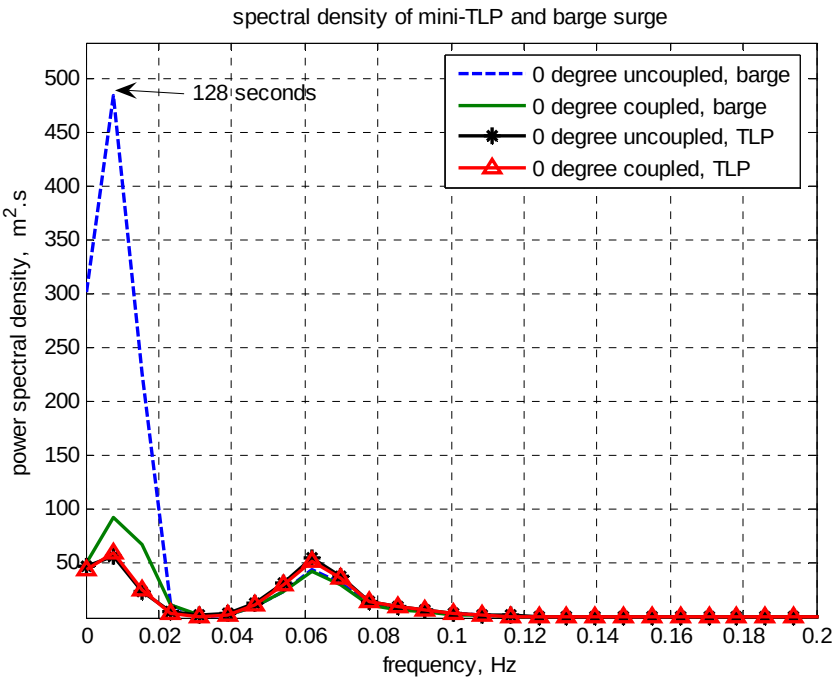

Fig. 22. Spectral density of both mini-TLP and barge surge in the 0° uncoupled and coupled cases

Note that in the case of the mini-TLP surge and heave, as well as the barge surge, a pronounced peak at the wave frequency can be observed. In all the three cases, the value of the spectrum at the wave frequency peak does not change regardless the existence of the connection. Only the low frequency peaks are reduced in the case of the barge surge when it is influenced by the adding of the breast lines and the fender system. It can be assumed that in the wave frequency those three motions are essentially influenced by the action of the wave and the connection system has little effect compared to the one of the wave.

One exception is however observed for the barge sway motion in the -90° configuration, illustrated by Fig. 23: the barge sway is not much affected by the connection system. Actually, in this configuration the barge is partly shielded behind the mini-TLP, the motions of all the 6 DOF have been more or less reduced. Moreover, the transverse incident forces have no significant influence over the sway motion in this configuration. Thereby, the coupling effect of the connection system is not very noticeable in this case.

As for the heave and pitch motions of the barge, they have similar spectrums for uncoupled and coupled cases, showing that the connection system does not have significant effect on these motions. This confirms the result of the analysis from the statistical parameters previously. Fig. 24 shows the example of the barge heave.

The roll motion of the barge is however reduced by the connection system in both 0° and -90° configurations, which is expected for the breast lines and the fender system provide a restoring force limiting the roll motion of the barge. Note that the magnitude of the roll motion in the -90° configuration, uncoupled or coupled, is much larger than in the 0° configuration for the barge is largely exposed to the environmental forces in this configuration even it is partly shielded by the mini-TLP.

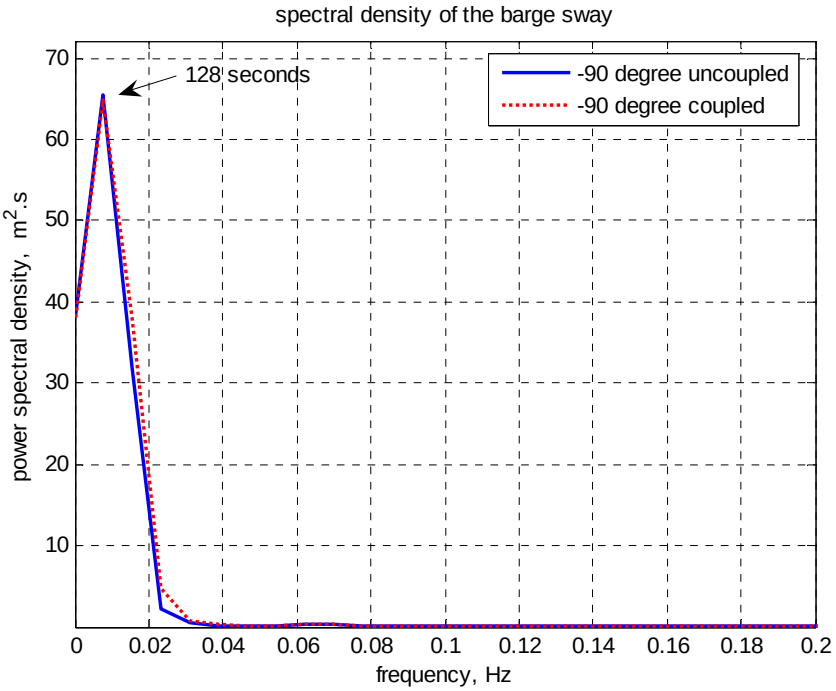

Fig. 23. Spectral density of the barge sway in the -90° uncoupled and coupled cases

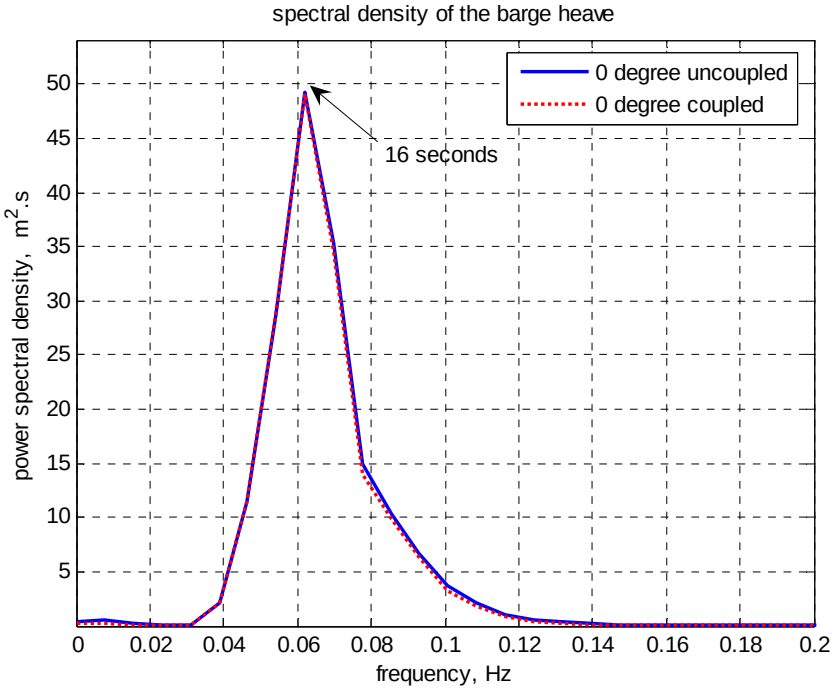

Fig. 24. Spectral density of the barge heave in the 0° uncoupled and coupled cases

The study of the yaw has objective to assess any risk of collision in the present two-body feature. The mini-TLP is very compliant to the yaw motion, thus it is important to know how the connection system will affect the yaw motion of the barge. In the 0° heading sea case, the barge yaw increases with the connection of the two platforms, and the peak value changes from 43 to 65 seconds (Fig. 25). Whereas in the -90° heading configuration, this value decreases with the adding of the connection and the same shift of peak can be observed as shown by Fig. 26. This difference can be explained by the fact that under the head sea the barge has a relatively small area exposed to the incident forces thus small yaw is generated, but when connected to the mini-TLP which is more compliant to the yaw motion the barge is given a certain additional yaw due to the coupling effect. In the beam sea condition however, the barge has a much larger area exposed to the combined environmental forces, it becomes probably more compliant to yaw than the mini-TLP does; as a consequence when the breast lines and the fender system are used the stiffer mini-TLP reduces the barge yaw. In either configuration, the experimental data of the yaw show that they are small enough to exclude the possibility of a collision between the two vessels.

The fender forces in the 0° and -90° coupled cases are compared (Fig. 27). This force is visibly more important in the beam sea condition and it has most of its energy in the wave frequency region. This because all the environmental forces are applied in the direction of the compression of the fender system.

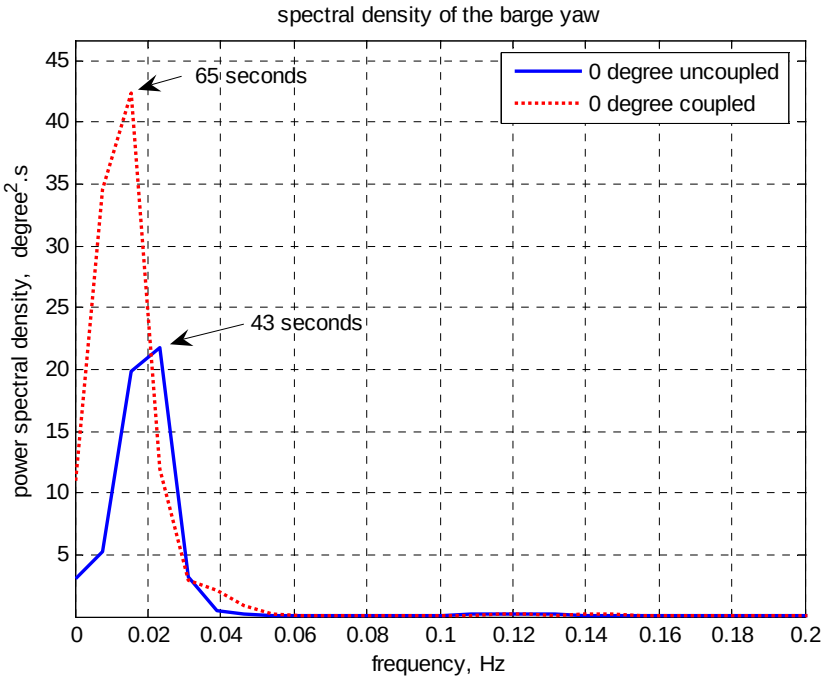

Fig. 25. Spectral density of the barge yaw in the 0° uncoupled and coupled cases

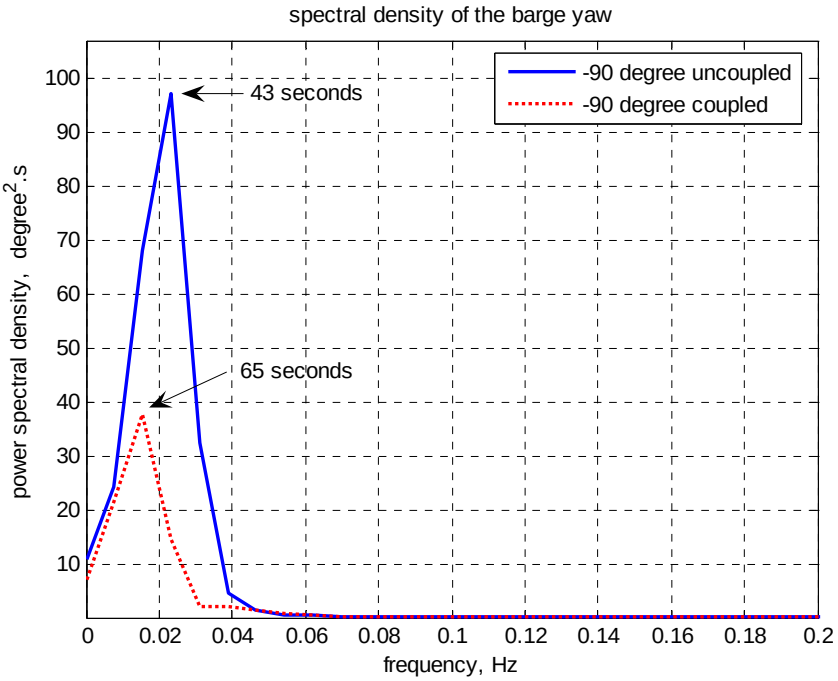

Fig. 26. Spectral density of the barge yaw in the -90° uncoupled and coupled cases

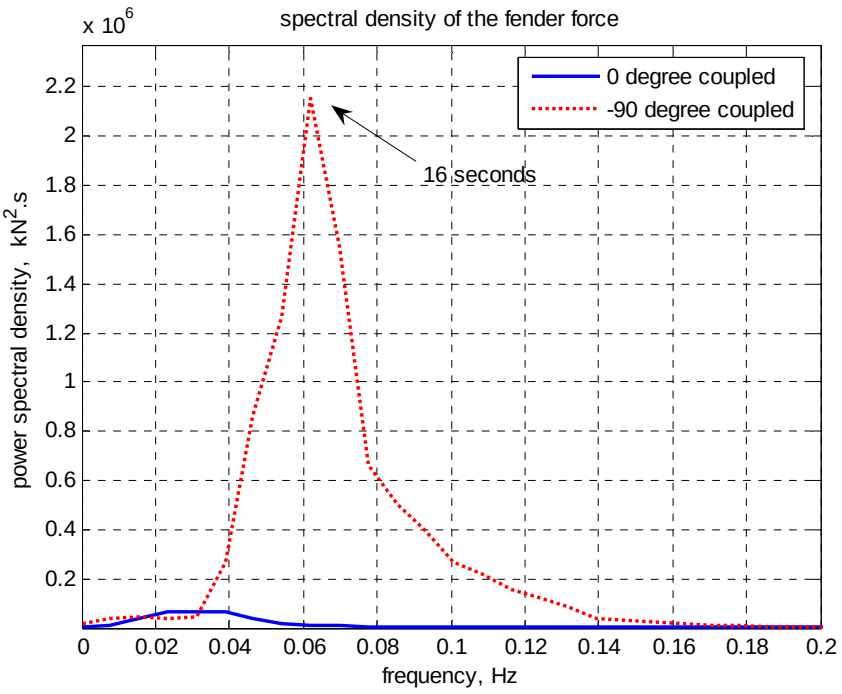

Fig. 27. Spectral density of the fender forces in the 0 and -90° coupled cases

The following points summarize the observations made in this section:

- The connection system does not have much influence upon the stiff mini-TLP, but changes the motion pattern of the less stiff barge, particularly those of the barge surge, sway, yaw and has some moderate limitation on roll.
- When changes occur with the adding of the connection system, in most cases the peaks remain the same and only the amplitudes change. Except the barge yaw which has a different peak frequency with the connection.
- When there are both low frequency and wave frequency peaks, only the low frequency peak will be affected if the motion is sensible to the coupling effect.
- The 0° and the -90° configurations have quite similar behavior face to the adding of the connection, but the initial values of the uncoupled barge motions are usually smaller in the -90° case due to the shielding effect provided by the mini-TLP.
- The barge yaw has a period of 43 seconds when uncoupled and a period of 65 seconds for the coupled case. The spectrum of the yaw increases in the 0° heading condition and decreases in the -90° configuration.
- The fender force is much higher for the -90° configuration because the incident forces are in the direction of the compression of the fender system.

4.5.2. Cross spectrum and coherence function

In the previous section, the auto-spectrums were used to study the behavior of each time series. In this section, the cross spectrum analysis will be proceeded to help the understanding of the coupling effect between two time series. The pairs of time series analyzed in the present study are those between the mini-TLP and the barge motions, as well as the fender wave and fender force with the above mentioned different motions. By comparing the cross spectrum in the uncoupled and coupled cases, it is possible to

see the change in the coupling effect caused by the connection system between these pairs of the time series. In the following presentations, three plots are generated by using MATLAB for each pair of data. The first plot is the amplitude spectrum; the peak indicates that both of the time series have a high energy for the corresponding frequency, which implies a possible high coupling effect between them at that specific frequency. The second plot is the phase spectrum which gives the information concerning the phase as indicated by its name. The third and the last plot is the squared coherence function; it is the tool for the correlation study in frequency domain, a close value to 1 means a high correlation between the two time series. These three information combined together gives a fair idea of the degree of coupling between each pair of time series. Again, only some most representative plots are shown in this section and the completed plots are listed in the Appendix D at the end of the text.

Fig. 28 shows the case of the TLP surge / barge surge couple in the 0° heading configuration. Two significant peaks can be observed for both uncoupled and coupled cases, one for the low frequency domain and the other for the wave frequency domain. The attention will be focused on the frequency domains corresponding to high energy because it is useless to consider the region where only few motions occur. These high energy frequency ranges are those corresponding to the peaks and are highlighted by the shaded areas. It can be observed that the low frequency peak is increased in the coupled case whereas the wave frequency peak remains the same. This means that there was initially a certain linear relationship between the mini-TLP surge and the barge surge, especially for the wave frequency range; this linearity is accentuated by the adding of the connection system in the low frequency range. The phase difference is smaller in the coupled case, near to 0, which implies that the two motions become almost in phase. The squared coherence function has very high values (near 1) for the wave frequency in both uncoupled and coupled cases, whereas it is significantly increased for the low frequencies with the connection system. This confirms the information given by the amplitude spectrum about the increase of the linear relationship between the two motions by adding the connection system. With this high correlation, one can almost

perfectly predict the barge surge motion at these frequencies by using the time series of the mini-TLP surge, without any phase shift for the phase difference in this case is nearly 0 for the considered frequencies.

Fig. 29 shows the cross spectrum of the TLP surge / barge surge couple in the -90° configuration. Compared to the 0° configuration, the -90° uncoupled case has the same peaks and similar amplitude for the cross spectrums, only with a bigger phase shift (about $-\pi/4$ for most of the considered frequencies). And the two time series show a similar relative behavior in the coupled case as in the 0° one: an increase in the low frequency peak range can be observed as well as an increase of correlation for the same frequencies. The correlation of the low frequencies in the -90° coupled case is slightly higher than the correlation in the 0° case, which suggests that the connection adds more linear relationship between the two motions in the beam sea condition. This because the surge motion is restrained by the breast lines and the fender system which are more linearly affected by the environmental forces in the surge direction in beam sea. All the three plots combined together shows that the change of configuration does not affect significantly the relative motion between the mini-TLP surge and the barge surge but a more linear relationship is created by the adding of the connection system for the low frequency ranges in the beam sea condition.

The cross spectrum analysis complements the information given by the auto-spectrums in the previous section. The auto-spectrums indicates that the spectrums of the surge motions in wave frequency does not change in either configuration for uncoupled or coupled cases, this corresponds to what is observed for the cross spectrum where the peak at the wave frequencies does not change. The auto-spectrums show that the less stiff barge has its surge motion changed to follow the mini-TLP surge motion. By the cross spectrum analysis, it is learnt that this relative surge/surge motion contains more energy (higher amplitude spectrum) and has actually a much higher linear correlation when the connection is set up.

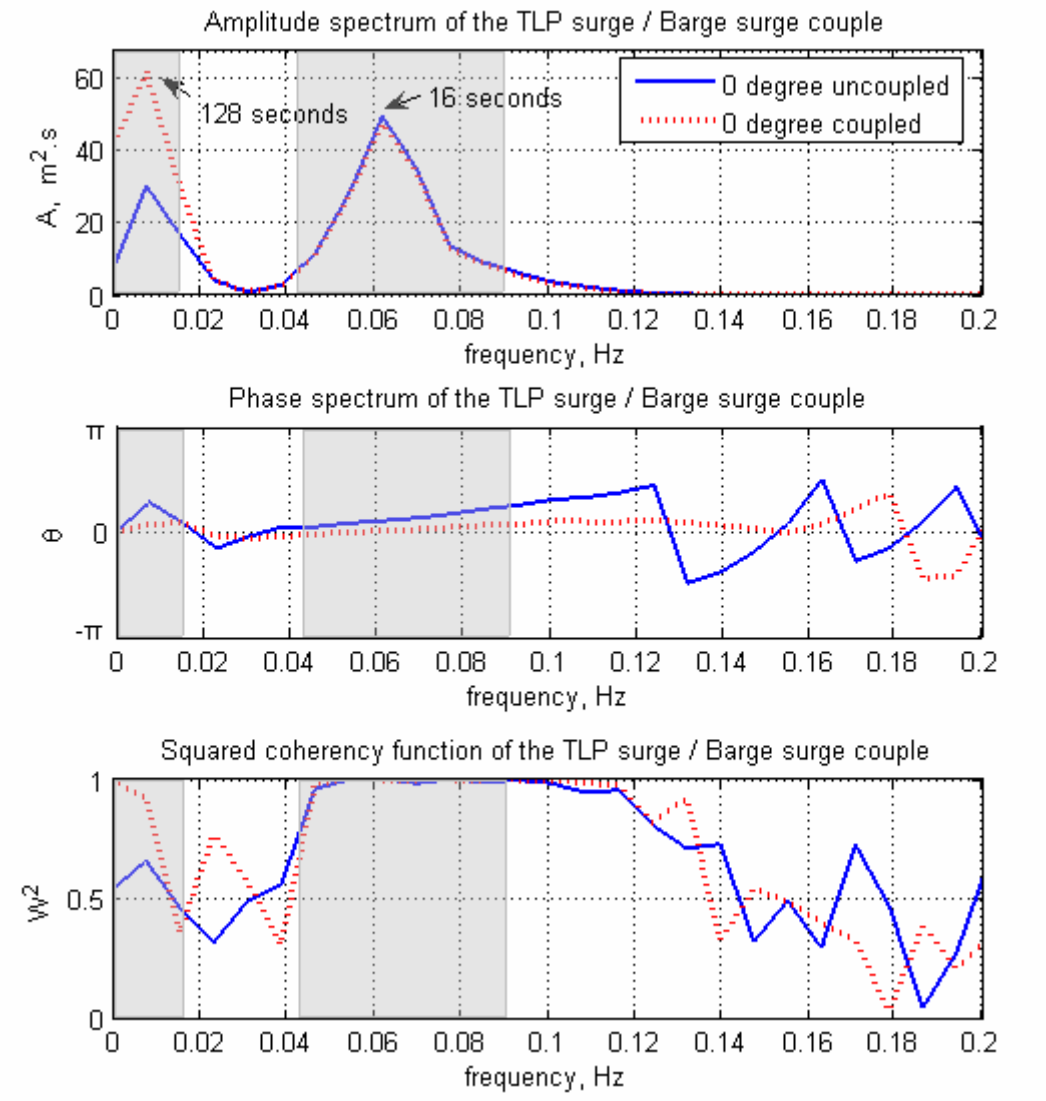

Fig. 28. Cross spectrums and coherence functions for the TLP surge / barge surge couple in the 0° configuration

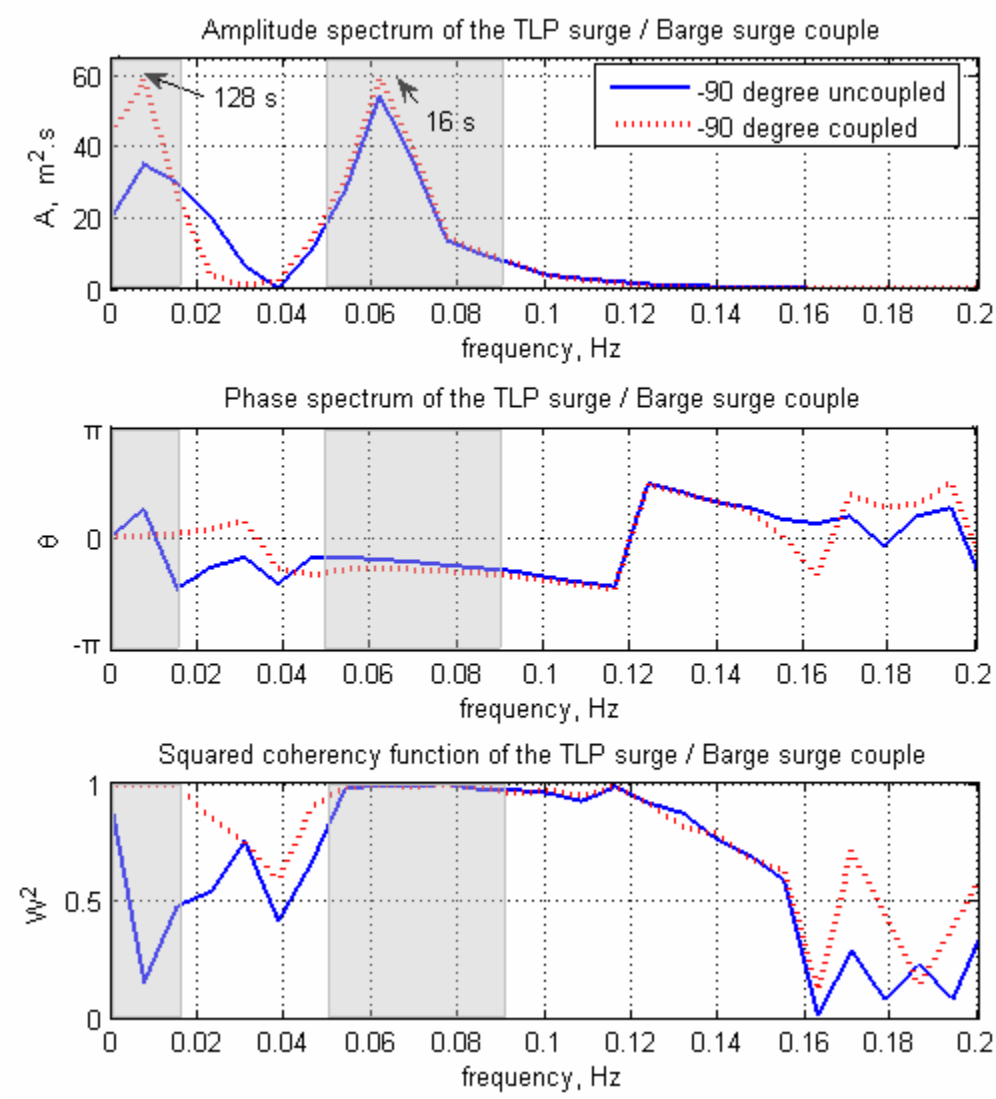

Fig. 29. Cross spectrums and coherence functions for the TLP surge / barge surge couple in the -90° configuration

Note that the coherence function is the equivalent of the cross-correlation function in the frequency domain, as stated before. Fig. 30 gives a comparison between the correlogram of the cross correlation coefficients and the amplitude spectrum of the cross spectrum obtained by using a same pair of time series. It is obvious that while the coherence function has an increase after the adding of the connection system, the cross correlation plot shows also an increase. The two plots give the same information respectively in frequency and time domain. However, some differences exists in practice: the time domain offers greater resolution in time for the time delay is more easily revealed, whereas the frequency domain gives more information concerning the frequency distribution but is less efficient to obtain accurate estimate of coherence when the data are of short length.

As stated at the beginning of this section, the data for both the mini-TLP and barge sway motions are of poor quality probably due to some measuring problems during the testing. As a consequence, except the sway / sway couple, all the other pairs of motions involving sway have quite spread out spectrums and small coherences which imply strong non-linear influences (Appendix D). It is difficult to tell if this corresponds to the real behavior of the system because of the problem of the data.

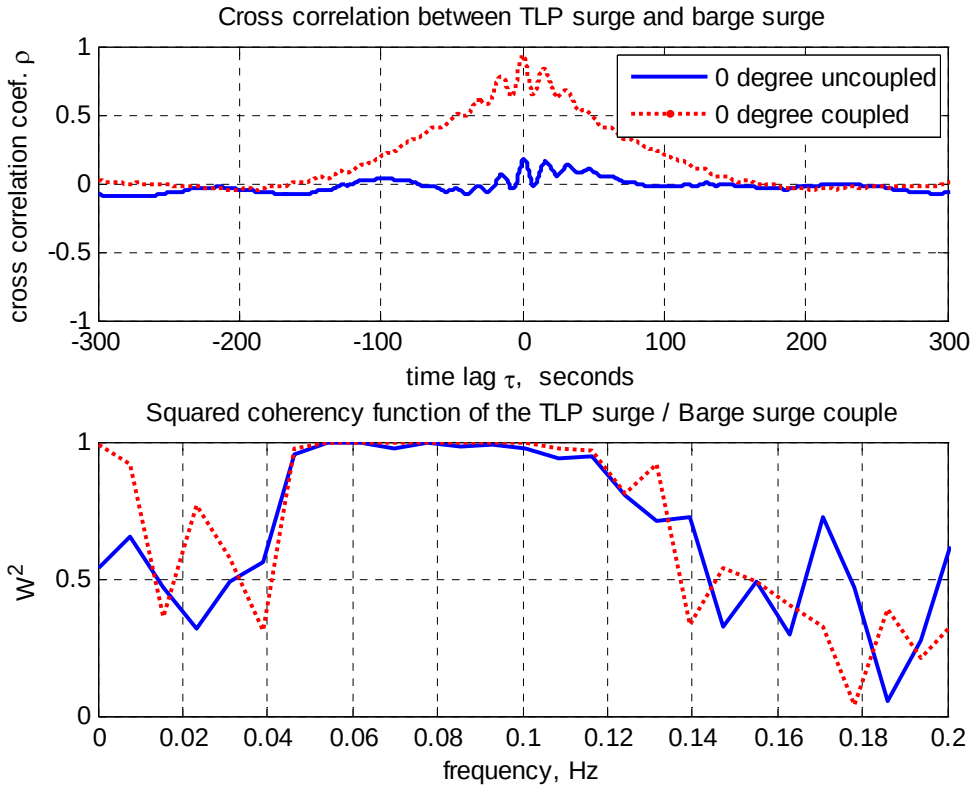

Fig. 30. Comparison between the cross correlation and the coherence function of the TLP surge / barge surge couple in the 0° head sea condition

The cross spectrums involving the mini-TLP heave motion have generally very small amplitudes even when the peaks are evident and the coherence high. Actually the auto-spectrum of this motion shows that it has a very small amplitude, this may be the reason for which the coherence is high as explained in section 2: the divisor in the formula of the squared coherency function is the product of the auto-spectrums of the two concerned motions, if at least one of the auto-spectrum has a very small value, the divisor can becomes very small and thereby the coherence becomes high without necessarily a real correlation between the two time series. In addition, the existence of the connection system or the change of configuration modifies the cross spectrums in different ways, but generally the amplitudes remain very small. Hence it can be concluded that the heave motion of the stiff mini-TLP does not have strong linear relationship with the motions of the barge and that the connection or the configuration does not affect significantly the coupling effect between the mini-TLP heave and the other motions.

The effect of the connection is obvious in the mini-TLP surge / barge roll couple in the 0° configuration: as shown in Fig. 31, whereas the spectrum has small amplitude and is spread out for the uncoupled case it is significantly increased in the coupled case and possesses a clear peak. This indicates that the mini-TLP surge / barge roll coupling is dominated by non-linear effect without the tie-off, and the connection makes this relationship much more linear. This because under the uncoupled condition the incident forces affect strongly the mini-TLP surge but much less the barge roll; the two separated bodies are hardly correlated for these motions. But once connected, the barge roll motion is restrained by the breast lines, thereby the correlation with the mini-TLP is more pronounced. However, the amplitude of the spectrum remains relatively small which shows that the effect of the connection is limited for this relative motion. In the -90° case the linearity is strong for both uncoupled and coupled cases for they have high amplitude of cross spectrums and high coherency, the connection does not change much the result (Fig. 32). Actually, in the -90° case the environmental forces influence largely both the mini-TLP and the barge, the effect of the connection can be hardly observed.

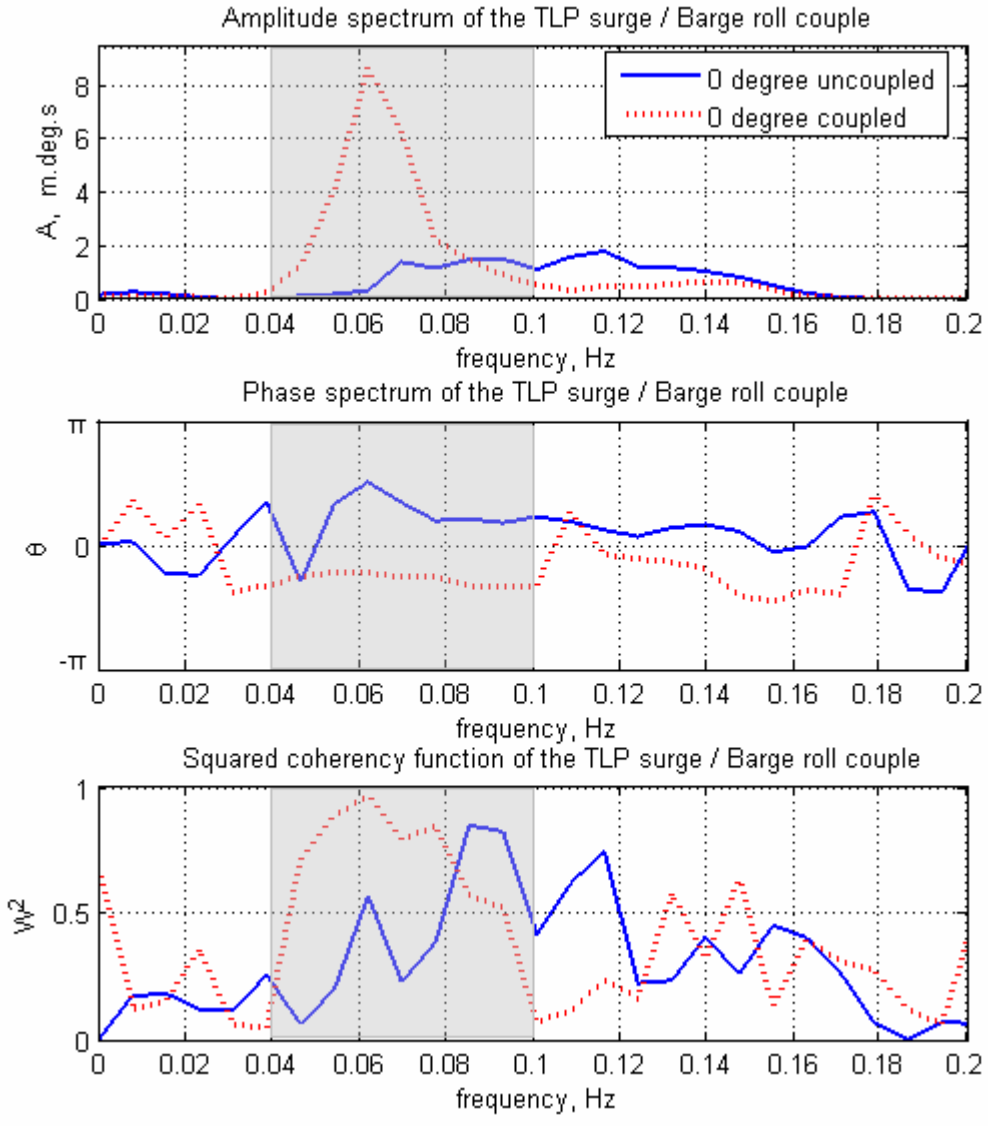

Fig. 31. Cross spectrums and coherence functions for the TLP surge / barge roll couple in the 0° configuration

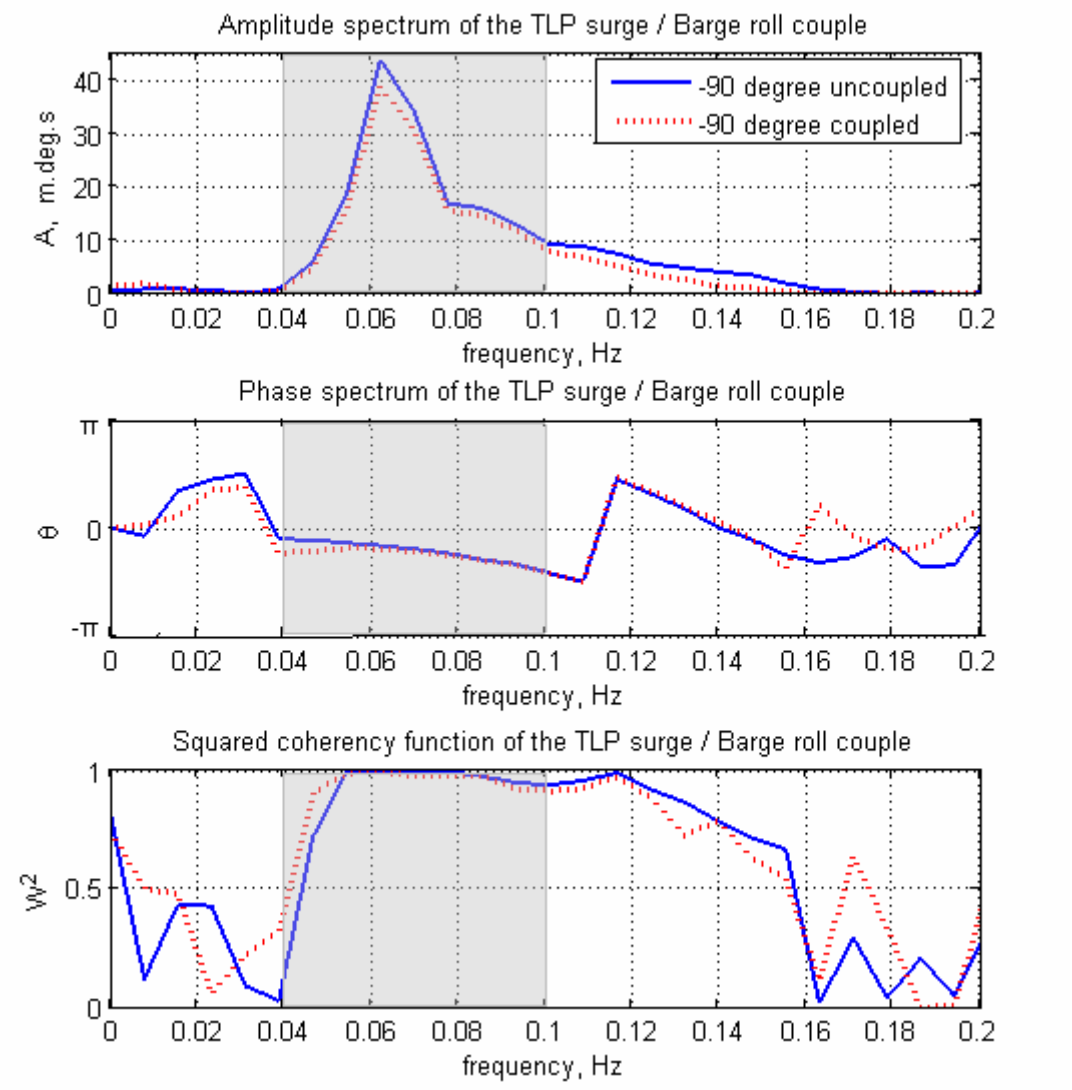

Fig. 32. Cross spectrums and coherence functions for the TLP surge / barge roll couple in the -90° configuration

Fig. 33 shows the comparison between the cross spectrums of the fender force / TLP surge couple in the coupled 0 and -90 degree configurations. The beam sea condition gives a much higher amplitude spectrum and a higher coherency value and the phase shift is almost constantly $-\pi/2$ over the whole shaded frequency range. In the 0 degree head sea configuration, no major forces tend to bring the two structures together so the fender receives relatively few loads. In the -90 degree configuration, the incident forces are in the same direction as the direction of the compression of the fender system, the higher the relative surge motion between the two structures, the higher the compression force in the fender system in order to keep the designed separation distance.

Fig. 34 shows the cross spectrums of the fender wave / fender force couple in the 0 and -90 degree configurations. These two time series are non-linearly related in the 0 degree configuration but have strong linear correlation in the 90 degree configuration. When the mini-TLP / barge system is set in the head sea condition, part of the wave can pass between the two bodies thus the water is hardly trapped in between and the rest of the wave hit the system from the bow. Since the fender wave elevation is not significant, it does not apply significant additional force on the hull of the structures to modify the separation distance, thereby there is no strong linear correlation between the fender wave elevation and the fender force. In the beam sea condition however, the incident wave is trapped between the two bodies because of the barge being perpendicular to the incident wave and creating a long barrier. This trapped water forms a considerable force applying on the barge in the direction of the incident wave and push the barge from the mini-TLP, as a consequence the fender system will respond and restrain the barge to keep the designed separation distance and this will result to a high tension in the fender.

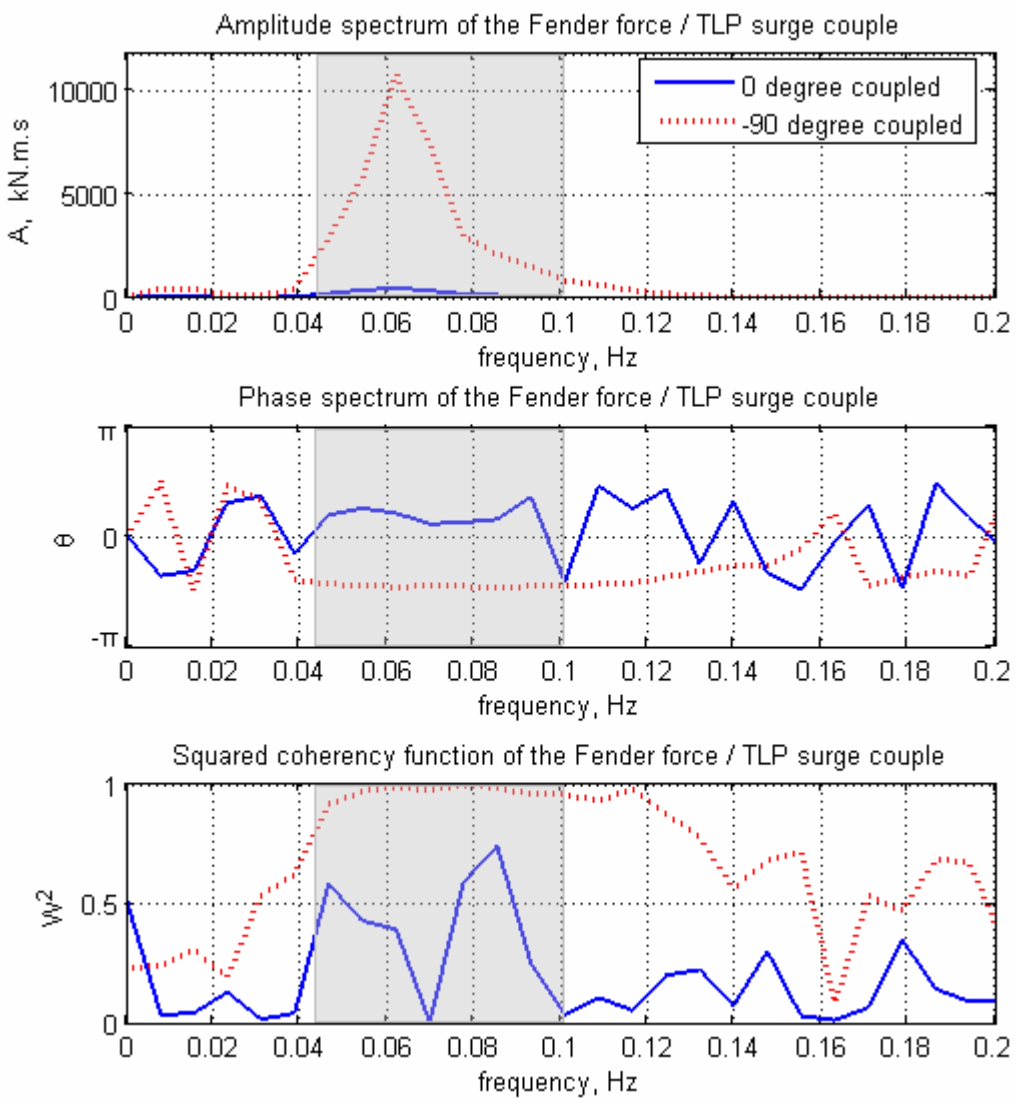

Fig. 33. Cross spectrums and coherence functions for the fender force / TLP surge couple in 0° and -90° configurations

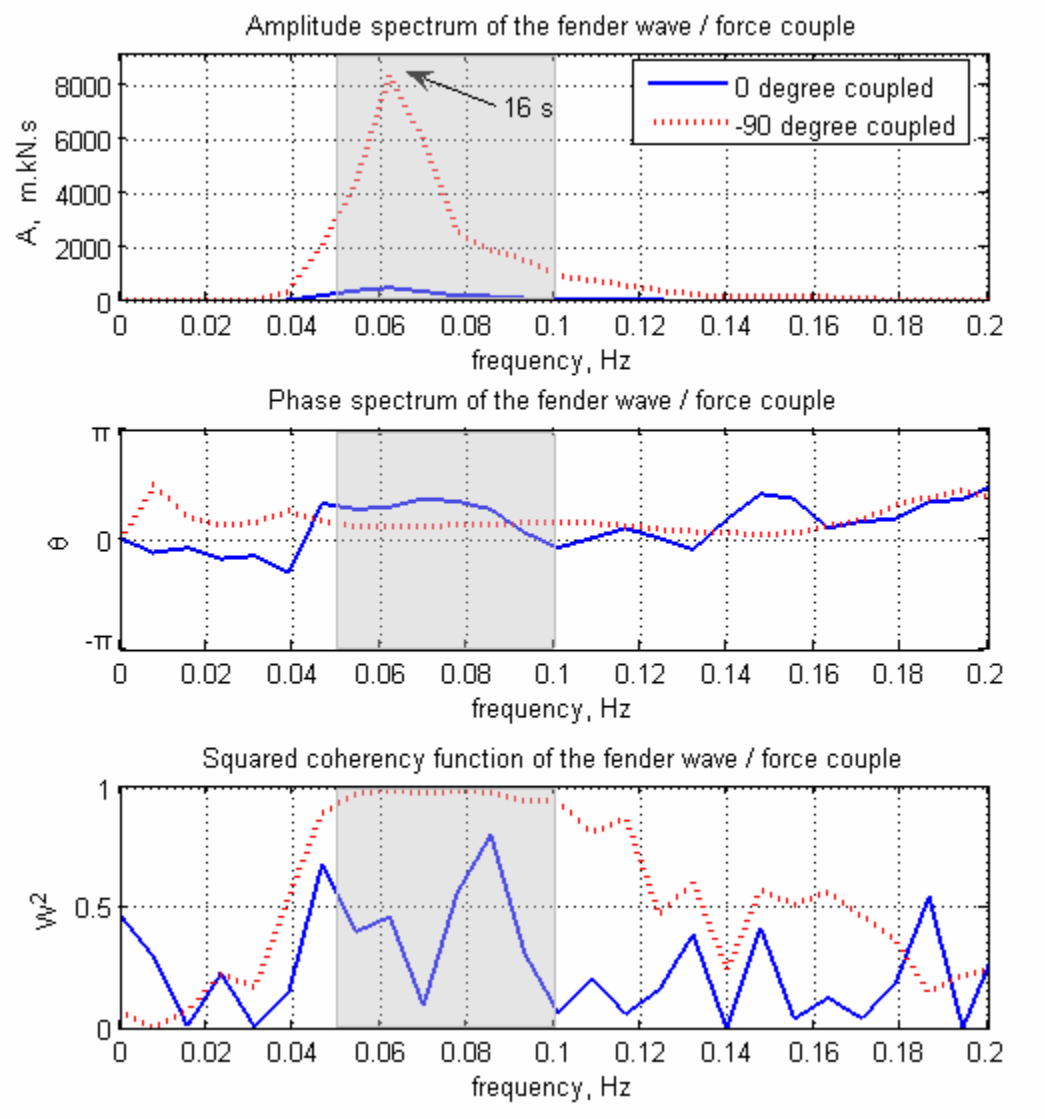

Fig. 34. Cross spectrums and coherence functions for the fender wave / fender force couple in 0° and -90° configurations

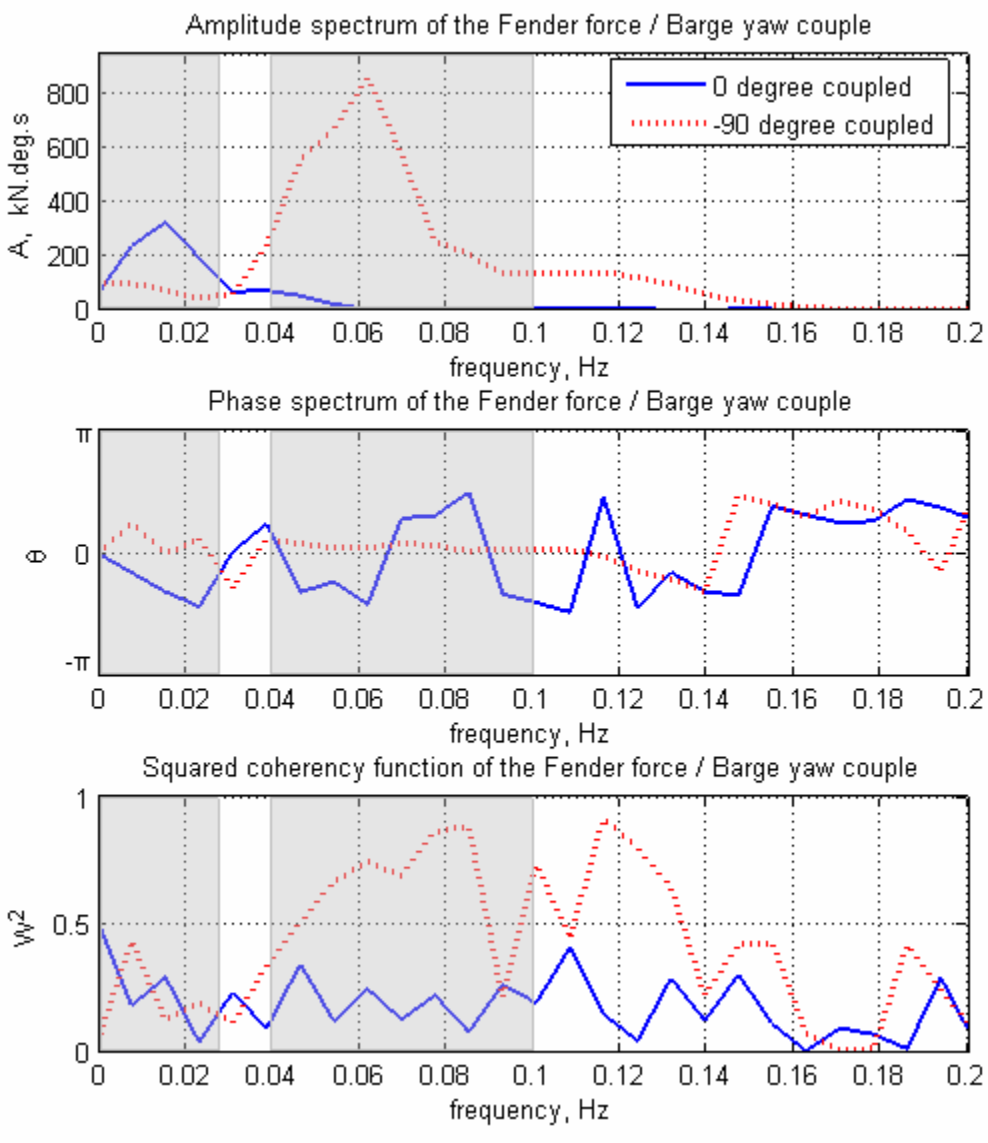

Fig. 35. Cross spectrums and coherence functions for the fender force / barge yaw couple in 0° and -90° configurations

Fig. 35 shows the analysis results of the fender force / barge yaw couple in both 0 and -90 degree configurations. It can be noticed that the two cross spectrums have different peak frequency values. For the 0 degree case, this peak frequency corresponds to a period of 65 seconds which is the natural period of the wind simulated in the testing; whereas the main period of the -90 degree case is 16 seconds, same as the wave and current period. It seems thereby that the fender force and the barge yaw are most related at the wind frequency but this relationship is mainly non-linear for the coherency values are low. They are more influenced by the wave and/or current in the -90 degree configuration and the coherence is much higher which implies a higher linear correlation between these two time series. The reason why the amplitude spectrum and the coherence function are higher in the -90 degree configuration is that the fender is in the same direction as the incident forces and the barge has a larger area exposed to these forces.

The following points summarize the analysis results obtained in this section concerning the cross spectrum study:

- Coherency function is the equivalent presentation of the correlation function in the frequency domain; it gives the correlation between the cyclical movements of the considered time series.
- The data of the sway motions are of poor quality, so the result in the cross spectrum analysis can be inaccurate when these time series are involved.
- In the case of the mini-TLP surge / barge surge couple, the connection system modifies the behavior of the system in the low frequency range by adding more linear relationship between the two motions. A slightly more linear relationship is observed for the -90° configuration for low frequencies.
- The mini-TLP heave motion is a small amplitude motion and it does not have any strong correlation with other motions of the barge. It can be concluded that the mini-TLP heave motion is hardly influenced by either the barge or the connection system.

- The connection adds a stronger linear relationship between the mini-TLP surge and the barge roll for the 0° configuration, but its effect is limited. This pair of motions is highly correlated in the -90° for both uncoupled and coupled cases.
- While the fender wave or fender force are involved, the cross spectrum and the coherency value are generally higher for the -90 degree case. This because the incident forces are in the same direction as the compression direction of the fender system, thereby a linear relationship is more likely in this case.

5. SUMMARY AND CONCLUSION

The behavior of the mini-TLP / barge system in both head sea (0°) and beam sea (-90°) conditions has been studied in order to determine the characteristics of each of the two vessels under combined wind, wave and current induced environmental forces. The comparison between the uncoupled and coupled cases allows the assessment of the effect of the connection system which is designed to restrain certain relative motions between the two bodies.

The use of the statistical methods is central in this study for the analysis of the mini-TLP / barge system. The tools used include basic statistical parameters, distribution functions, correlation function and spectral analysis. Except for the sway data which was judged to be of poor quality, all the available motion data of the mini-TLP and the barge as well as the data related to the fender system were of excellent quality and were analyzed in detail by using these methods.

Some of the results presented can be evaluated using different methods, and was employed as a check on various computations. For instance the basic statistical parameters give a general idea as to how the analysis has to proceed and the information that they provide at the beginning of the studies can be found in a more detailed way in the analysis which follows it. In the same way, cross correlation and coherency function may both measure the correlation between two time series but they are values in the time and frequency domains respectively.

The analysis of the distribution functions shows that most of the data follow Gaussian distributions which imply a strong linearity. However the extreme values are better fitted into Weibull distributions; this indicates a non-linearity in the system for these values. Although the Weibull distribution tends to overestimate the large values, it is considered to be adequate in this study. However, additional analyses should be pursued in design practice.

Three major features can be observed in the study regarding of the cross-correlation. A first group of motion pairs was verified to have a significant increase of

cross-correlation with the adding of the connection system, whereas the second group includes those pairs whose correlations are only affected slightly; the effect of the connection is negligible for the remaining time series pairs which form the third group. The first feature includes the pairs of motions such as mini-TLP surge / barge surge, mini-TLP sway / barge sway, mini-TLP heave / barge surge in 0 degree configuration and mini-TLP sway / barge sway in -90 degree configuration. They all have a high correlation after the set up of the connection which means that that the latter provides a strong linear relationship to these relative motions. The -90 degree surge / surge and heave / surge couples also have a high correlation with the adding of the connection but the initial correlation is high, this because the environmental forces which act in the direction of the surge motion have more impact in this configuration and a linearity can exist between the two vessels due to some common influence from these forces. The second feature includes the pairs of motions such as TLP surge / barge heave, TLP surge / barge pitch, TLP heave / barge pitch, TLP surge / barge yaw and TLP heave / barge yaw in both 0 and -90 degree configurations. And the others pairs of motions are part of the third feature and they are also similar for the two different configurations. The biggest difference between the 0 and -90 degree configurations is the correlation between the fender wave and fender force: the correlation is much higher in the beam sea condition for the fender compression springs are in the same direction as the incident forces.

The studies in the frequency domain complement the information obtained previously. The comparison between the auto-spectra of the uncoupled and coupled cases shows that the mini-TLP is not much affected by the connection system because of its relative stiffness due to the mooring system provided by tendons. The barge, which is less stiff, is pulled along the mini-TLP via the connection system thus some of its motions changed to follow that of the mini-TLP. In particular the barge surge, sway and yaw motions were most affected. The motions within the wave frequencies remain intact and only those motion responses in the low frequency range were changed by the addition of the connection system. The -90 degree configuration has smaller initial

values in certain DOF of the barge in the uncoupled case, this because of the shielding effect provided by the mini-TLP which is not very significant though. Once the vessels are coupled, the tendency of the change is the same. More specifically, if there is an increase of spectrum amplitude in the 0 degree case, the same thing can be observed in the -90 degree case although the magnitudes are different. The barge yaw motion is an exception. It has different peak frequencies for the uncoupled and coupled cases, which are 43 seconds for the uncoupled case and 65 seconds for coupled one. The related energy increases in 0 degree configuration and decreases in the -90 degree configuration for the mini-TLP yaw may be more compliant in the 0 degree case and less in the -90 degree case compared to the barge yaw.

The cross spectrums show the relationships between two time series. It is observed that the adding of the connection increases the linear relationship between the mini-TLP surge and the barge surge for the low frequency range in both 0 and -90 degree configurations, with a slightly higher correlation for the beam sea condition. The mini-TLP heave motion is a small amplitude motion and it does not have any strong correlation with other motions of the barge even if the coherency values may be high. It can be concluded that the mini-TLP heave motion is hardly influenced by either the barge or the connection system. The tie-up adds a certain linearity between the mini-TLP surge and the barge roll in the 0° case due to the restriction of the movement by the breast lines, whereas it is already high for the -90° case even when uncoupled because of the direction of the environmental forces. The cross spectrum and the coherency value are generally higher for the -90 degree case when either the fender wave or fender force is involved in the considered time series couple. This again is because the incident forces are in the same direction as the compression direction of the fender system, which may add a stronger linear relationship in this case.

Thus, the connection system coupling of the barge to the mini-TLP does not significantly modify the motion response of the mini-TLP, but it has big impact on the barge surge, sway and yaw motions. Other motions such as the barge roll can also be influenced by the addition of the connection, but by design this should be minimal.

Moreover, this effect is not as visible as the horizontal motions and the yaw. The influence of the connection system is manifested by a certain reduction of motion amplitude and an increase of the linear relationship between some pairs of the motions. The -90 degree configuration presents the advantage of the shielding effect, but the loading on the fender system and the barge mooring system is observed to be much bigger.

Overall, the use of the statistical methods is proved to be a direct and efficient way to characterize the studied system. It is seen that the change of the environmental forces heading and the existence of the connection system can affect substantially the behavior of the vessels, which are among the factors to be considered during the design process of a multiple body system.

Note that the present thesis is focused on the study of the behavior of the two vessels only. A similar study has been conducted by Pillai and Niedzwecki (2005) which is dedicated to the analysis of the mooring lines and tendons of the same two-body system. These two texts are complementary to each other in the study of the whole system.

REFERENCES

Buchner, B., van Dijk, A.W.V., de Wilde, J.J., 2001. Numerical multiple-body simulations of side-by-side mooring to an FPSO. 11th International Offshore and Polar Engineering Conference, ISOPE'01, Stavanger, Norway, vol.1, 343-353.

Chen, S., Mahrenholtz, O., Zhu, T., 1991. Gravity waves and their interaction with floating twin bodies. 10th International Conference on Offshore Mechanics & Arctic Engineering, OMAE'91, Stravanger, Norway, vol.1.B, 481-487.

Handbook of Statistical Methods (online version), National Institute of Standards and Technology (NIST) / SEMATECH, 2005.

Hong, S.Y., Kim, J.H., Cho, S.K., Choi, Y.R., Kim, Y.S., 2005. Numerical and experimental study on hydrodynamic interaction of side-by-side moored multiple vessels. Ocean Engineering, vol.32, 783-801.

Hong, S.Y., Kim, J.H., Kim, H.J., Choi, Y.R., 2002. Experimental study on behavior of tandem and side-by-side moored vessels. 12th International Offshore and Polar Engineering Conference, ISOPE'02, Kyushu, Japan, vol.3, 841-847.

Huang, M.C., Hudspeth, R.T., Leonard, J.W., 1985. FEM solutions of 3D wave interference problems. Journal of Waterway, Port, Coastal and Ocean Engineering, ASCE, vol.111, No. 4, 661-677.

Ikegami, K., Matsuura, M., 1981. Study on motions of floating bodies under composite external loads. Proceedings of International Symposium on Hydrodynamics in Ocean Engineering, NIT, Trondheim vol.2, 799-816.

Inoue, Y., Seif, M.S., Asada, H., Yamashita S., 1996. Motion analysis of parallely connected FPSO and LNG carrier. 15th International Conference on Offshore Mechanics & Arctic Engineering, OMAE'96, Florence, ITALY, vol.1.A, 415-421.

Kim, C.H., 1972. The hydrodynamic interaction between two cylindrical bodies floating in beam seas. SIT Report OE-72-10, Stevens Institute of Technology, Hoboken, NJ.

Kodan, N., 1984. The motions of adjacent floating structures in oblique waves. 3rd International Conference on Offshore Mechanics & Arctic Engineering, OMAE'84, New Orleans, vol.1, 481-487.

Korvin-Kroukovsky, B.V., 1955. Investigation of ship motions in regular waves. Transaction Society of Naval Architects and Marine Engineers, vol 63, 386-433.

Lee, C.H., Newman, J.N., 2004. Computation of wave effects using the panel method. Numerical Models in Fluid-Structure Interaction, Preprint, WIT Press, Southampton, UK.

Løken, A.E., 1981. Hydrodynamic interaction between several floating bodies of arbitrary form in waves. Proceedings of International Symposium on Hydrodynamics in Ocean Engineering, NIT, Trondheim vol.2, 745-779.

Newton, H.J., 1996. TIMESLAB: A Time Series Analysis Laboratory. Wadsworth & Brooks/Cole Publishing Company, Pacific Grove, California, US.

Niedzwecki, J.M., 2004-2005. Personal correspondence.

Ohkusu, M., 1976. Ship motions in vicinity of a structure. Proceedings of International Conference on Behavior of Offshore Structure, BOSS'76, NIT, Trondheim vol 1, 284-306.

Sannasiraj, S.A., Sundaravadivelu, R., Sundar, V., 2001. Diffraction-radiation of multiple floating structures in directional waves. Ocean Engineering, vol.28, 201-234.

Taylor, E.R., Zietsman, J., 1982. Hydrodynamic loading on multi-component bodies. Proceedings of the Third International Conference on Behavior of Offshore Structure, BOSS'82, MIT, Cambridge, MA, 424-443.

Teigen, P., Niedzwecki, J.M., 1999. Experiments and analysis with fully coupled mini-TLP / Barge system. 9th International Offshore and Polar Engineering Conference, ISOPE'99, Brest, France.

Van Oortmerssen, G., 1979. Hydrodynamic interaction between two structures, floating in waves. Proceedings of the Second International Conference of Behavior of Offshore Structures, BOSS'79, London, 339-356.

Van der Valk, C., Watson, A., 2005. Mooring of LNG carriers to a weathervaning floater – side-by-side or stern-to-bow. OTC 17154. OTC'05.

APPENDIX A

CHARACTERISATION PARAMETERS OF WEIBULL DISTRIBUTION

Shape and scale parameters for Weibull distribution in the 0° uncoupled case

	Shape parameters		Scale parameters	
	p_max	n_min	p_max	n_min
TLP surge	1.37	1.32	2.20	2.48
TLP sway	0.98	1.28	0.88	1.03
TLP heave	1.37	1.25	0.08	0.09
Barge surge	1.33	1.33	2.07	2.04
Barge sway	1.30	1.38	1.26	1.28
Barge heave	1.28	1.14	0.75	0.72
Barge roll	1.89	1.83	0.55	0.55
Barge pitch	1.75	1.74	1.48	1.49
Barge yaw	1.27	1.32	0.44	0.42
Fender wave	NA	NA	NA	NA
Fender force	NA	NA	NA	NA

Shape and scale parameters for Weibull distribution in the 0° coupled case

	Shape parameters		Scale parameters	
	p_max	n_min	p_max	n_min
TLP surge	1.22	1.32	1.96	1.92
TLP sway	1.65	1.15	0.90	0.73
TLP heave	1.73	1.39	0.07	0.06
Barge surge	1.30	1.27	1.78	1.56
Barge sway	1.27	1.21	0.82	0.81
Barge heave	1.37	1.25	0.76	0.74
Barge roll	1.72	1.72	0.44	0.44
Barge pitch	1.77	1.81	1.43	1.43
Barge yaw	1.24	1.27	0.63	0.65
Fender wave	1.24	0.86	0.89	0.47
Fender force	1.29	1.27	34.51	34.34

Shape and scale parameters for Weibull distribution in the -90° uncoupled case

	Shape parameters		Scale parameters	
	p_max	n_min	p_max	n_min
TLP surge	1.37	1.48	2.20	1.90
TLP sway	0.96	1.59	1.16	1.53
TLP heave	1.32	1.27	0.07	0.07
Barge surge	1.31	1.22	2.30	2.35
Barge sway	1.49	1.21	0.79	0.72
Barge heave	1.35	1.30	0.96	0.91
Barge roll	1.75	1.63	2.04	2.08
Barge pitch	1.67	1.54	0.24	0.23
Barge yaw	1.18	1.30	0.88	0.87
Fender wave	NA	NA	NA	NA
Fender force	NA	NA	NA	NA

Shape and scale parameters for Weibull distribution in the -90° coupled case

	Shape parameters		Scale parameters	
	p_max	n_min	p_max	n_min
TLP surge	1.43	1.55	1.99	1.94
TLP sway	1.27	1.55	0.98	1.10
TLP heave	1.25	1.25	0.06	0.06
Barge surge	1.39	1.33	2.02	1.94
Barge sway	1.25	1.38	0.78	0.81
Barge heave	1.40	1.31	0.97	0.90
Barge roll	1.67	1.62	1.73	1.77
Barge pitch	1.53	1.40	0.26	0.25
Barge yaw	1.23	1.33	0.56	0.57
Fender wave	1.66	1.39	0.82	0.91
Fender force	1.18	1.26	181.02	181.57

APPENDIX B

CROSS CORRELATIONS

	0° head sea	-90° beam sea
TLP surge / Barge Surge	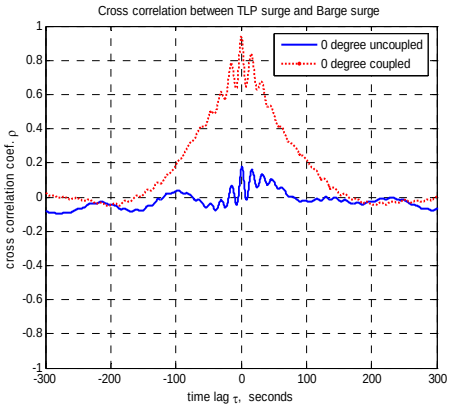	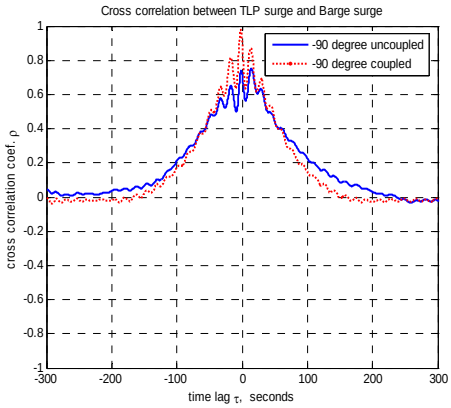
TLP surge / Barge sway	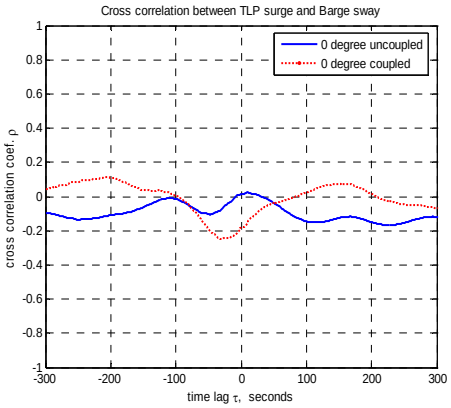	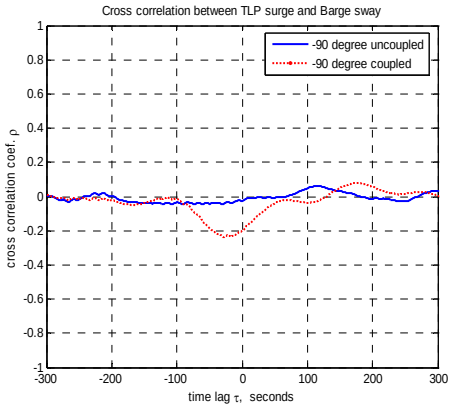
TLP surge / Barge heave	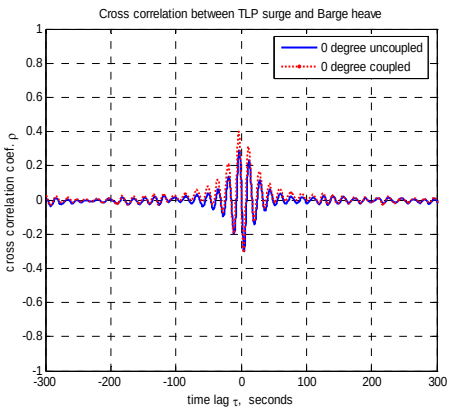	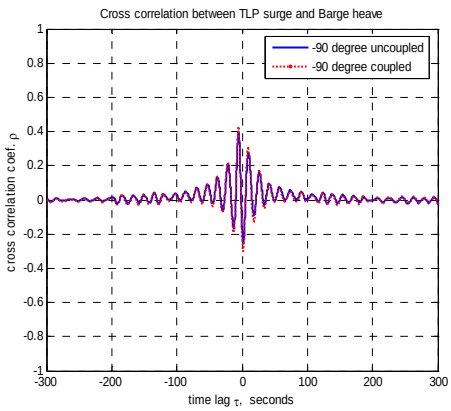

	0° head sea	-90° beam sea
TLP surge / Barge roll	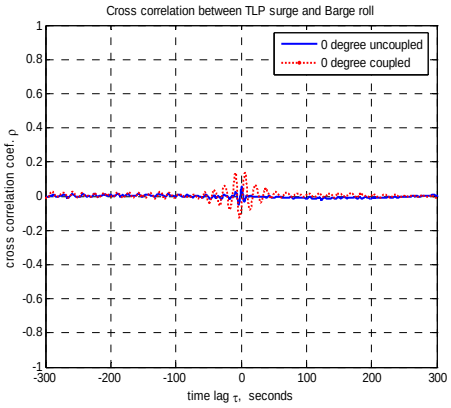	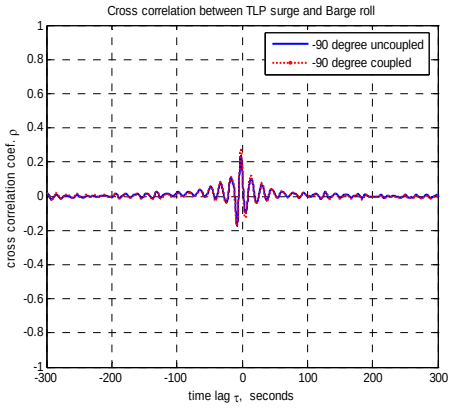
TLP surge / Barge pitch	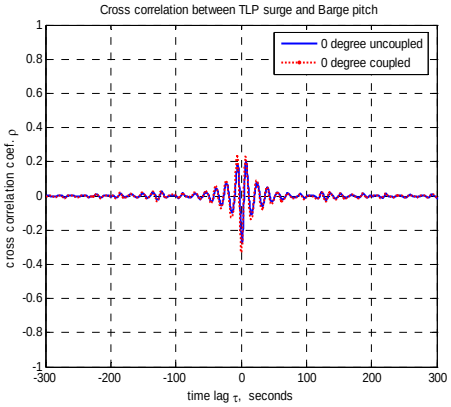	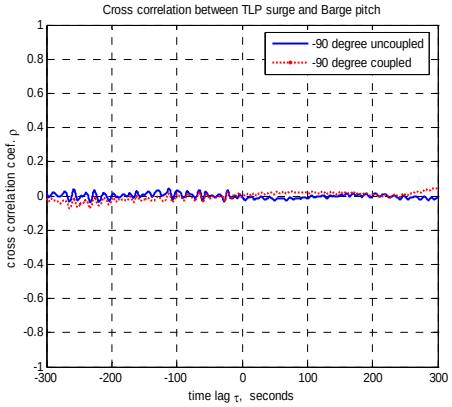
TLP surge / Barge yaw	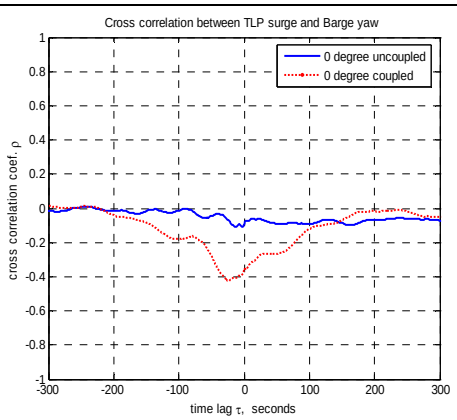	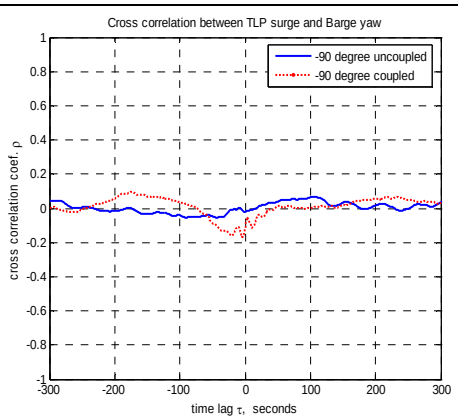

	0° head sea	-90° beam sea
TLP sway / Barge surge	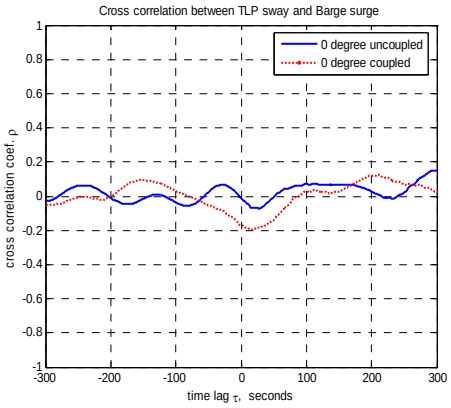	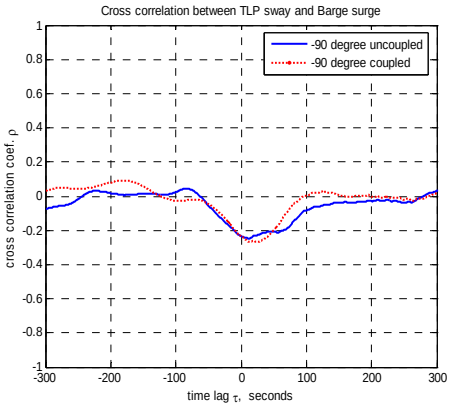
TLP sway / Barge sway	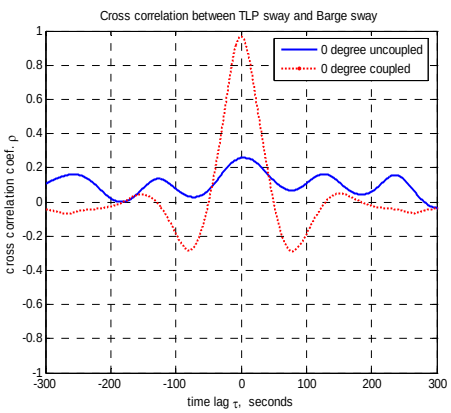	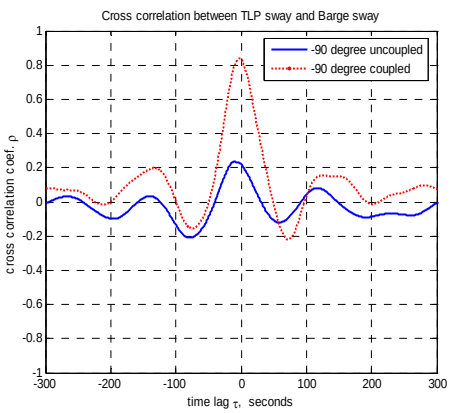
TLP sway / Barge heave	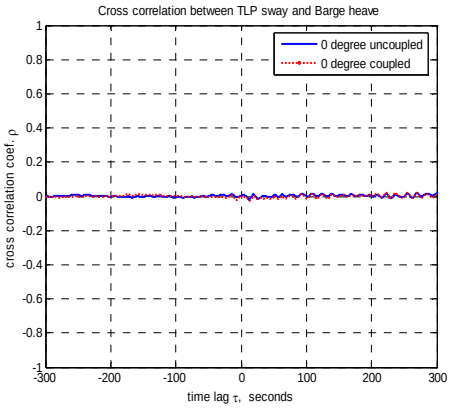	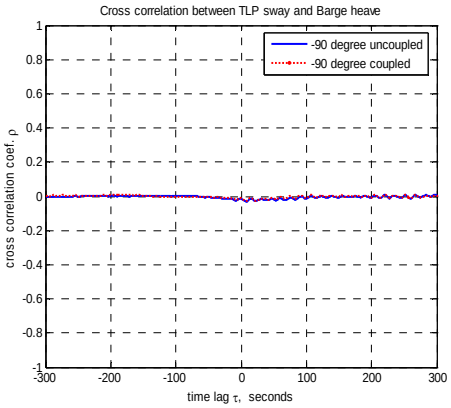

	0° head sea	-90° beam sea
TLP sway / Barge roll	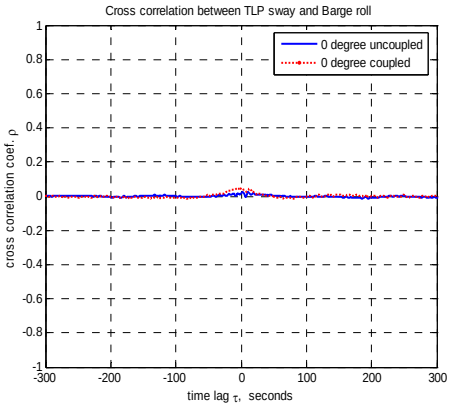	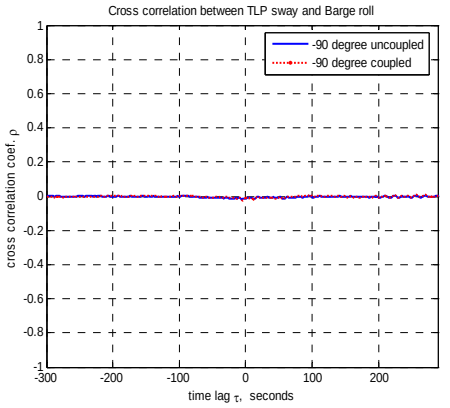
TLP sway / Barge pitch	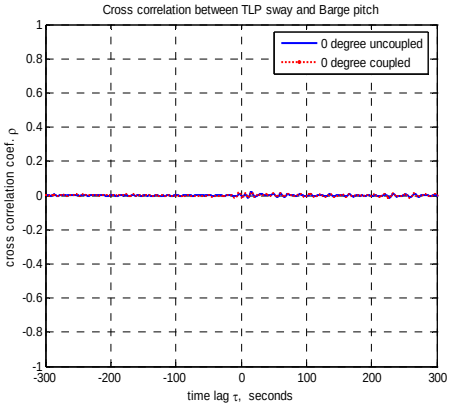	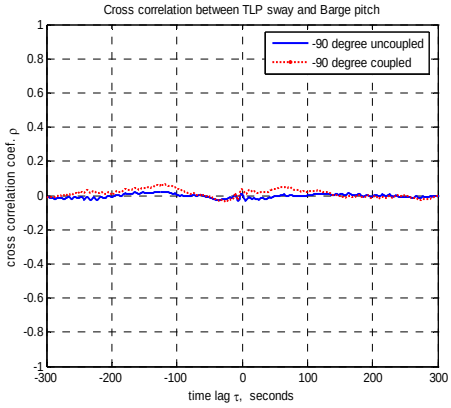
TLP sway / Barge yaw	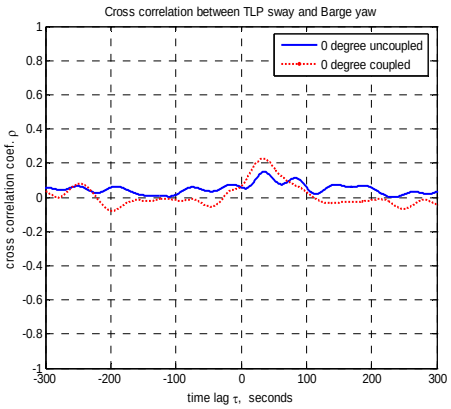	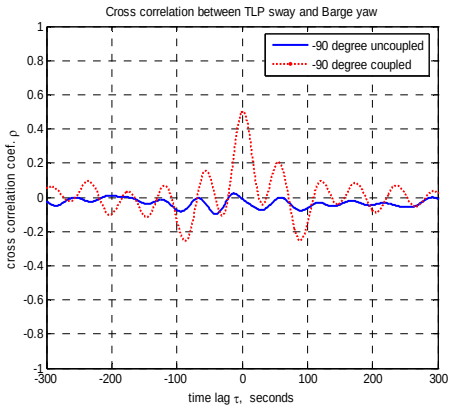

	0° head sea	-90° beam sea
TLP heave / Barge surge	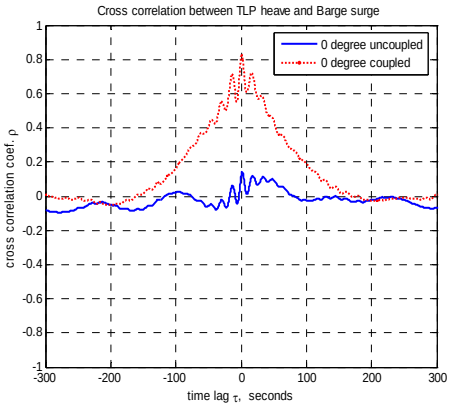	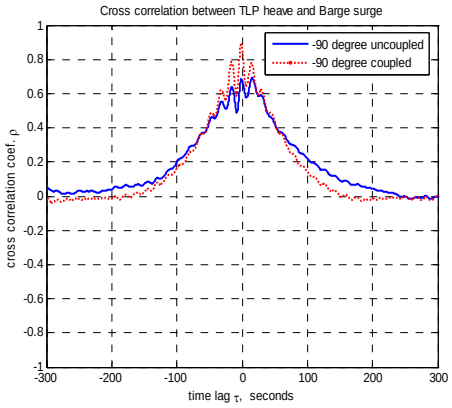
TLP heave / Barge sway	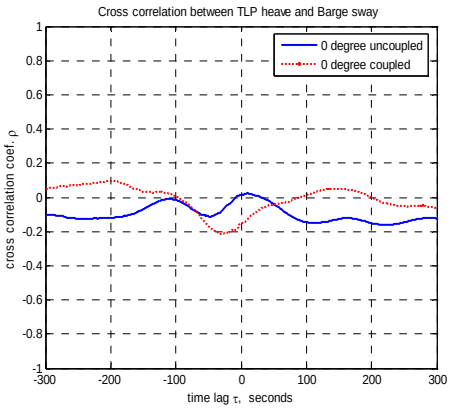	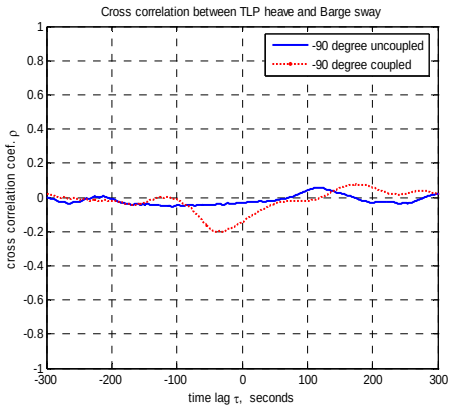
TLP heave / Barge heave	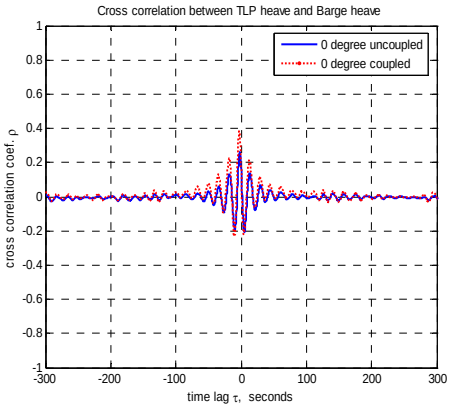	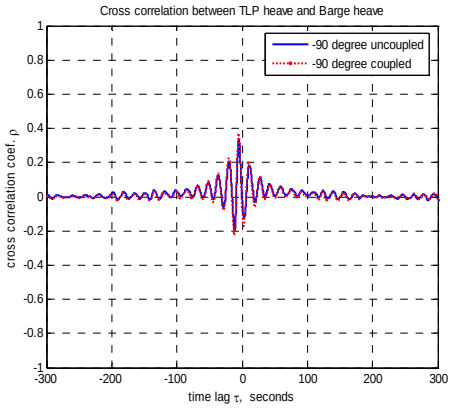

	0° head sea	-90° beam sea
TLP heave / Barge roll	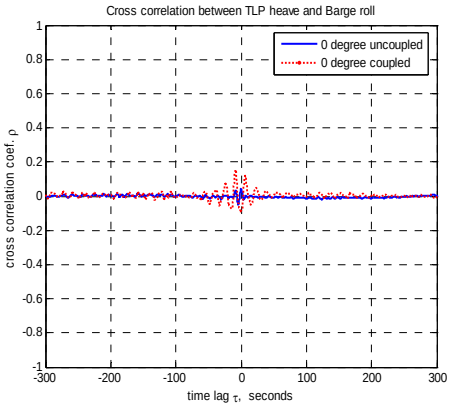	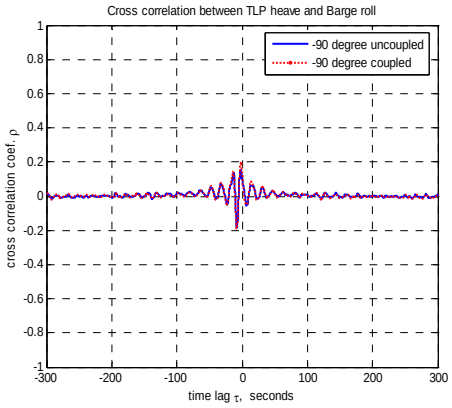
TLP heave / Barge pitch	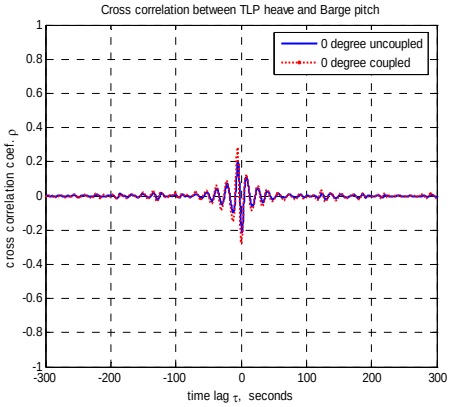	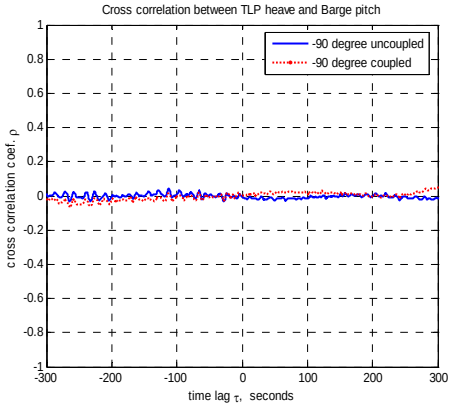
TLP heave / Barge yaw	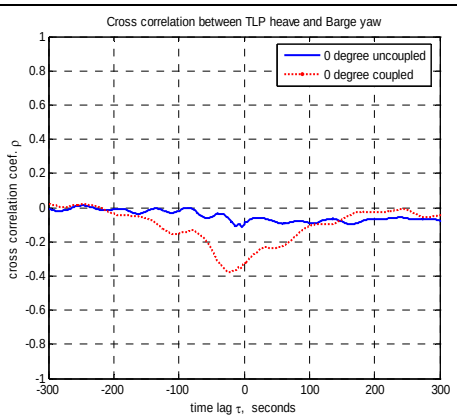	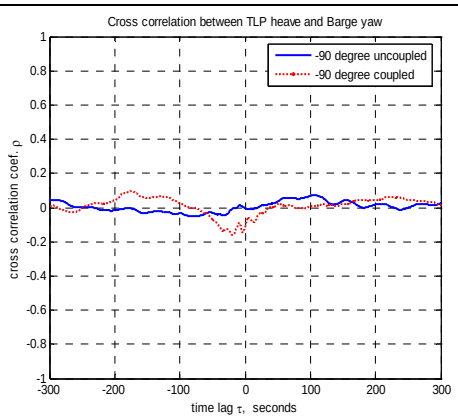

	0° head sea, coupled case	-90° beam sea, coupled case
Fender wave and TLP surge	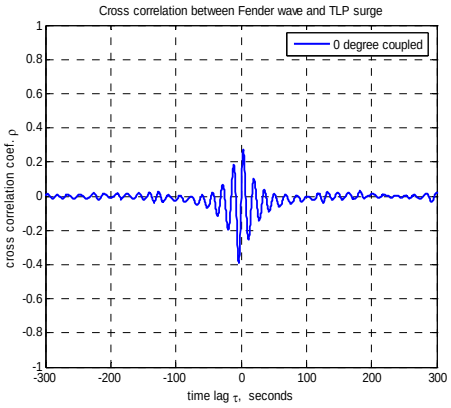	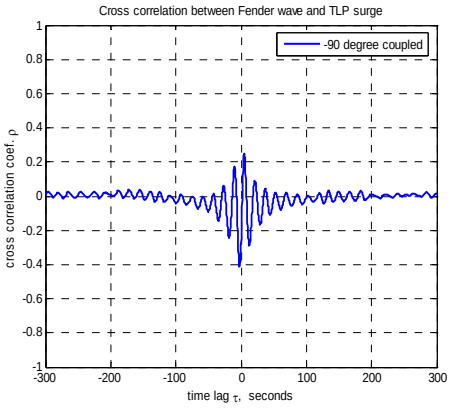
Fender wave and TLP sway	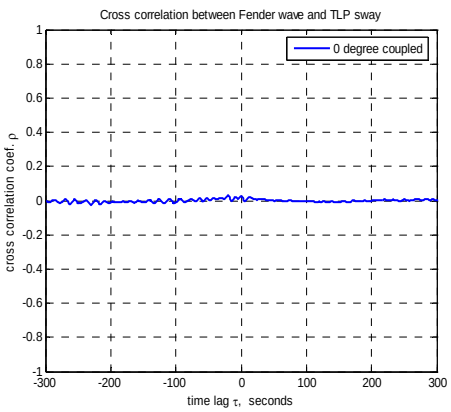	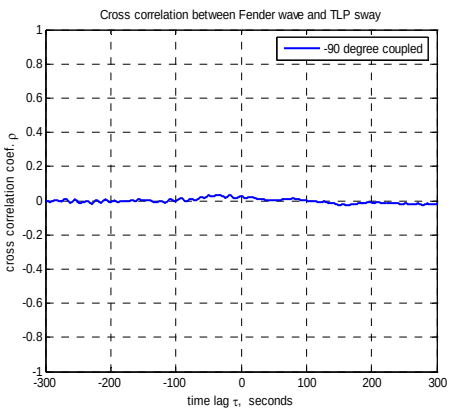
Fender wave and TLP heave	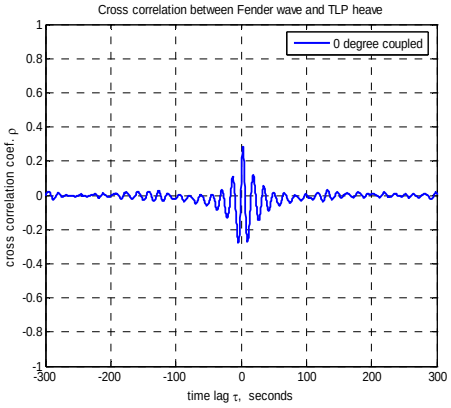	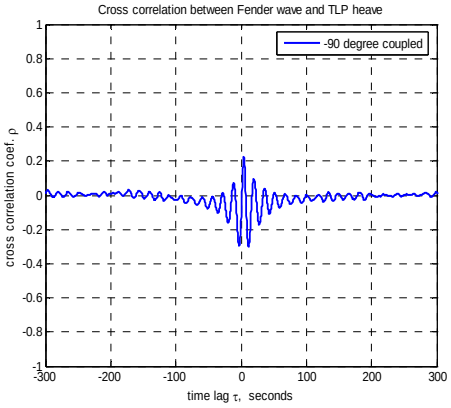

	0° head sea, coupled case	-90° beam sea, coupled case
Fender wave and Barge surge	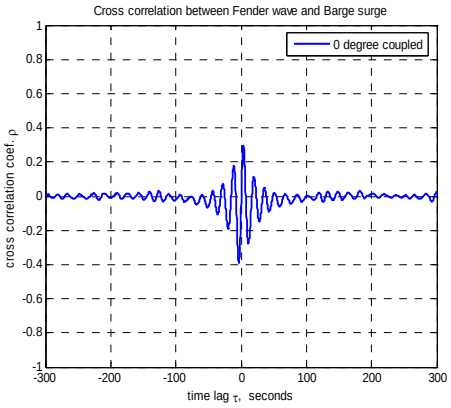	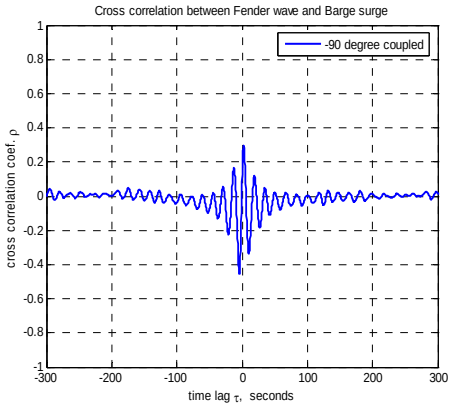
Fender wave and Barge sway	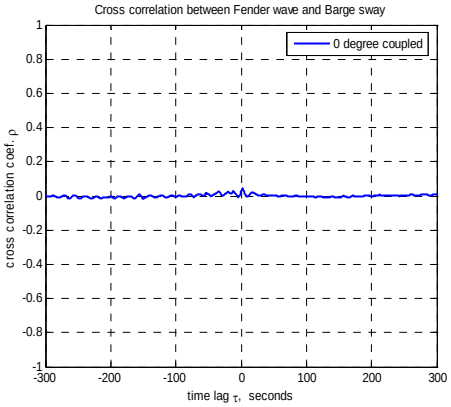	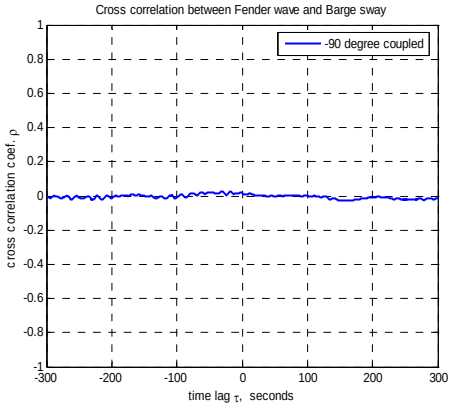
Fender wave and Barge heave	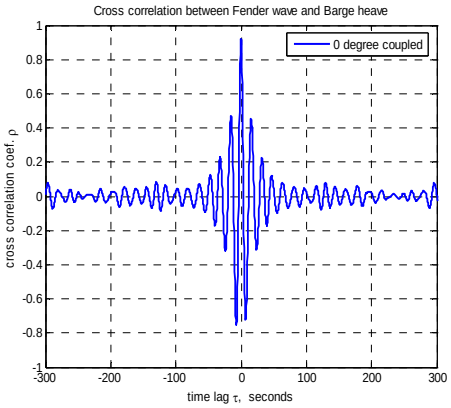	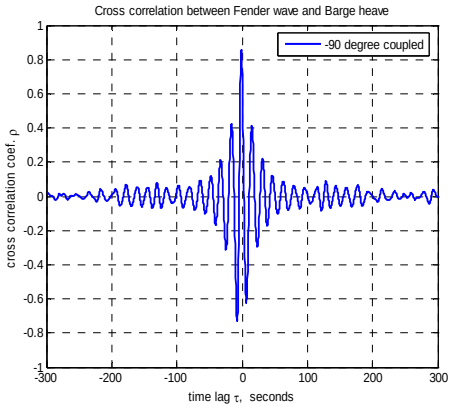

	0° head sea, coupled case	-90° beam sea, coupled case
Fender wave and Barge roll	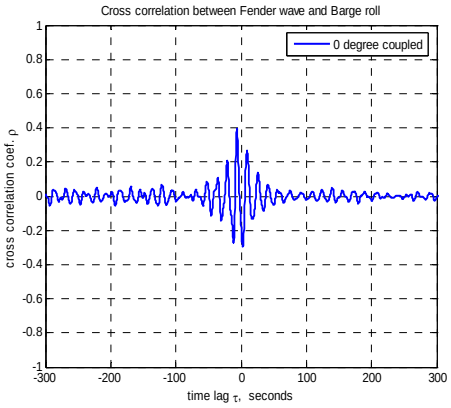	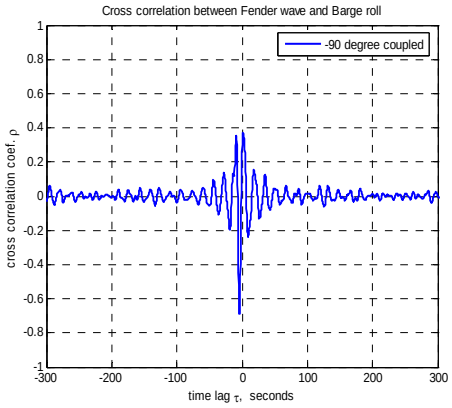
Fender wave and Barge pitch	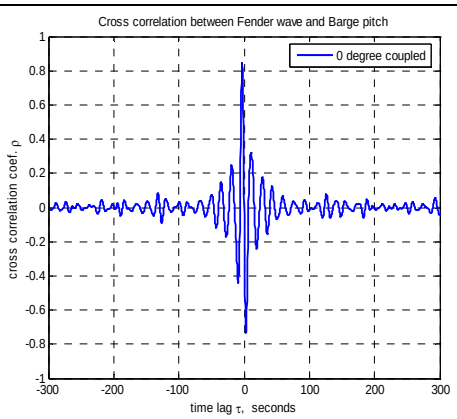	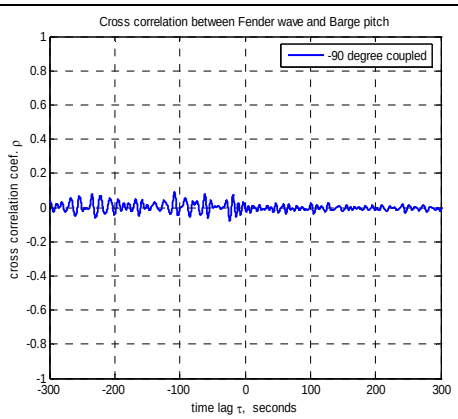
Fender wave and Barge yaw	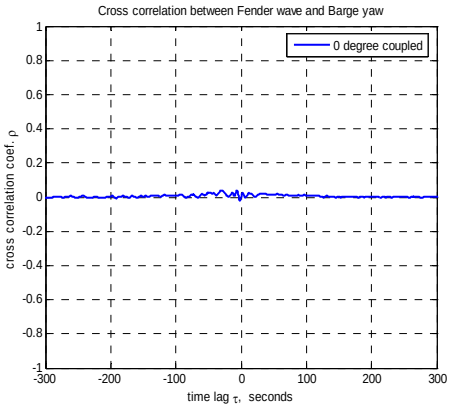	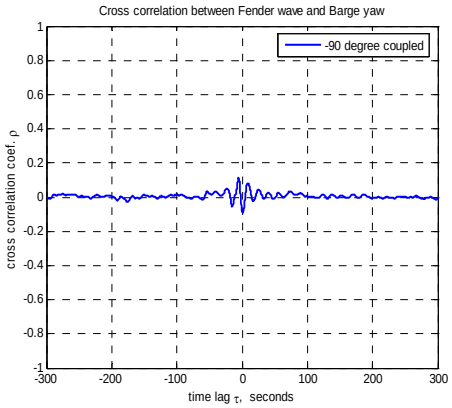

	0° head sea, coupled case	-90° beam sea, coupled case
Fender force and TLP surge	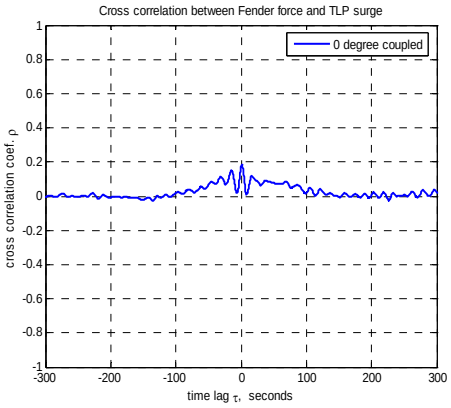	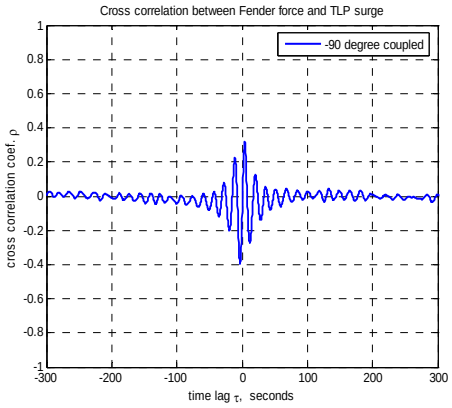
Fender force and TLP sway	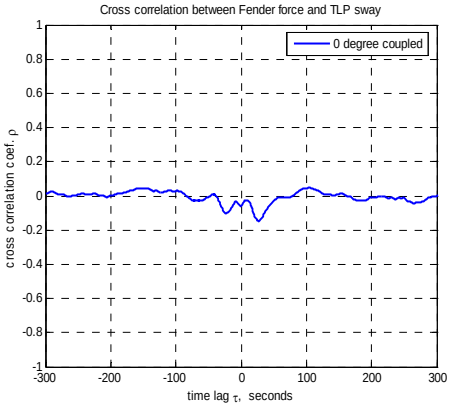	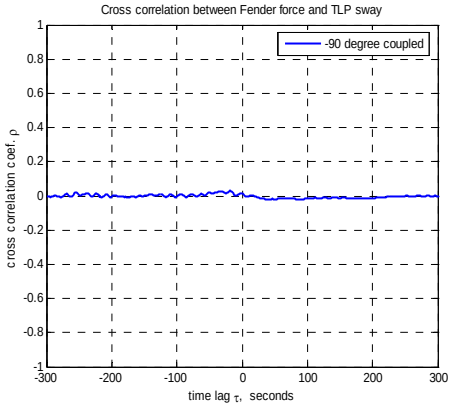
Fender force and TLP heave	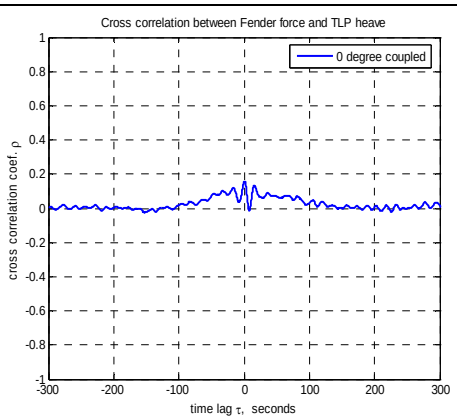	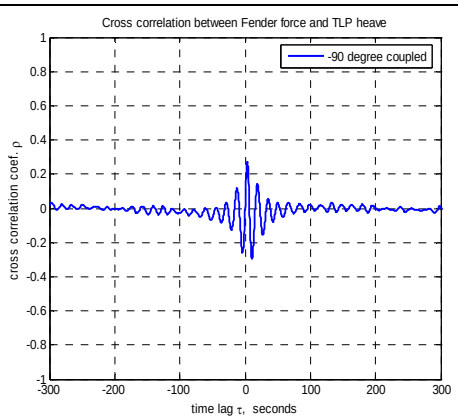

	0° head sea, coupled case	-90° beam sea, coupled case
Fender force and Barge surge	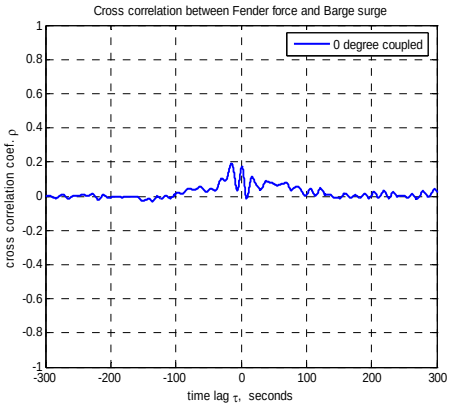	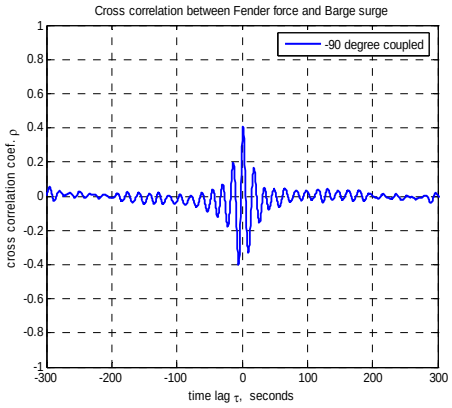
Fender force and Barge sway	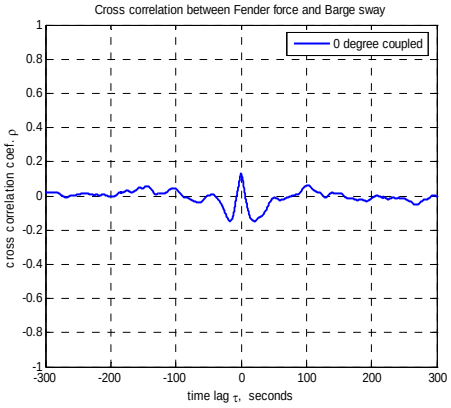	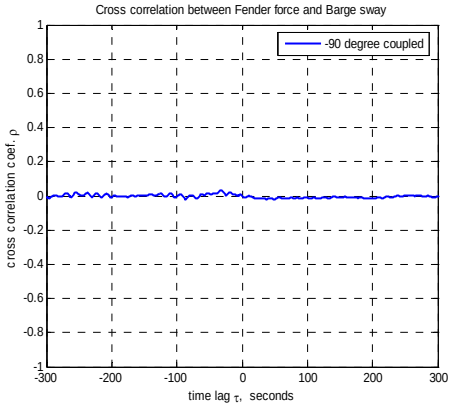
Fender force and Barge heave	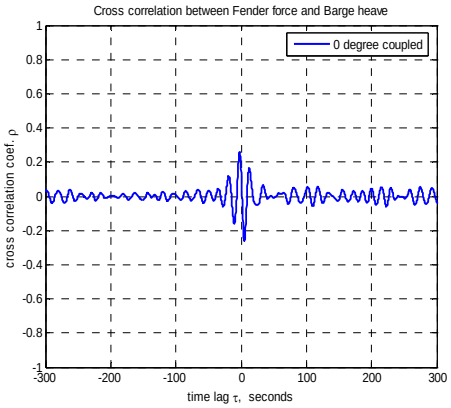	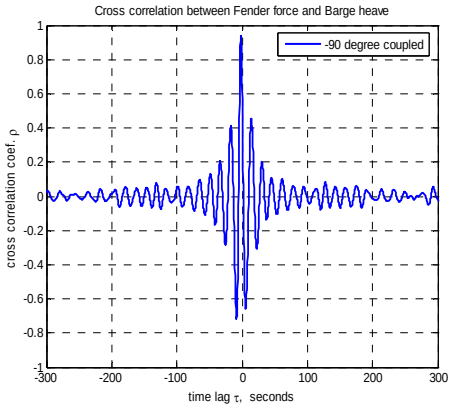

	0° head sea, coupled case	-90° beam sea, coupled case
Fender force and Barge roll	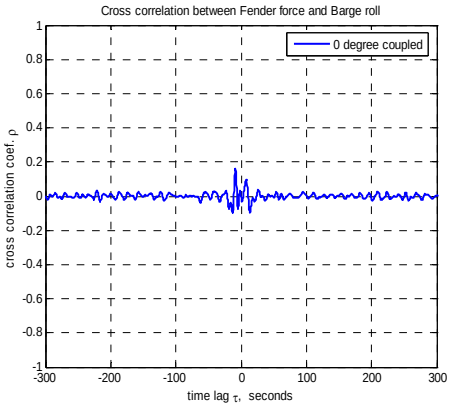	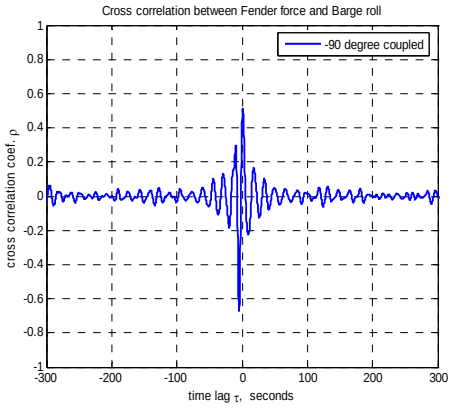
Fender force and Barge pitch	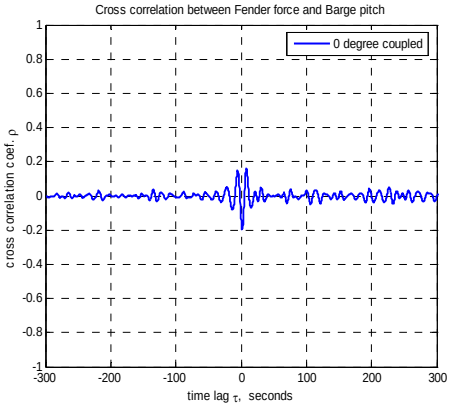	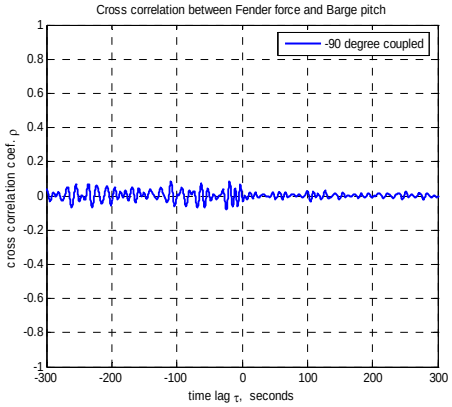
Fender force and Barge yaw	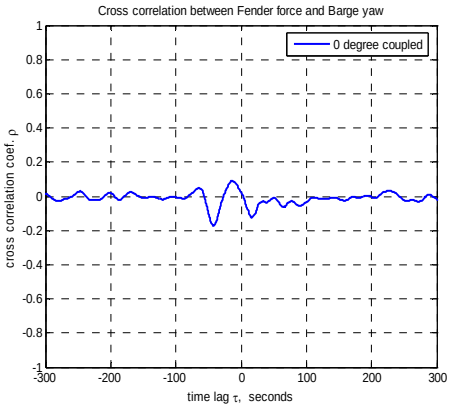	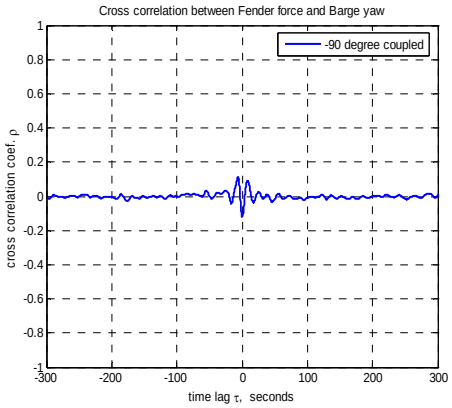

	0° head sea, coupled case	-90° beam sea, coupled case
Fender wave and Fender force	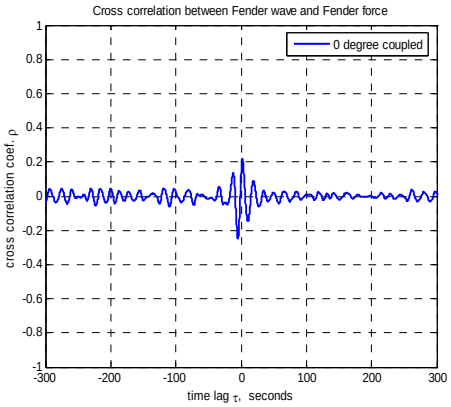	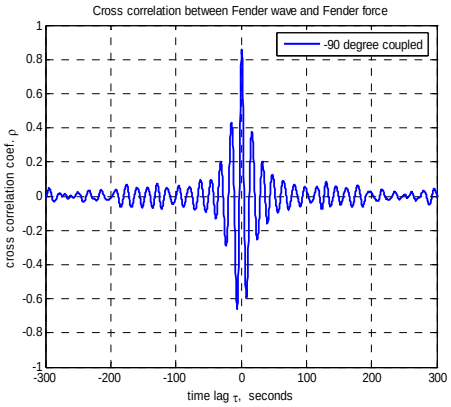

APPENDIX C

AUTO-SPECTRUMS*

	0° head sea	-90° beam sea
Wind	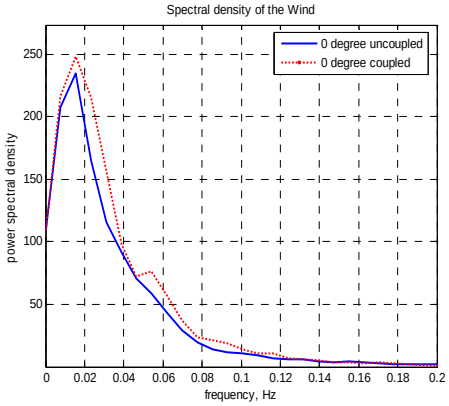	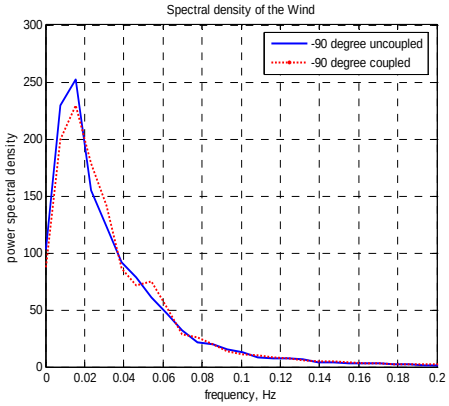
Wave	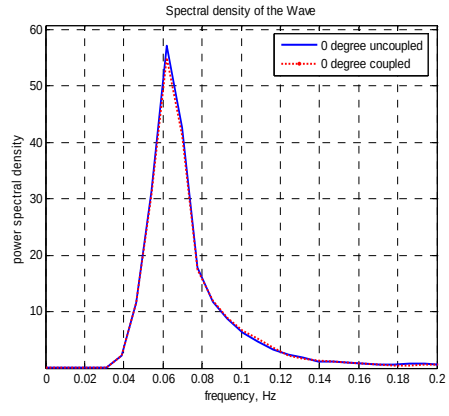	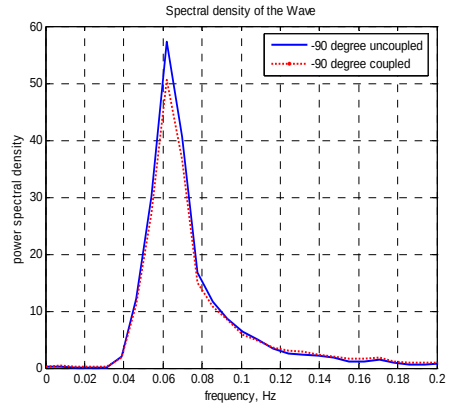

* The scale of the amplitude are not always the same for the head sea and the beam sea, because in some cases there is a large difference in the amplitude for these two configurations, a normalized scale will not allow a detailed view of the smaller spectrum.

	0° head sea	-90° beam sea
Current X	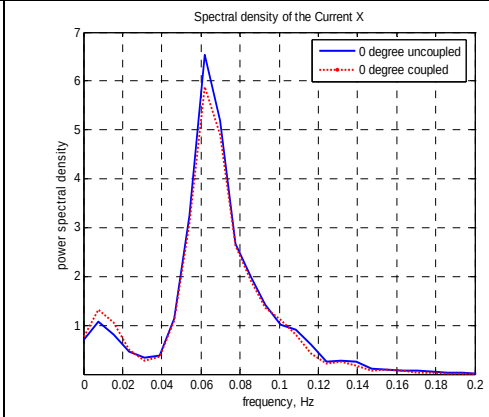	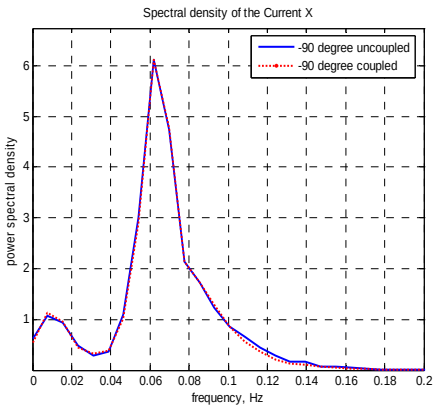
Current Y	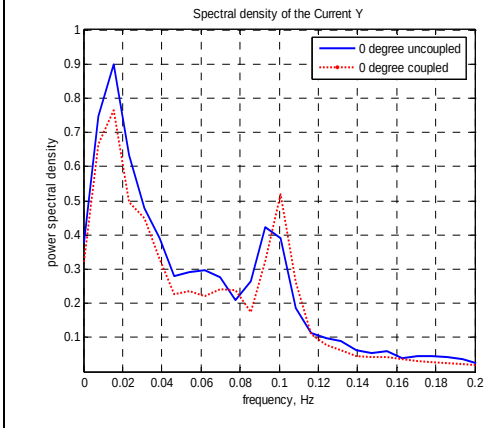	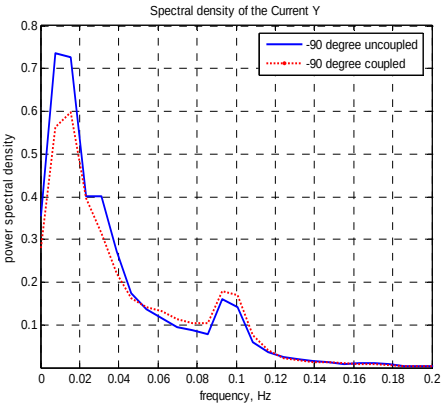

	0° head sea	-90° beam sea
TLP surge	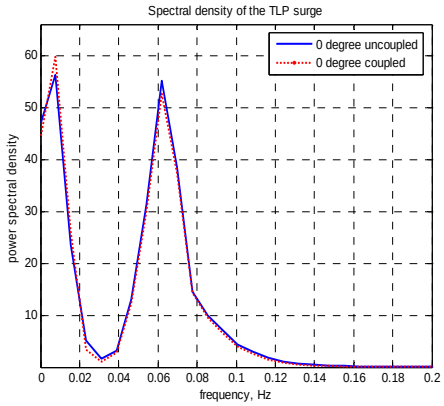	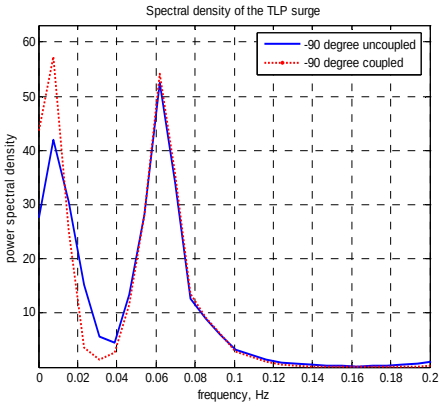
TLP sway	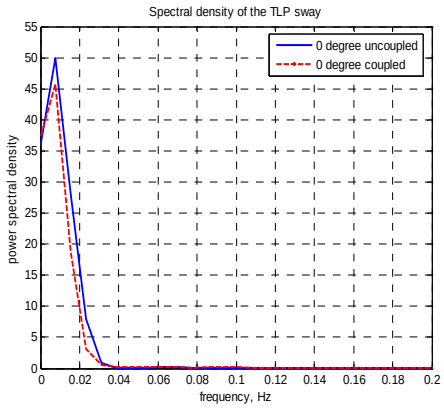	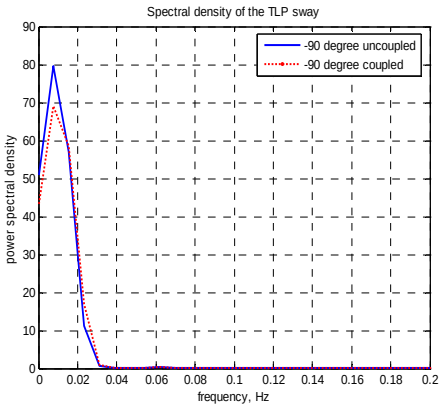
TLP heave	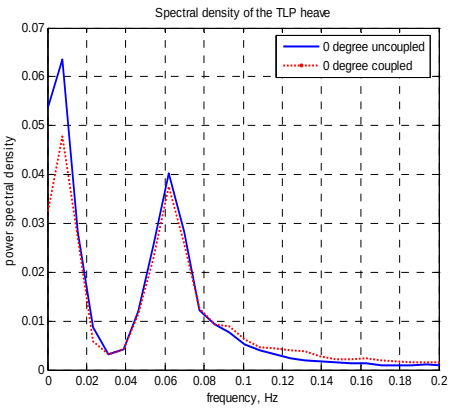	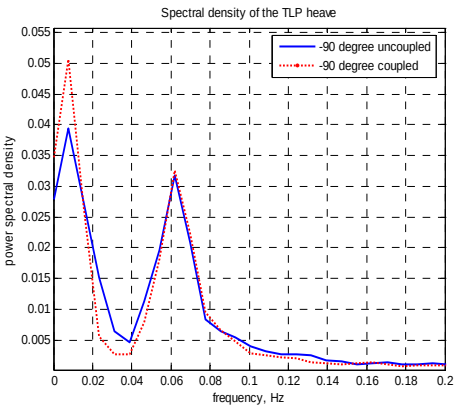

	0° head sea	-90° beam sea
Barge surge	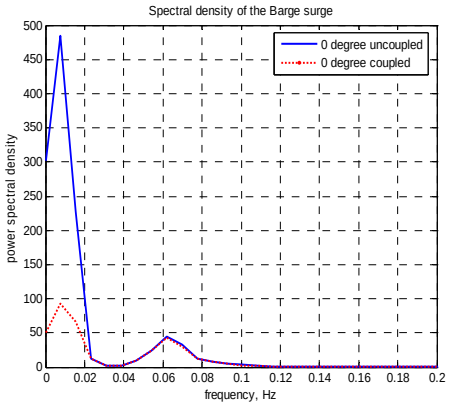	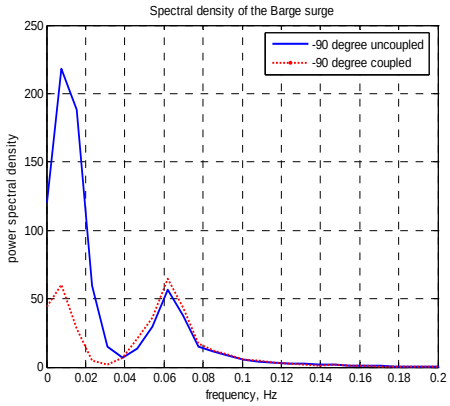
Barge sway	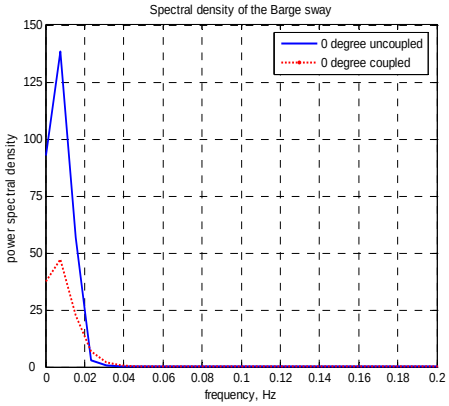	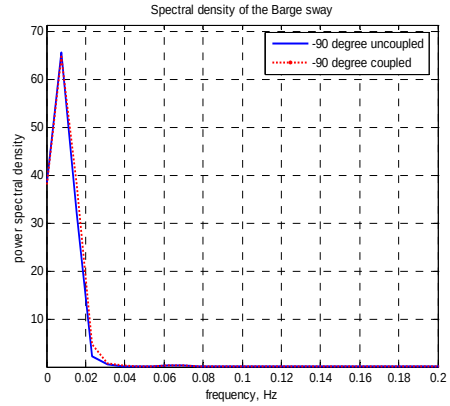
Barge heave	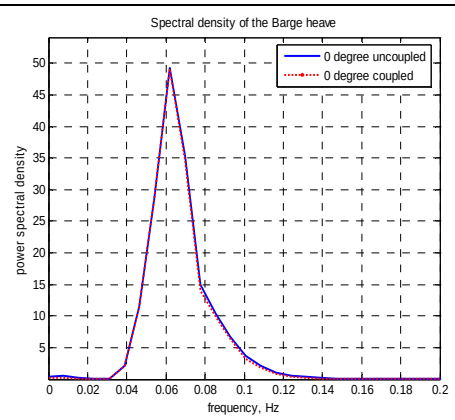	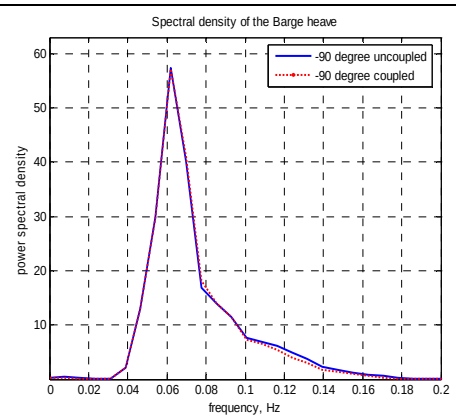

	0° head sea	-90° beam sea
Barge roll	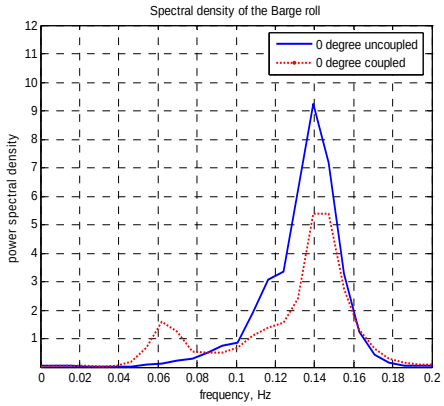	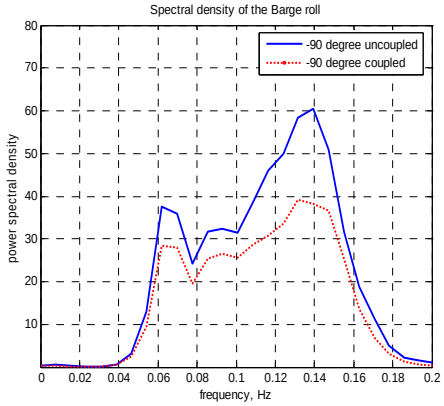
Barge pitch	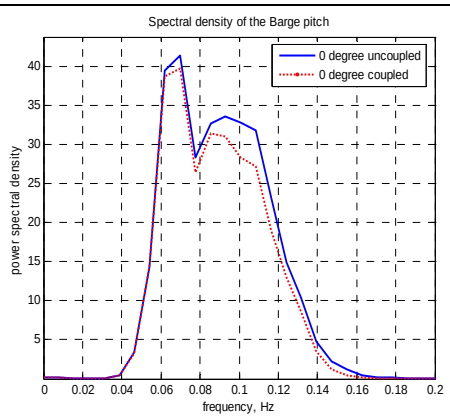	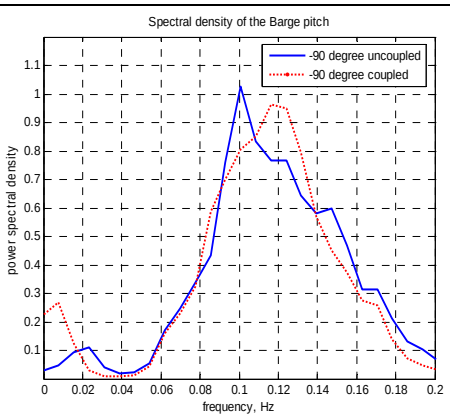
Barge yaw	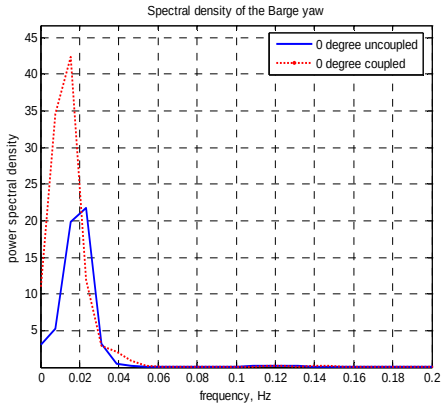	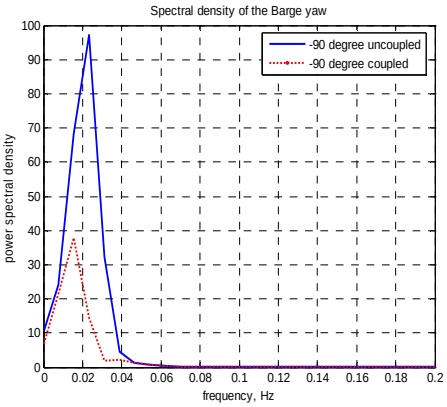

	0° head sea	-90° beam sea
Fender wave	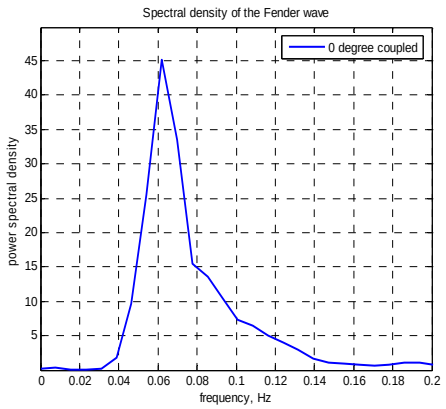	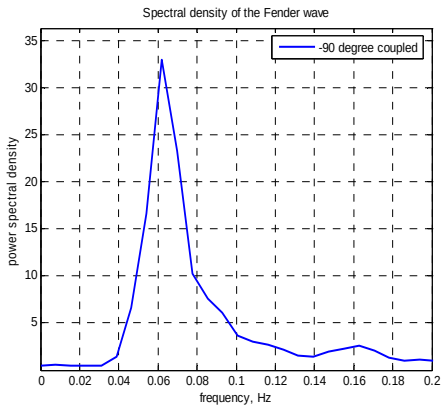
Fender force	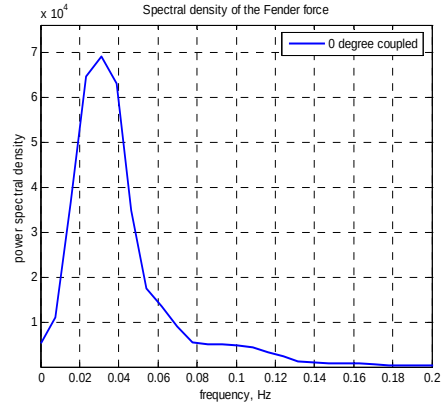	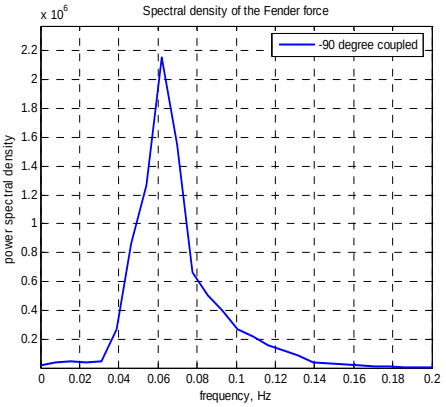

APPENDIX D

CROSS SPECTRUMS AND COHERENCE FUNCTIONS*

	0° head sea	-90° beam sea
TLP surge / Barge Surge	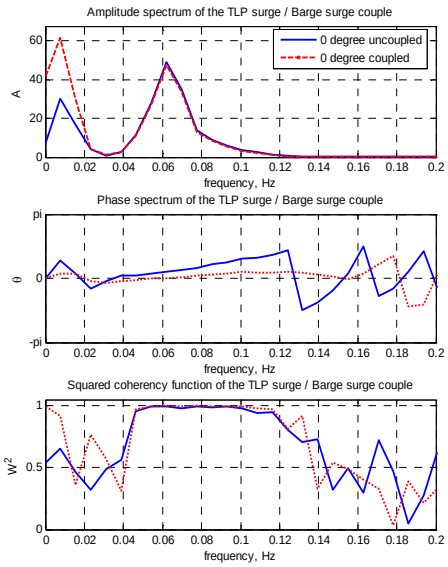	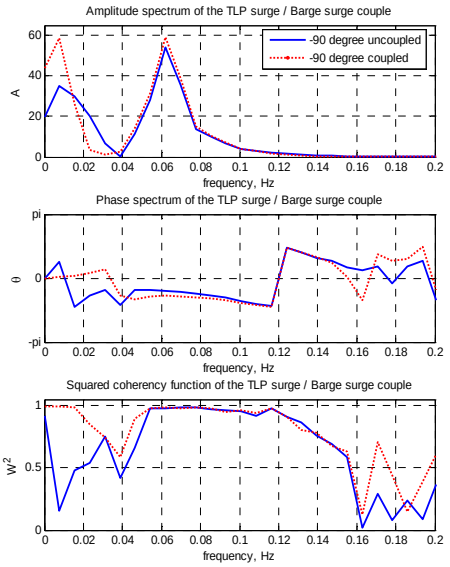
TLP surge / Barge sway	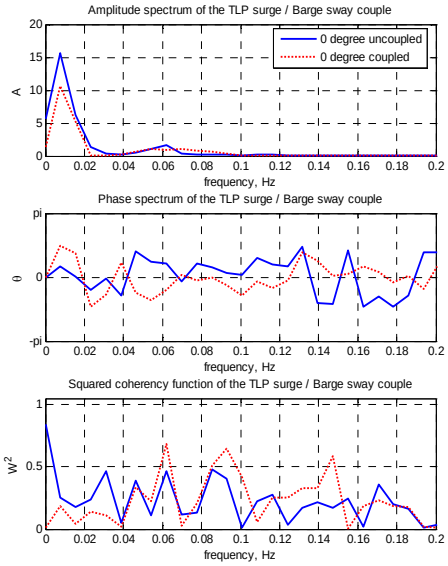	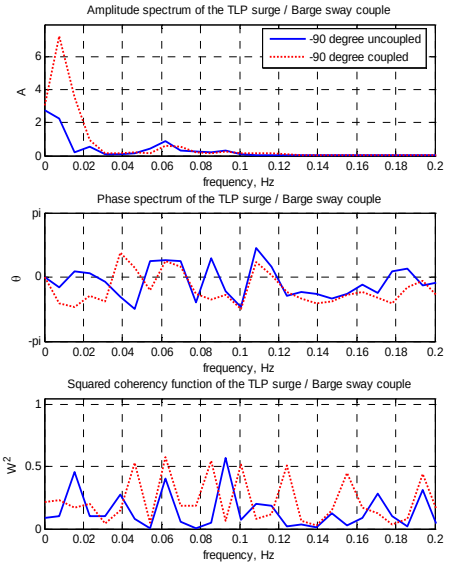

* Same as in the Appendix C, the scale are not the same for the amplitudes in 0 and -90 degree configurations.

	0° head sea	-90° beam sea
TLP surge / Barge heave	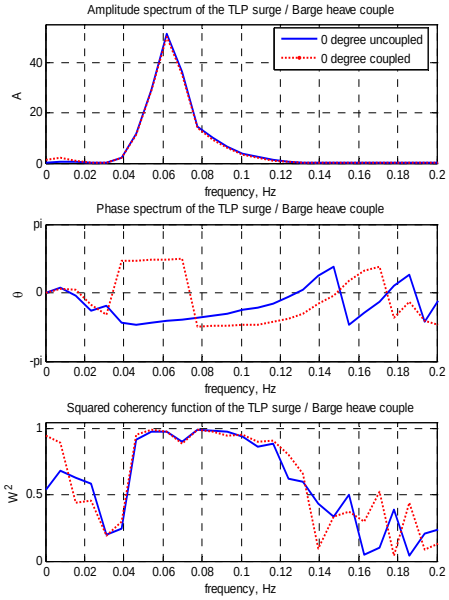	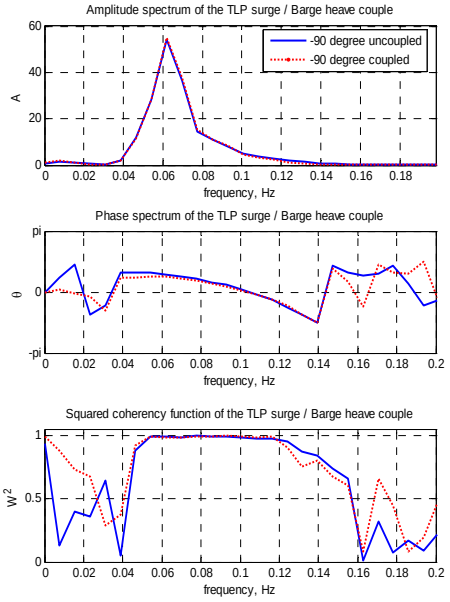
TLP surge / Barge roll	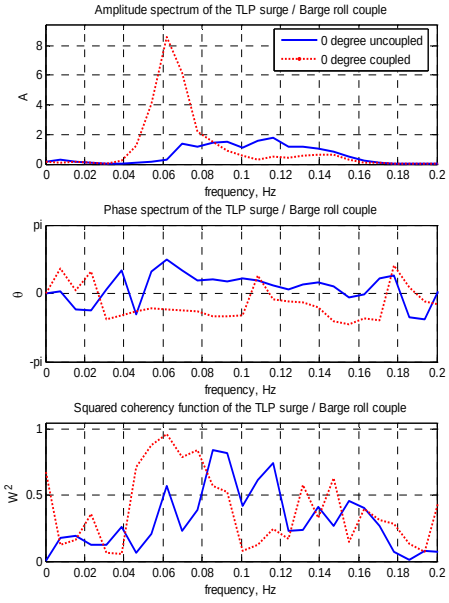	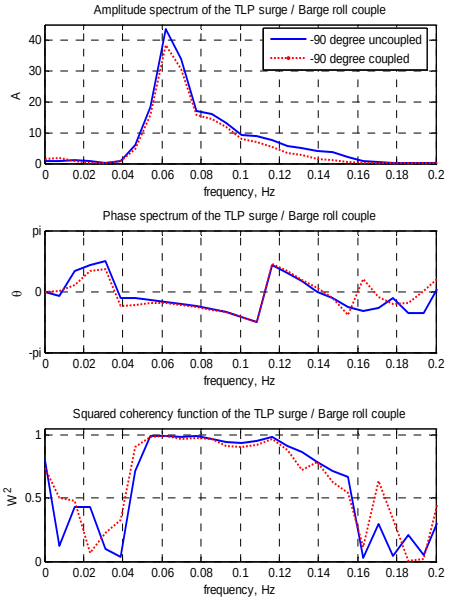

	0° head sea	-90° beam sea
TLP surge / Barge pitch	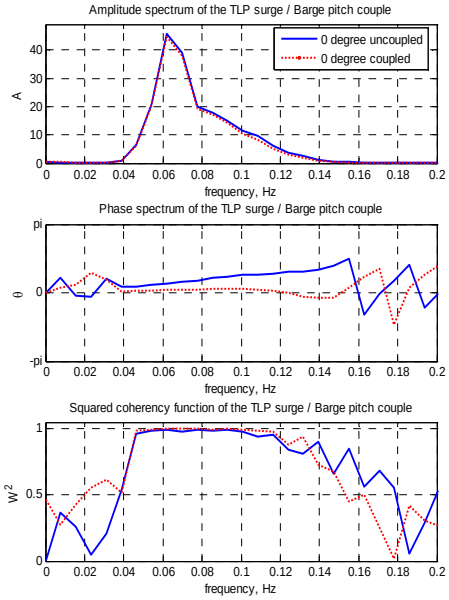	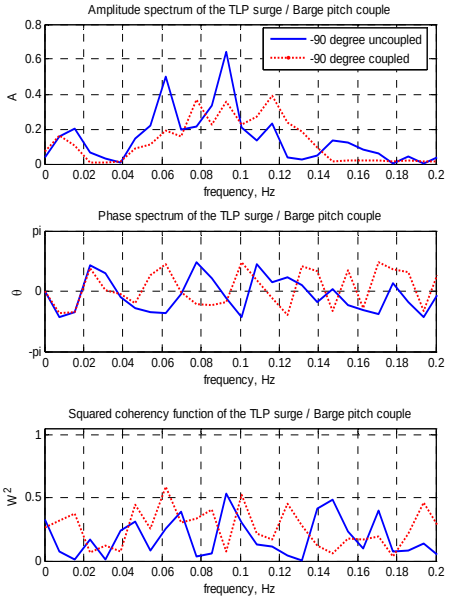
TLP surge / Barge yaw	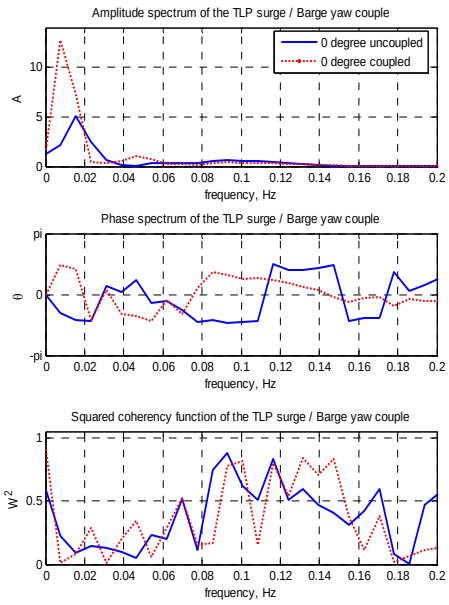	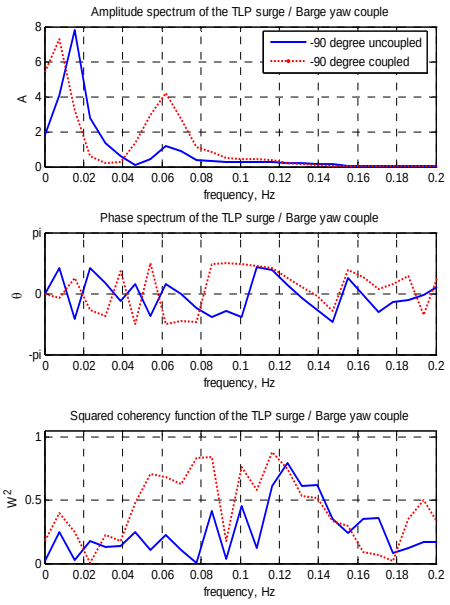

	0° head sea	-90° beam sea
TLP sway / Barge surge	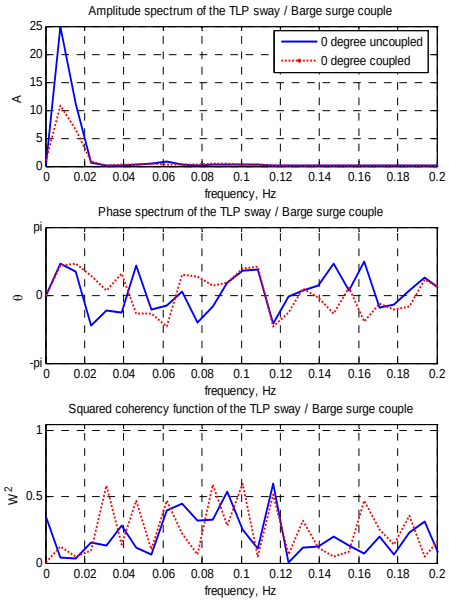	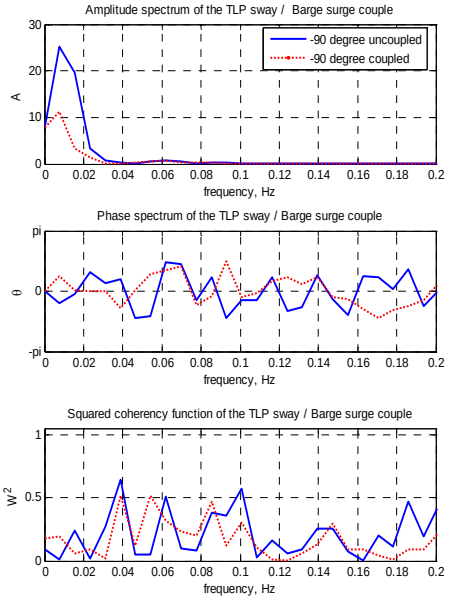
TLP sway / Barge sway	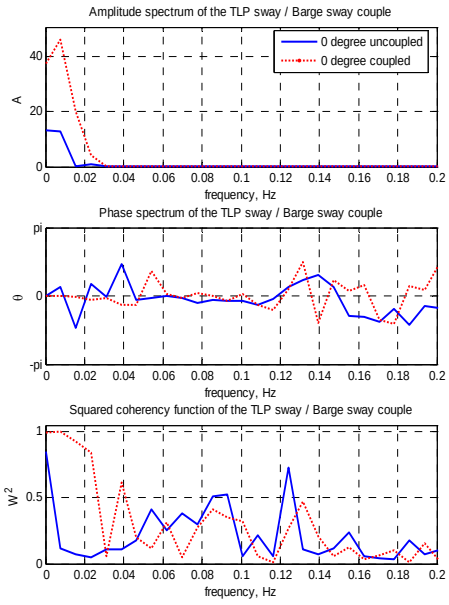	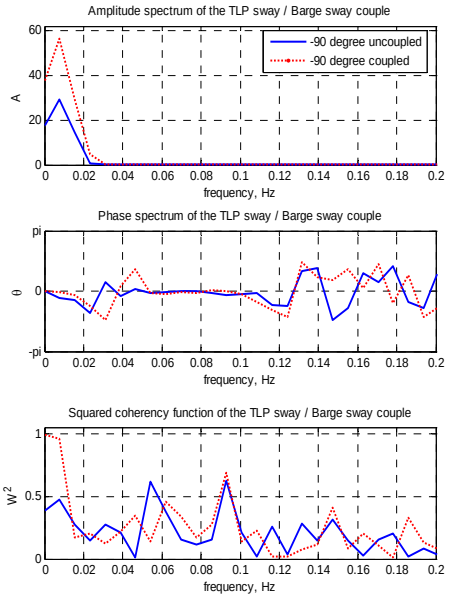

	0° head sea	-90° beam sea
TLP sway / Barge heave	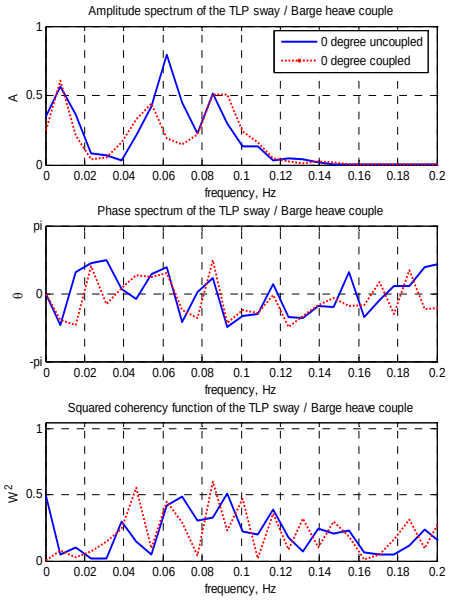	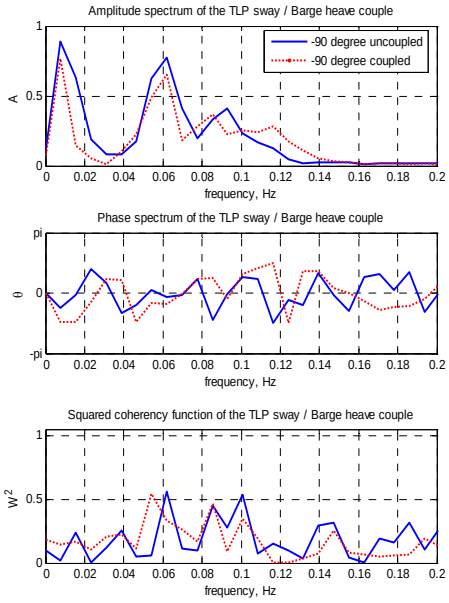
TLP sway / Barge roll	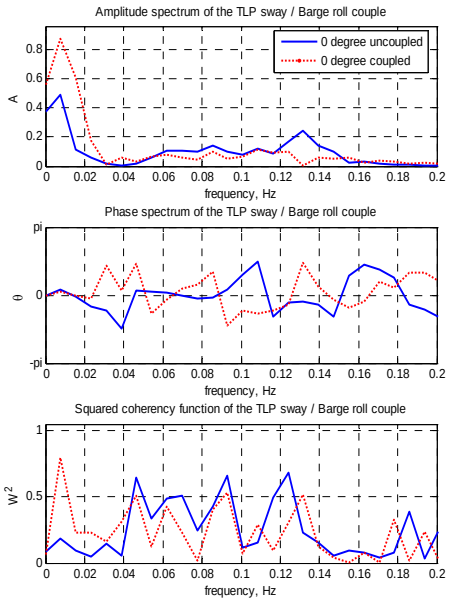	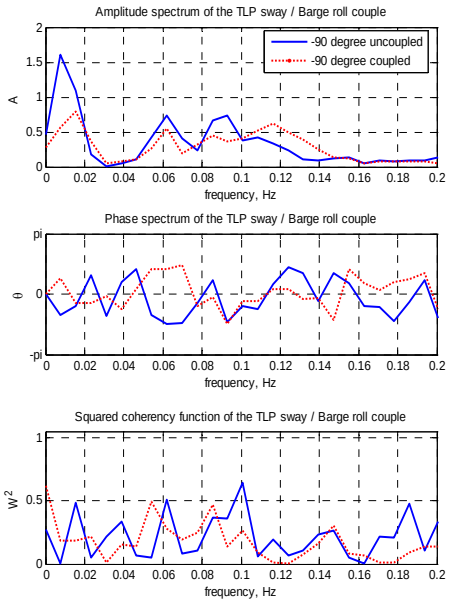

	0° head sea	-90° beam sea
TLP sway / Barge pitch	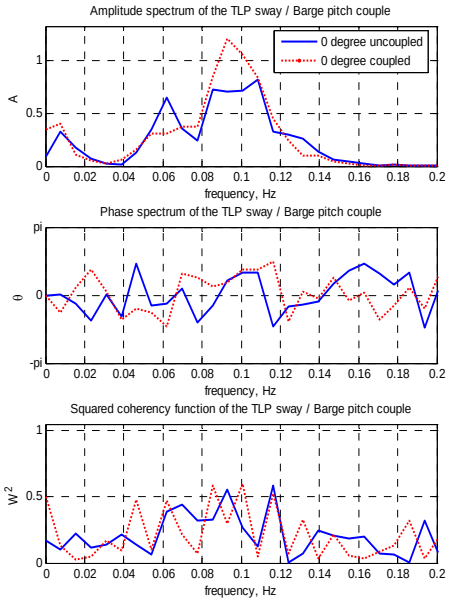	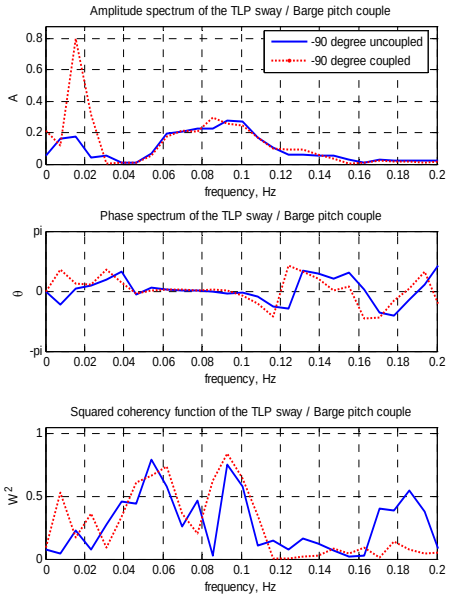
TLP sway / Barge yaw	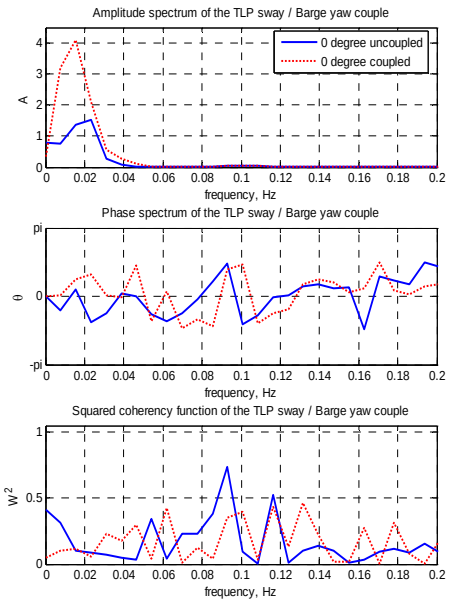	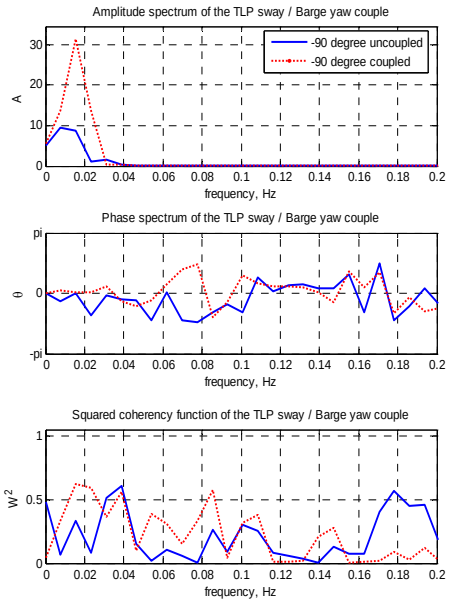

	0° head sea	-90° beam sea
TLP heave / Barge surge	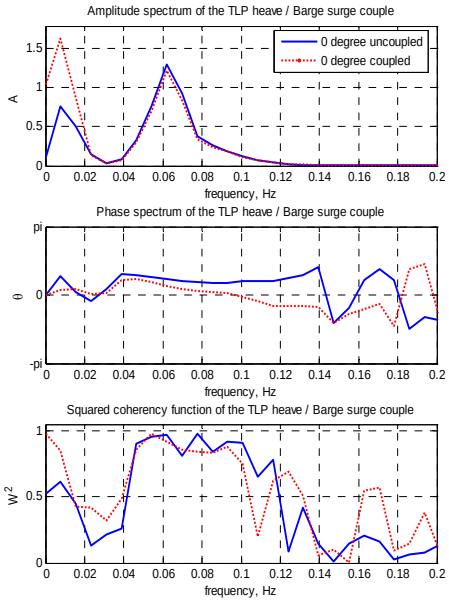	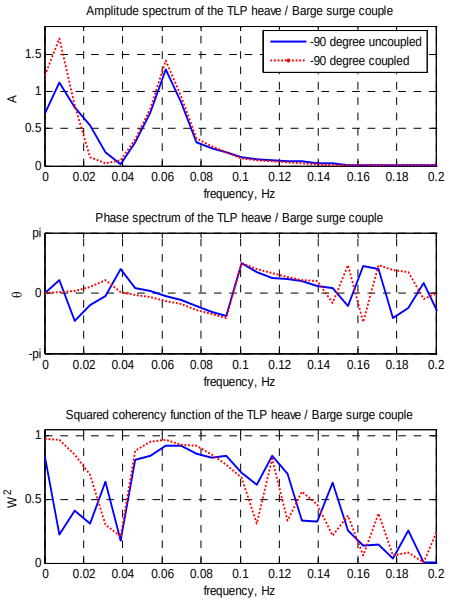
TLP heave / Barge sway	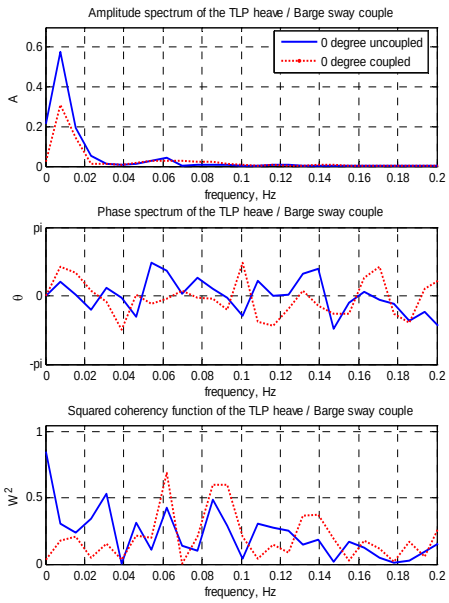	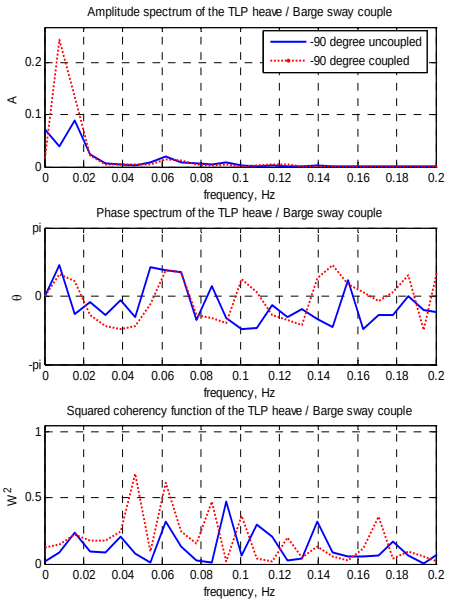

	0° head sea	-90° beam sea
TLP heave / Barge heave	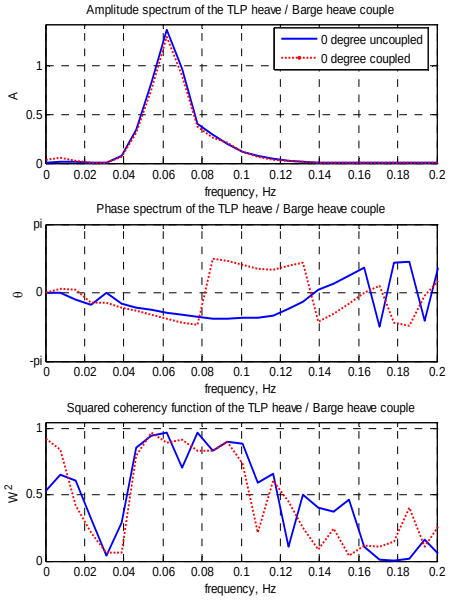	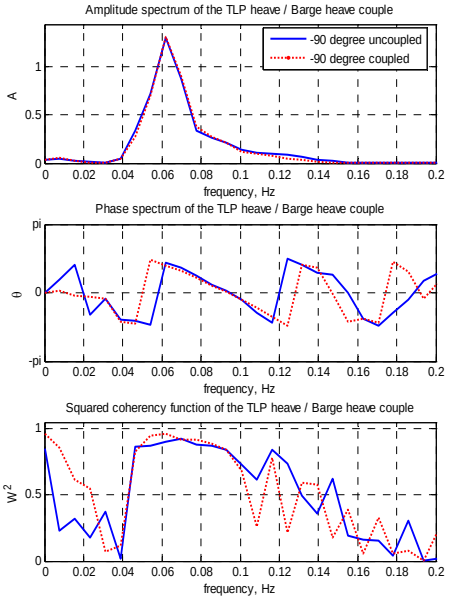
TLP heave / Barge roll	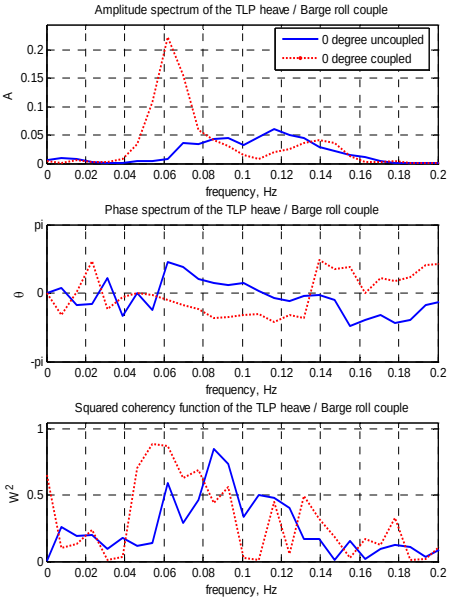	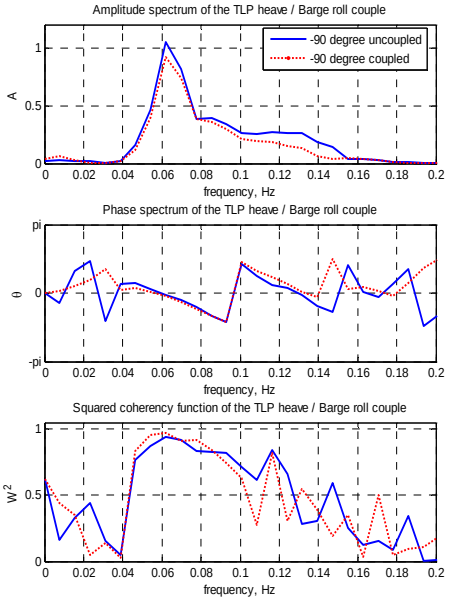

	0° head sea	-90° beam sea
TLP heave / Barge pitch	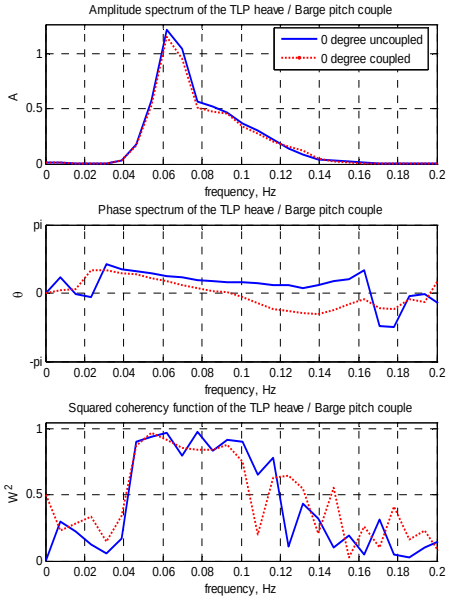	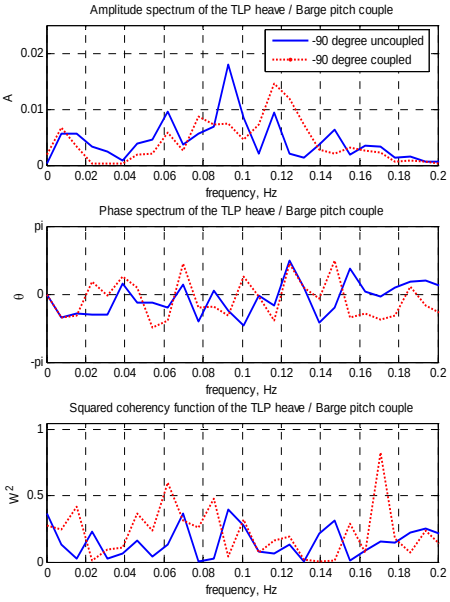
TLP heave / Barge yaw	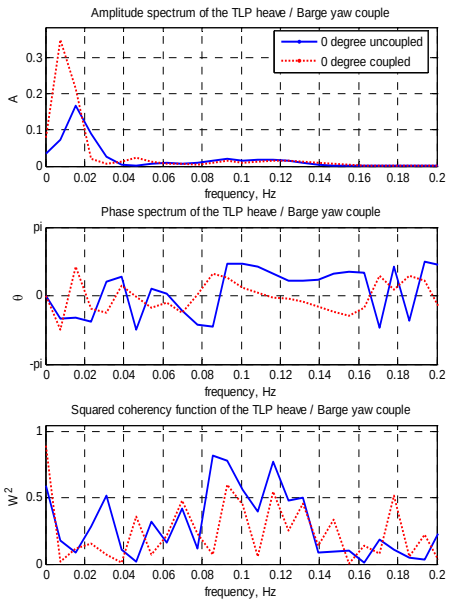	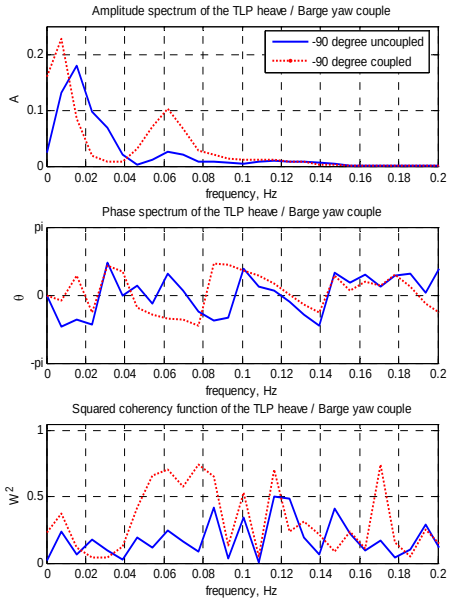

	0° head sea, coupled	-90° beam sea, coupled
Fender wave and TLP surge	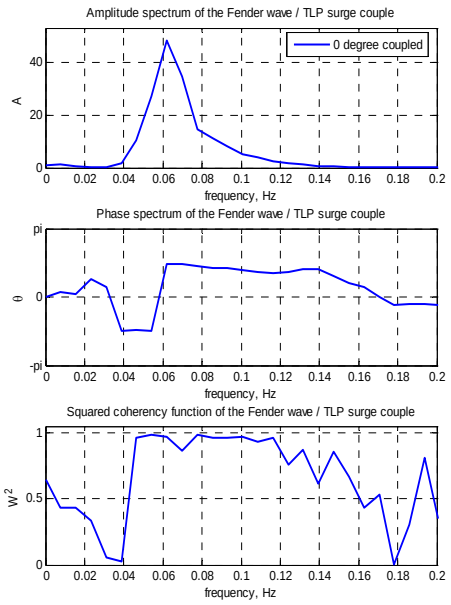	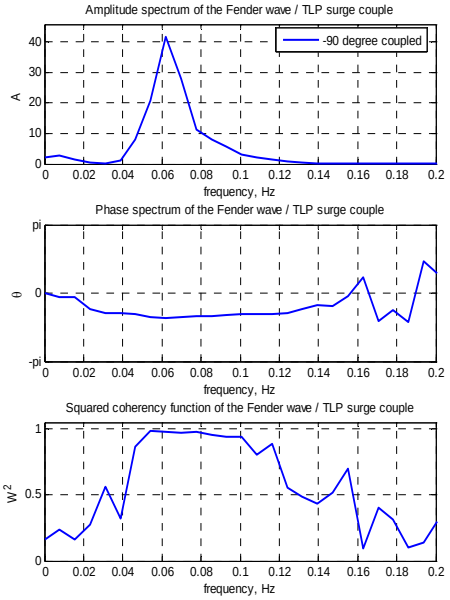
Fender wave and TLP sway	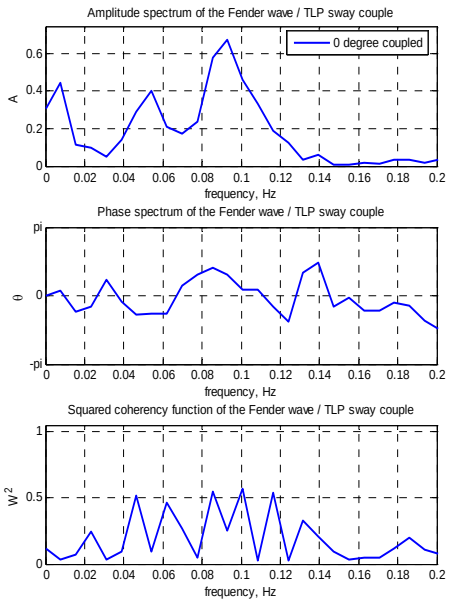	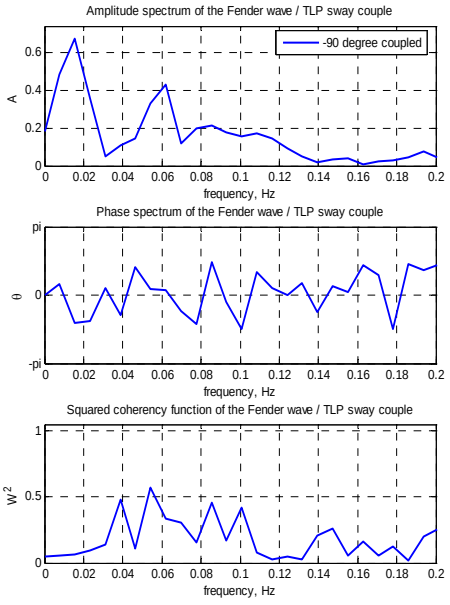

	0° head sea, coupled	-90° beam sea, coupled
Fender wave and TLP heave	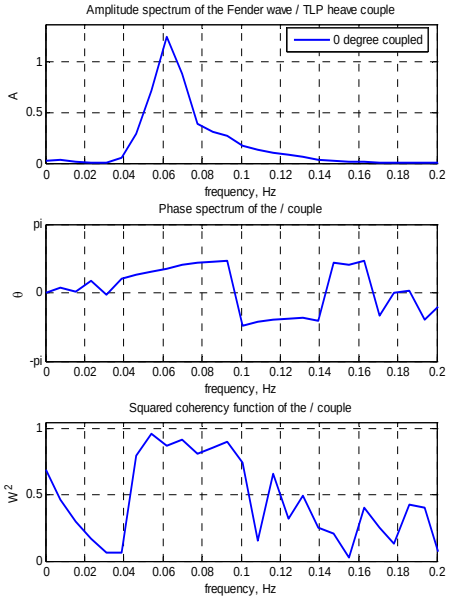	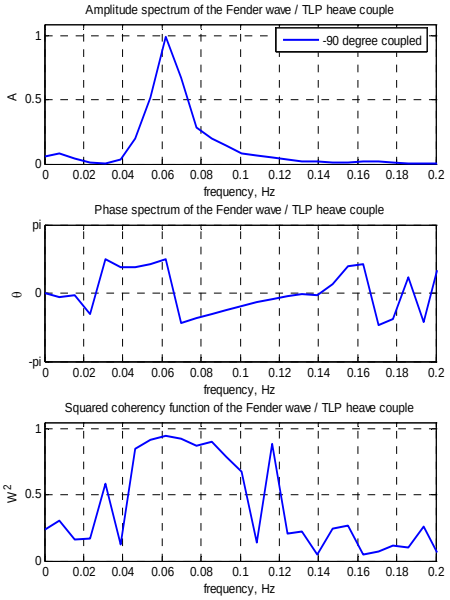
Fender wave and Barge surge	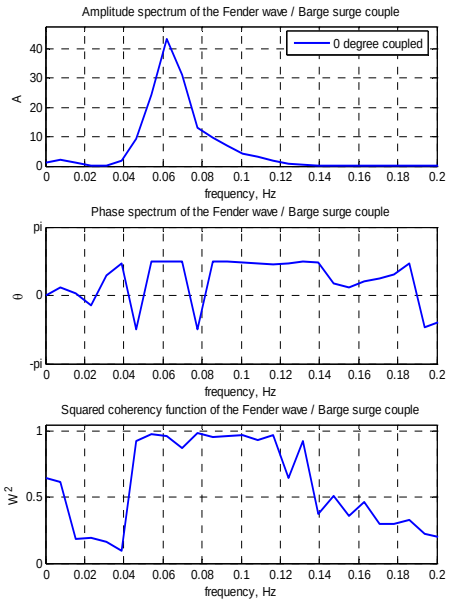	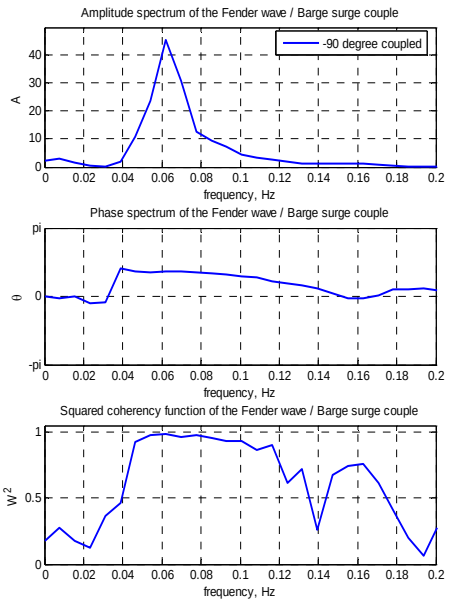

	0° head sea, coupled	-90° beam sea, coupled
Fender wave and Barge sway	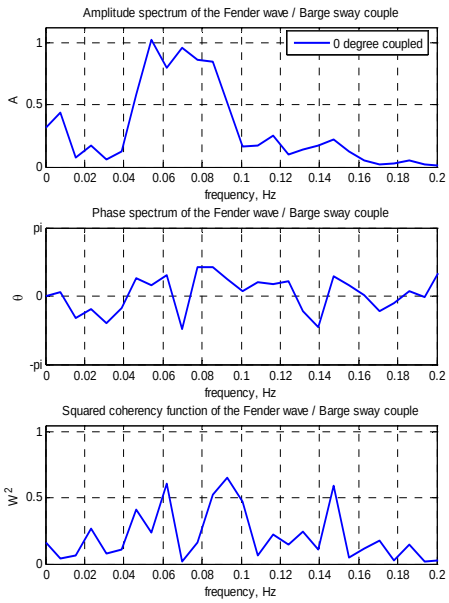	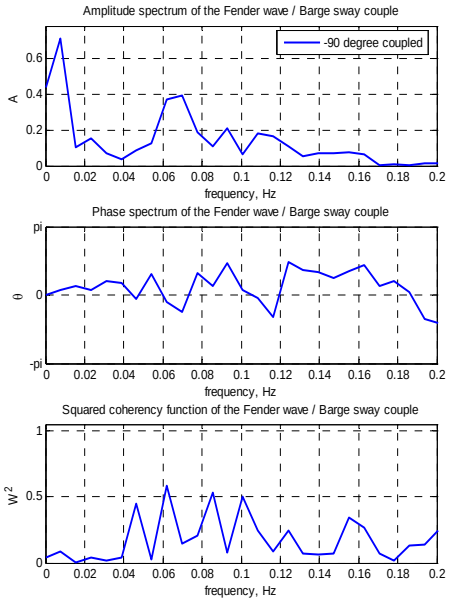
Fender wave and Barge heave	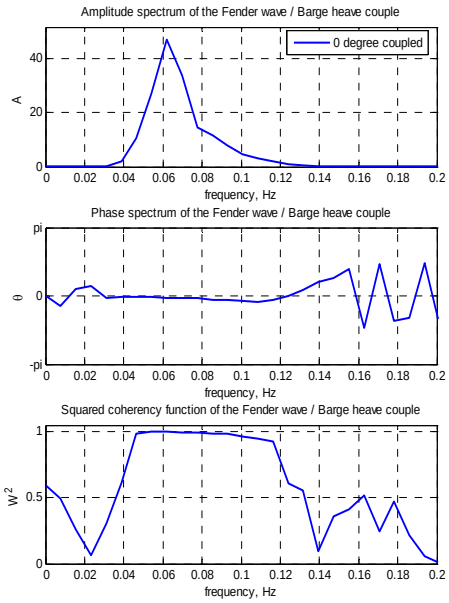	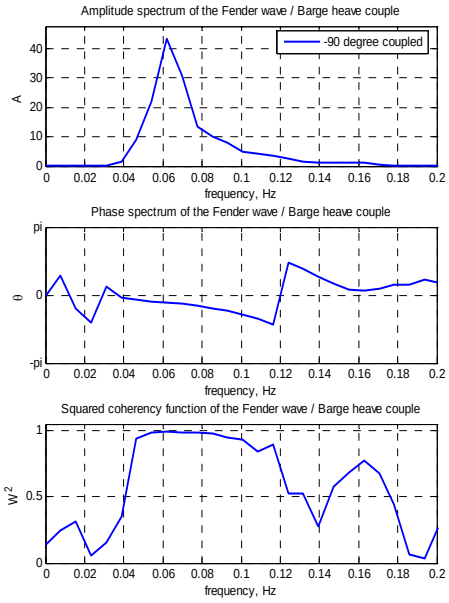

	0° head sea, coupled	-90° beam sea, coupled
Fender wave and Barge roll	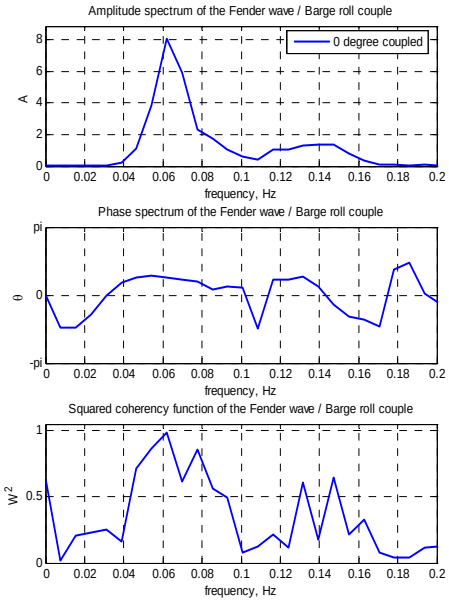	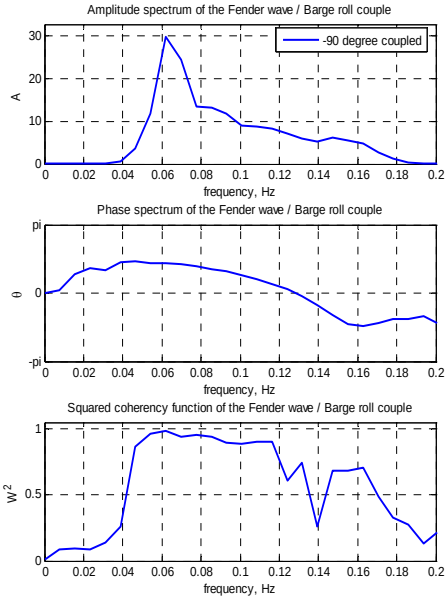
Fender wave and Barge pitch	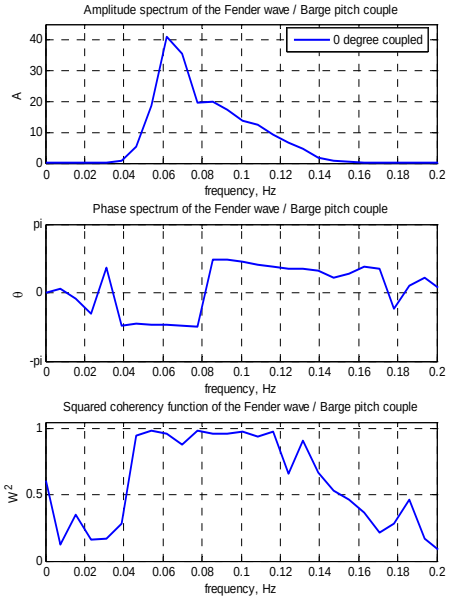	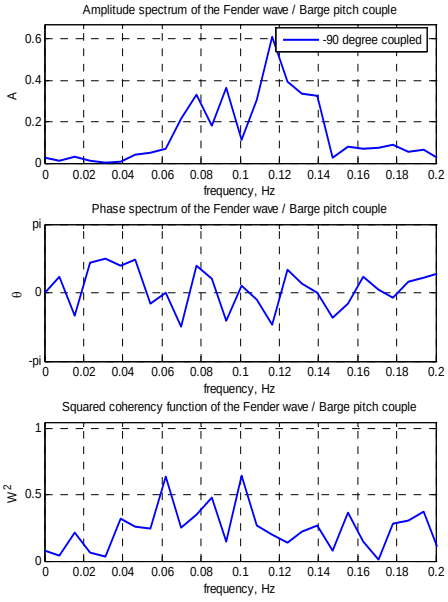

	0° head sea, coupled	-90° beam sea, coupled
Fender wave and Barge yaw	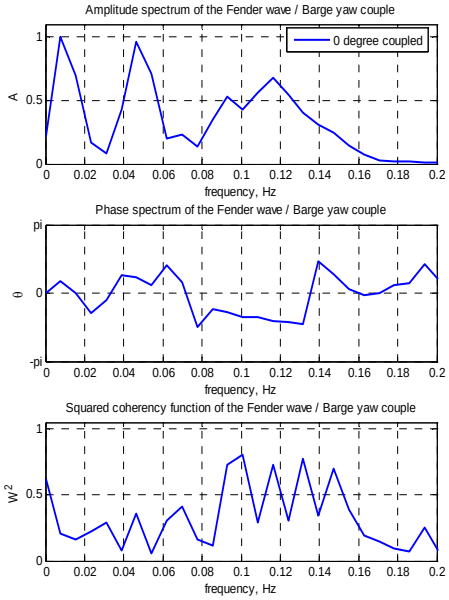	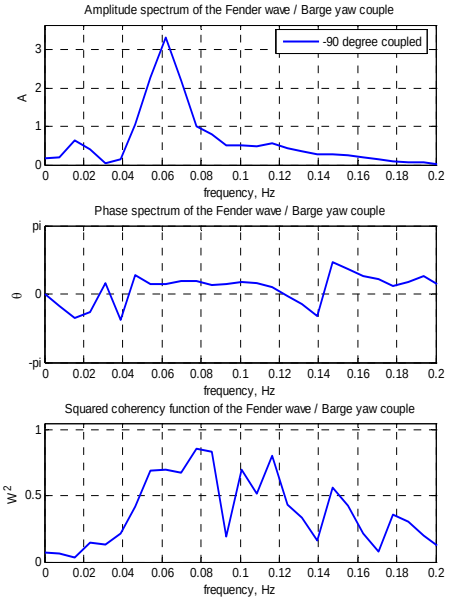
Fender force and TLP surge	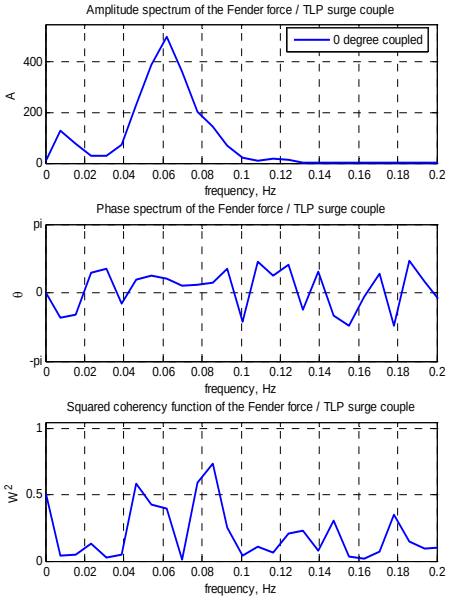	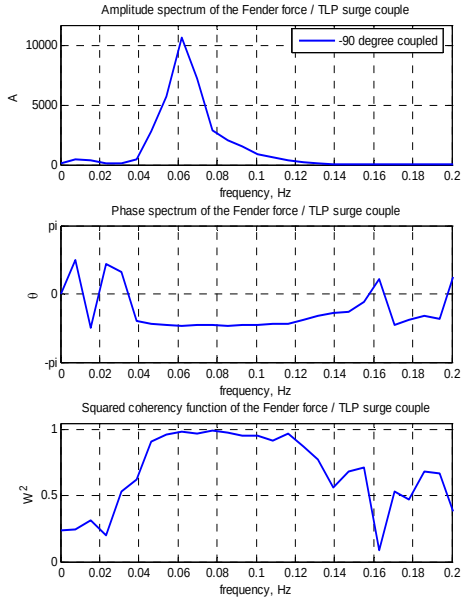

	0° head sea, coupled	-90° beam sea, coupled
Fender force and TLP sway	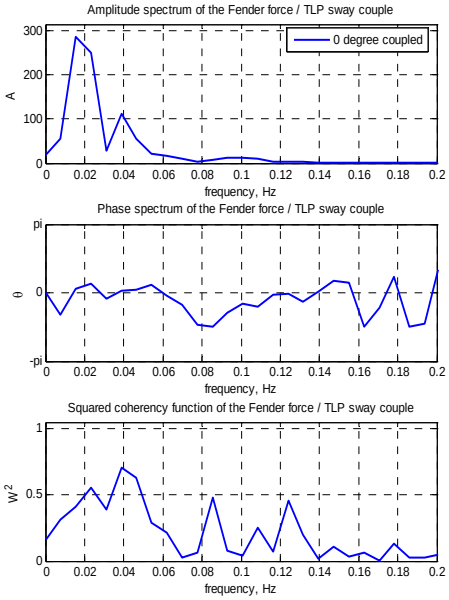	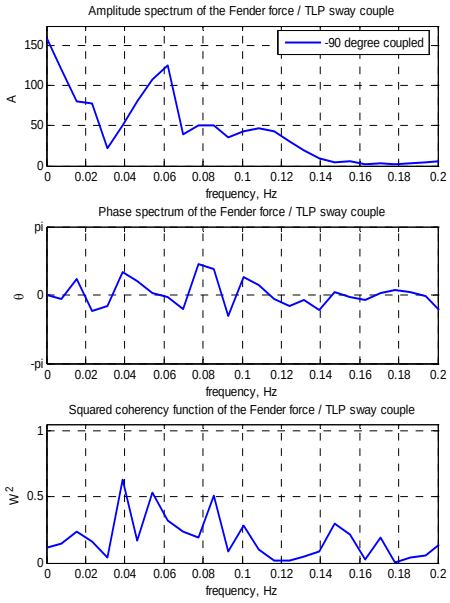
Fender force and TLP heave	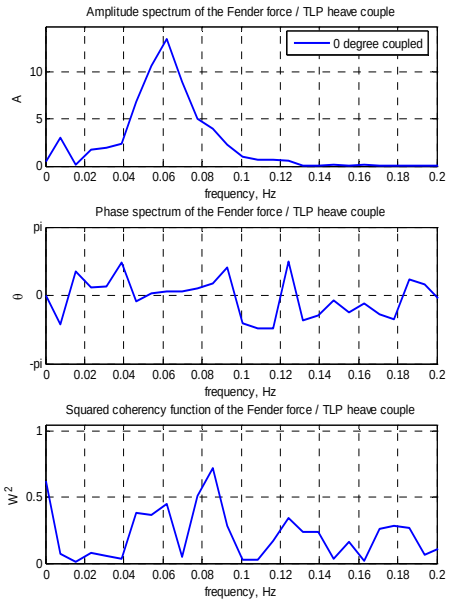	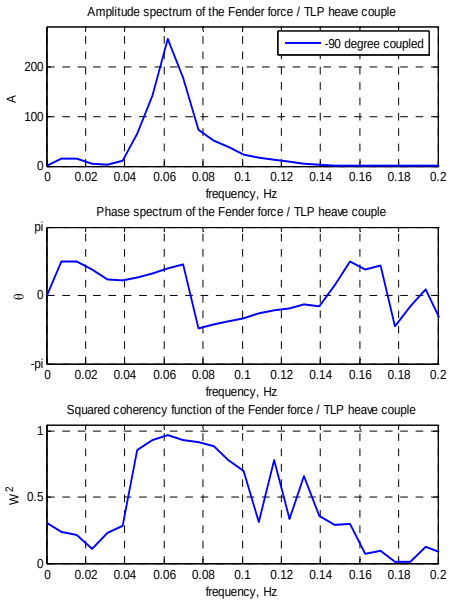

	0° head sea	-90° beam sea
Fender force and Barge surge	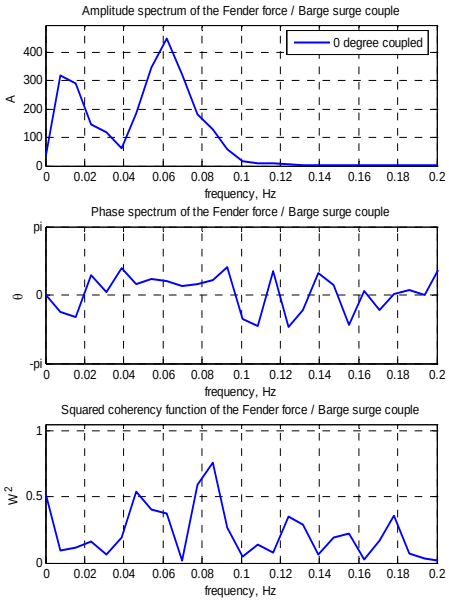	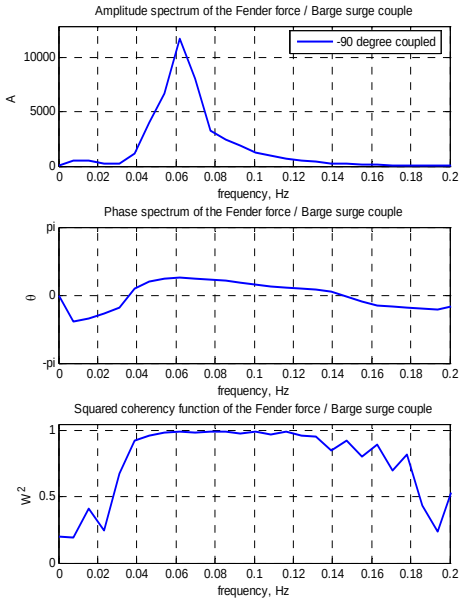
Fender force and Barge sway	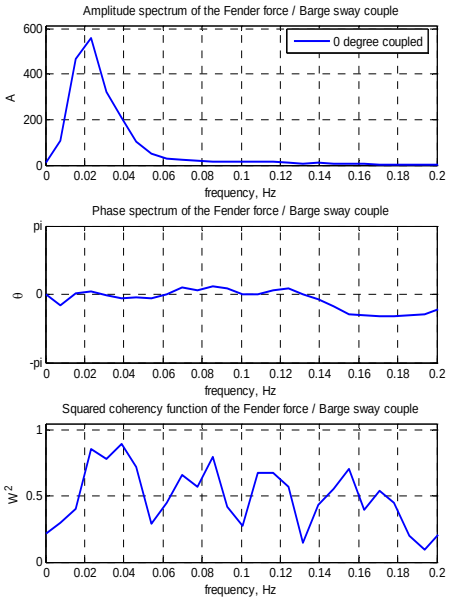	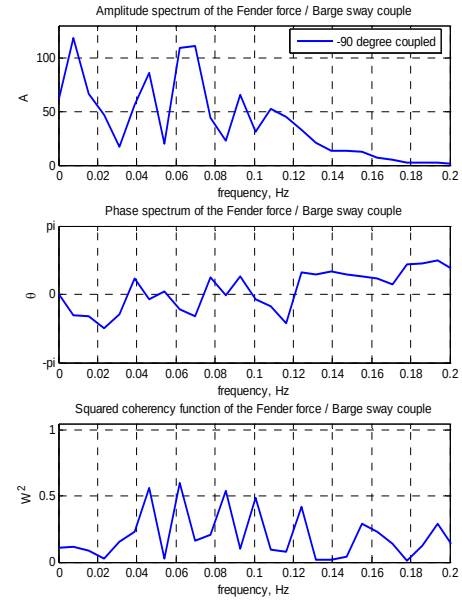

	0° head sea	-90° beam sea
Fender force and Barge heave	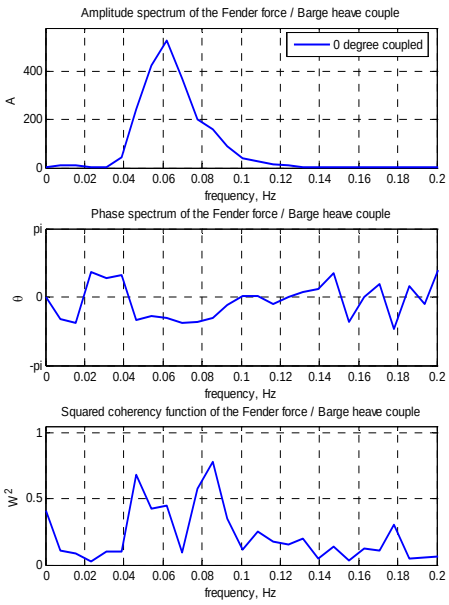	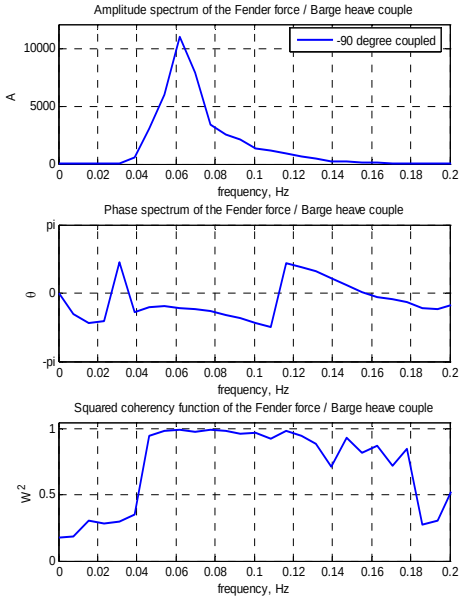
Fender force and Barge roll	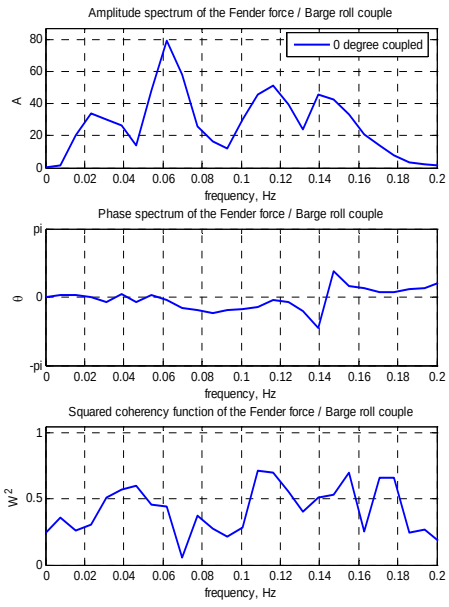	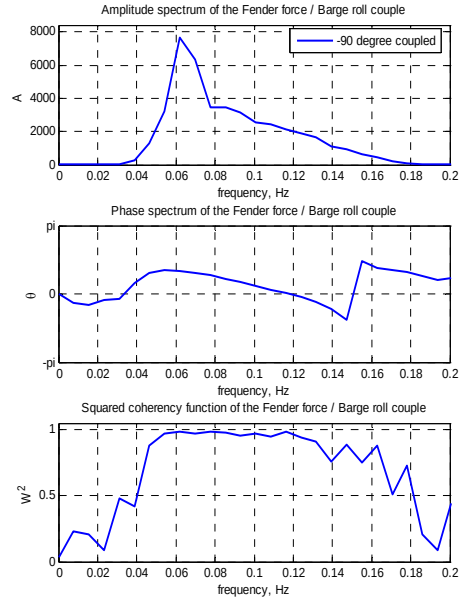

	0° head sea, coupled case	-90° beam sea, coupled case
Fender force and Barge pitch	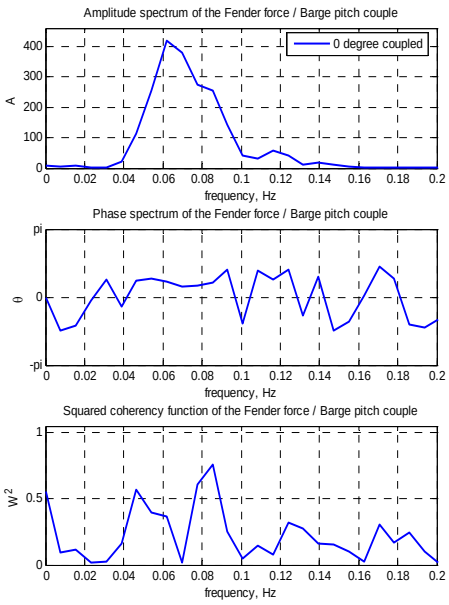	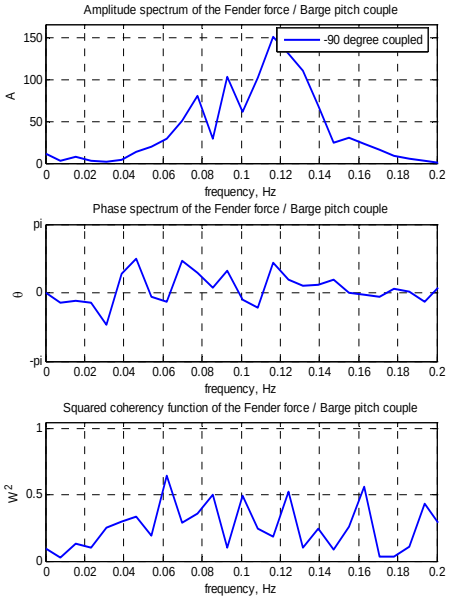
Fender force and Barge yaw	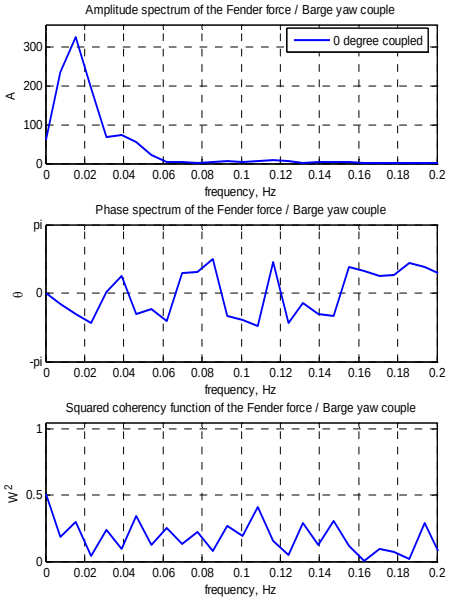	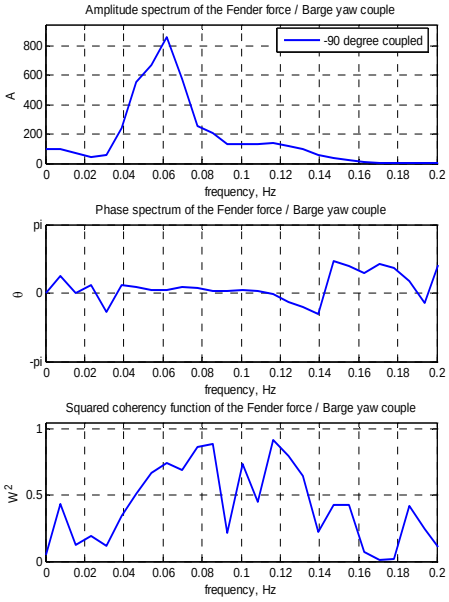

	0° head sea, coupled case	-90° beam sea, coupled case
Fender wave and Fender force	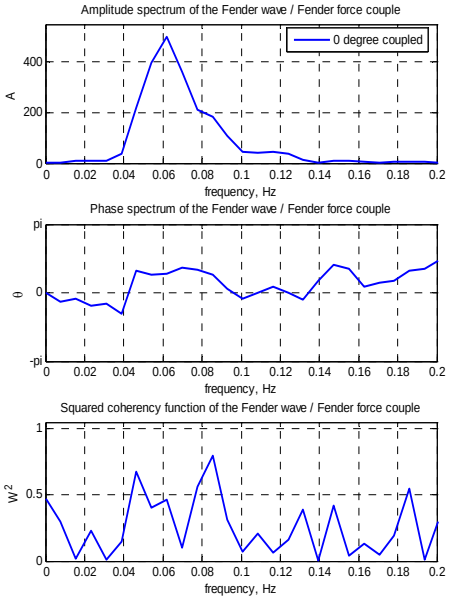	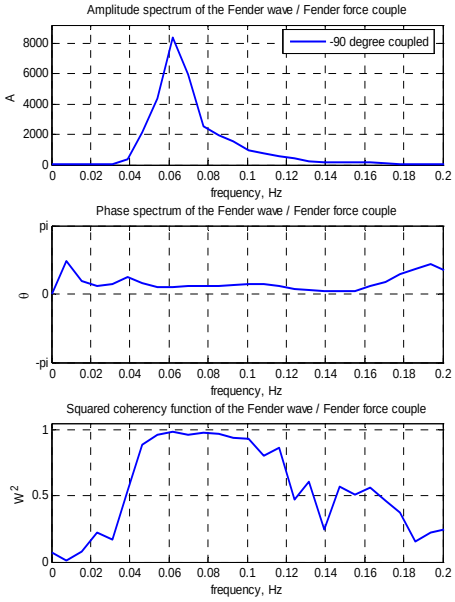

VITA

Chen Xie

EDUCATION

- Master of Science, in Ocean Engineering
  Graduation date: December 2005
  Texas A&M University, College Station, USA

- Diplôme d'ingénieur, in Constructing Engineering
  Graduation date: December 2005
  Ecole Spéciale des Travaux Publics, Paris, France

EXPERIENCE

- Texas A&M University, College Station, Texas (Jan. 2004 – Dec. 2005)
  Research Assistant for Dr. John M.Niedzwecki

- Bouygues Construction, Paris, France (Jun. 2003 - Aug. 2003)
  Assistant site manager (internship)

- Technip China, Shanghai, China (Jun. 2002 – Aug. 2002)
  Assistant structure designer (internship)